

**An Investigation into Dystroglycan Deficiency in
Fibroblasts and a Role for Dystroglycan in
Cytokinesis**

Jennifer R. Higginson B.Sc.(Hons)

A thesis submitted to the University of Glasgow
for the Degree of Doctor of Philosophy

Institute of Biomedical and Life Sciences,

University of Glasgow

July 2007

Table of Contents

List of Figures.....	ix
List of Tables.....	xi
Acknowledgements.....	xii
Declaration.....	xiii
Summary.....	xiv
Abbreviations.....	xvi

Chapter 1: Introduction

1.1	<i>Introduction.....</i>	2
1.2	<i>The dystrophin-glycoprotein complex.....</i>	2
1.3	<i>Dystroglycan complex in non-muscle cells.....</i>	3
1.4	<i>Dystroglycan biosynthesis and protein structure.....</i>	4
	1.4.1 <i>Dystroglycan gene.....</i>	4
	1.4.2 <i>Pro-peptide biosynthesis and processing.....</i>	5
	1.4.3 <i>Structure of α-dystroglycan.....</i>	5
	1.4.4 <i>Structure of β-dystroglycan.....</i>	6
1.5	<i>Dystroglycan binding partners.....</i>	6
	1.5.1 <i>α-Dystroglycan interactions.....</i>	7
	1.5.2 <i>β-Dystroglycan interactions.....</i>	7
	1.5.2.1 <i>Dystrophin and utrophin.....</i>	7
	1.5.2.2 <i>Caveolin-3.....</i>	8
	1.5.2.3 <i>GRB2.....</i>	9
	1.5.2.4 <i>Other proteins.....</i>	9
	1.5.3 <i>Dystroglycan phosphorylation.....</i>	11

1.6	<i>Development</i>	12
1.6.1	<i>Basement membrane formation</i>	12
1.6.2	<i>Muscle</i>	13
1.6.3	<i>Neuromuscular junction</i>	14
1.6.4	<i>Epithelial morphogenesis</i>	15
1.6.5	<i>Central and peripheral nervous system</i>	15
1.7	<i>Dystroglycan depletion in model organisms</i>	16
1.8	<i>Signal transduction</i>	17
1.8.1	<i>SH2 and SH3 domain containing signalling molecules</i>	17
1.8.2	<i>ERK-MAP kinase signalling</i>	18
1.8.3	<i>PI3K/AKT signalling</i>	19
1.8.4	<i>ERM proteins and Rho GTPase signalling</i>	20
1.9	<i>Dystroglycan and disease</i>	21
1.9.1	<i>Duchenne muscular dystrophy and secondary dystroglycanopathies</i>	21
1.9.2	<i>Cancer</i>	22
1.9.3	<i>Viral infection</i>	25
1.10	<i>Summary and aims</i>	25

Chapter 2: Materials and Methods

2.1	<i>Materials</i>	29
2.1.1	<i>Molecular biology reagents</i>	29
2.1.2	<i>Cells, cell culture vessels and reagents</i>	30
2.1.3	<i>SDS-PAGE, Western blotting and detection reagents</i>	32

2.1.4	<i>Antisera</i>	32
2.1.5	<i>Miscellaneous lab equipment</i>	33
2.2	Methods	33
2.2.1	<i>Molecular biology techniques</i>	33
2.2.2	<i>Polymerase chain reaction</i>	34
2.2.3	<i>RT-PCR</i>	35
2.2.4	<i>Northern blotting</i>	35
2.2.5	<i>Growth and maintenance of mammalian tissue culture cells</i>	36
2.2.6	<i>Maintenance and differentiation of embryonic stem cells</i>	36
2.2.7	<i>Generation of stable dystroglycan RNAi knockdown cells</i>	37
2.2.8	<i>Cryogenic preservation and storage</i>	38
2.2.9	<i>LipofectAMINE transfection</i>	38
2.2.10	<i>Generation of stable transfected cell lines</i>	39
2.2.11	<i>Cell fixation</i>	39
2.2.12	<i>Immunocytochemistry</i>	40
2.2.13	<i>Morphological analysis</i>	40
2.2.13.1	<i>Area and circularity quantification</i>	40
2.2.13.2	<i>Focal adhesion quantification</i>	41
2.2.14	<i>Cell proliferation assay</i>	41
2.2.15	<i>BrdU (5-bromo-2-deoxyuridine) incorporation</i>	42
2.2.16	<i>Cell synchronisation methods</i>	42
2.2.16.1	<i>Double thymidine block and transfection</i>	42
2.2.16.2	<i>Cell Synchronisation by double block with thymidine and mimosine</i>	43
2.2.17	<i>Time-lapse microscopy</i>	44

2.2.18 Wound healing assays.....	44
2.2.19 Annexin V apoptosis assay.....	45
2.2.20 Actin fractionation.....	45
2.2.21 Total cell lysates.....	46
2.2.22 Determination of protein concentration.....	46
2.2.23 SDS-polyacrylamide gel electrophoresis.....	47
2.2.24 Western analysis.....	47
2.2.25 Western blot detection.....	48
2.2.25.1 ECL detection.....	48
2.2.25.2 Alkaline phosphatase detection.....	48

Chapter 3: Isolation and analysis of dystroglycan null-derived fibroblasts

3.1 Introduction.....	50
3.2 Results.....	52
3.2.1 Generation of fibroblasts from dystroglycan null embryonic stem cells.....	52
3.2.2 Characterisation of DG <i>-/-</i> cell clones.....	53
3.2.2.1 DG <i>-/-</i> cells displayed typical fibroblast morphology.....	53
3.2.2.2 Determination of DG <i>-/-</i> cell lineage.....	54
3.2.2.3 DG <i>-/-</i> cells exhibited a multinucleate phenotype.....	55
3.2.3 DG <i>-/-</i> cells expressed dystroglycan.....	55
3.2.4 Proposed re-initiation of dystroglycan expression.....	57
3.2.4.1 RT-PCR analysis.....	58
3.2.4.2 DG <i>-/-</i> cells express full-length <i>Dag1</i> mRNA.....	60
3.2.5 3C12 epithelial-like DG <i>-/-</i> derived cells expressed dystroglycan.....	61
3.2.6 DG <i>-/-</i> cells and 3C12 cells did not contain gene disrupting cassette	

4.2.14.1	<i>Dystroglycan deficiency reduces filopodia in cells transfected with DA Cdc42.....</i>	97
4.2.14.2	<i>Dystroglycan deficiency prevents formation of lamellipodia in DA Rac1 transfected cells.....</i>	99
4.2.14.3	<i>Effect of dystroglycan deficiency on RhoA activity.....</i>	102
4.2.14.4	<i>Effect of dystroglycan deficiency on dominant negative Rho GTPases.....</i>	103
4.2.15	<i>Ezrin expression is upregulated but mislocalised in DG - fibroblasts....</i>	105
4.3	Discussion.....	107

Chapter 5: Investigating dystroglycan localisation during cytokinesis

5.1	Introduction.....	120
5.2	Results.....	124
5.2.1	<i>Dystroglycan localises to the cleavage furrow and midbody of dividing Ref52 fibroblasts.....</i>	124
5.2.2	<i>Dystroglycan-GFP localises to the cleavage furrow of stably-expressing Swiss 3T3 fibroblasts.....</i>	125
5.2.3	<i>Dystroglycan co-localises with ezrin in dividing Ref52 cells.....</i>	126
5.2.4	<i>Investigating the localisation of dystroglycan-GFP constructs during cytokinesis.....</i>	128
5.2.4.1	<i>Dystroglycan-GFP localisation in dividing HeLa cells.....</i>	130
5.2.4.2	<i>Myristolated-GFP does not localise to the cleavage furrow or midbody in dividing HeLa cells.....</i>	132
5.2.4.3	<i>Dystroglycan requires its C-terminal cytoplasmic tail for cleavage furrow localisation.....</i>	134

5.2.4.4	<i>Expression of the cytoplasmic tail of β-dystroglycan</i>	135
5.2.4.5	<i>Dystroglycan does not require ezrin binding for cleavage furrow localisation</i>	136
5.3	<i>Discussion</i>	138
Chapter 6:	Final Discussion	148
Appendix I:	Plasmid Maps	159
Appendix II:	DNA Constructs	161
Appendix III:	Cell lines and Primary Cells	162
Appendix IV:	Primary Antisera	163
Appendix V:	Secondary Antisera	164
Appendix VI:	Stock Solutions, Buffers and Media Compositions	165
Appendix VII:	RT-PCR Primers	169
Appendix VIII:	Genomic PCR Primers	169
Appendix IX:	Secondary Antisera Cross-reactivity	170
Appendix X:	Experimental Timeline	171
References		172
Publications		187

List of Figures

1.1	Dystroglycan structure and binding partners.....	10
3.1	Phase contrast images of DG -/- embryonic stem cells.....	52
3.2	Cellular morphology of DG -/- clones.....	53
3.3	Determination of cell lineage.....	54
3.4	Immunofluorescence staining of DG -/- fibroblasts.....	55
3.5	DG -/- cells expressed dystroglycan.....	56
3.6	Potential re-initiation of dystroglycan expression.....	58
3.7	RT-PCR analysis of DG -/- cells.....	60
3.8	Northern blot of <i>Dag1</i> mRNA.....	61
3.9	Detection of β -dystroglycan in 3C12 cells.....	62
3.10	Genomic PCR of DG -/- and 3C12 cells.....	64
4.1	Comparison of different shRNA sequences on dystroglycan knockdown.....	73
4.2	Phase contrast image of negative control.....	74
4.3	Quantification of dystroglycan expression following shRNA knockdown.....	75
4.4	Effect of dystroglycan knockdown on size and shape of Swiss 3T3 fibroblasts....	77
4.5	Effect of dystroglycan knockdown on number and size of focal adhesion complexes.....	79
4.6	Quantification of F-actin content.....	81
4.7	Dystroglycan deficiency does not affect cell motility.....	83
4.8	Dystroglycan deficiency does not affect cell polarity.....	85
4.9	DG - cells have a reduced proliferation rate.....	86
4.10	Effect of dystroglycan deficiency on mitotic index.....	88

4.11	Effect of dystroglycan deficiency on the degree of multinucleation.....	89
4.12	Cell cycle profile of DG + and DG - cells.....	92 - 93
4.13	Dystroglycan deficiency causes increased apoptosis.....	95
4.14	ERK-MAP kinase expression is reduced in DG - cells.....	96
4.15	Dystroglycan depletion reduces filopodia formation.....	99
4.16	Dystroglycan depletion reduces lamellipodia formation.....	101
4.17	Effect of dystroglycan depletion on RhoA activity.....	103
4.18	Effect of dystroglycan deficiency on dominant negative Rho GTPases.....	104
4.19	Effect of dystroglycan deficiency on ezrin expression and localisation.....	106
5.1	Changes in the cytoskeleton during cytokinesis.....	122
5.2	Endogenous dystroglycan localises to the cleavage furrow of Ref52 cells.....	125
5.3	Dystroglycan-GFP localises to the cleavage furrow of dividing Swiss 3T3 cells.....	126
5.4	Dystroglycan co-localises with ezrin at the cleavage furrow.....	127
5.5	Schematic representation of the dystroglycan-GFP fusion constructs.....	130
5.6	Dystroglycan-GFP concentrates at the midbody in dividing HeLa cells.....	131
5.7	Dystroglycan-GFP localises to the cleavage furrow of dividing HeLa cells.....	132
5.8	Myristoyl-tagged GFP does not localise to the cleavage furrow of dividing HeLa cells.....	133
5.9	Dystroglycan requires its cytoplasmic domain for cleavage furrow localisation.....	134
5.10	Myristoyl-tagged C β -GFP is correctly targeted to the plasma membrane in HeLa cells.....	136

5.11 Dystroglycan does not require ezrin binding for cleavage furrow
localisation.....137

5.12 Model of dystroglycan function at the cleavage furrow.....146

List of Tables

Table I Percentage DG + and DG - cells in each phase of the cell cycle following
synchronisation91

Acknowledgements

I would like to thank my supervisor, Professor Steve Winder, for the support and encouragement he has provided during my time as his student. His sound advice and enthusiasm has kept me motivated throughout the course of this research and for that I am sincerely grateful.

To all members of both Steve's lab and Kathryn Ayscough's lab, past and present, thank you for making the last few years so enjoyable. Special thanks go to Clare Batchelor, Heather Spence, Campbell Gourlay and Jeelan Moghraby for sharing their superb post-doc expertise! I am indebted to Rosaria, Sarah, Emma, Ellen and Tommy for their excellent technical support. To my fellow PhD students Jen, Oliver, Mike, Dana, Fiona, Mitch, Werner, Du Wei and Alistair, thank you for being fantastic lab mates! Thank you to the Biomedical Science Department at Sheffield University for a very warm welcome. I would also like to thank Mark Jones in the Sheffield University Flow Cytometry Facility for his patient and helpful advice and Dr Jane Limer in Peter Andrews's lab for generously supplying me with reagents. Thanks to the BBSRC for financial support and the University of Glasgow for awarding me this studentship.

Thanks to my good friends Jennifer Mackley for inspiration and helpful suggestions, Oliver 'Rodriguez' Thompson for his wit and confidence boosts and my housemates Caroline Parkin and Claire Badger for making Hunter's Bar a home from home! Big thanks to Skully for printing and binding my thesis!

Thank you to all my friends and family, especially Mum, Dad, Fiona and Nicholas for their love and encouragement throughout. Nick, your patience and emotional support has been wonderful and your ability to calm me down when I'm being a stress-head is incredible - thank you so much!

Declaration

I hereby declare that this thesis is my own work and that, to the best of my knowledge and belief, it contains no material previously published or written by another person unless otherwise stated. Information derived from the published or unpublished work of others has been acknowledged in the text and a list of references is given.

Jennifer R. Higginson B.Sc.(Hons)

Summary

Dystroglycan is a heterodimeric cell adhesion molecule consisting of α and β subunits, which links the actin cytoskeleton to the extracellular matrix. Dystroglycan has an important structural role and is integral for maintaining tissue integrity, but new avenues of research have implicated it in other roles within the cell due to its ability to bind a number of interacting proteins including cytoskeletal components and proteins involved in signal transduction. To elucidate the functions of dystroglycan at the cellular level, fibroblasts were differentiated from dystroglycan null embryonic stem cells. Analysis of these cells by western blot, however, showed them to be expressing dystroglycan and this was confirmed by RT-PCR, genomic PCR and northern blot. Subsequently, Swiss 3T3 fibroblasts with greater than 60% reduction in dystroglycan expression were generated by stable retroviral infection of a shRNA construct. Dystroglycan deficient cells were smaller and were found to have a reduction in cell-substrate adhesions, when compared to a control cell line. Dystroglycan deficiency did not affect cell motility or polarity in fibroblasts, but did result in a reduction in the rate of cell proliferation, which was thought to be the consequence of an increase in apoptosis. Dystroglycan deficiency also inhibited the formation of filopodia and lamellipodia in response to dominant active Cdc42 or Rac1 respectively, suggesting that it is an important mediator of Rho GTPase-mediated cytoskeletal rearrangements. This study has also identified a possible new function for dystroglycan during cytokinesis. Endogenous dystroglycan was localised to the cleavage furrow and midbody of dividing fibroblasts, where it was found to co-localise with the ERM family member, ezrin. Expression of mutated and truncated dystroglycan-GFP constructs in dividing HeLa cells revealed that the cytoplasmic domain is required for cleavage furrow localisation, but ezrin-binding is not. A model for dystroglycan function at the cleavage furrow is presented whereby dystroglycan recruits ezrin to the site of

furrow ingression and together they serve to tether the actomyosin contractile ring to the plasma membrane during cytokinesis. These findings provide further insight into the multifaceted functions of dystroglycan within the cell and also raised interesting questions about possible new roles for dystroglycan.

Abbreviations

AchR	- Acetylcholine receptor
AP	- Alkaline phosphatase
APS	- Ammonium persulphate
BCIP	- 5-Bromo-4-chloro-3'-indolyphosphate p-Toluidine salt
BrdU	- 5-Bromo-2-deoxyuridine
BSA	- Bovine serum albumin
CMD	- Congenital muscular dystrophy
DAPI	- 4', 6-Diamidino-2-phenylindole
DGC	- Dystrophin-glycoprotein complex
DIG	- Digoxigenin
DMD	- Duchenne muscular dystrophy
DMEM	- Dulbecco's Modified Eagle Medium
DNA	- Deoxyribonucleic acid
DRP	- Dystrophin-related protein
ECL	- Enhanced chemiluminescence
ECM	- Extracellular matrix
ERK	- Extracellular signal-regulated kinase
ERM	- Ezrin/Radixin/Moesin
ES cells	- Embryonic stem cells
FAK	- Focal adhesion kinase
FBS	- Fetal bovine serum
FCMD	- Fukuyama congenital muscular dystrophy
GFP	- Green fluorescent protein
GRB2	- Growth factor receptor bound protein 2

GTPases	- Guanosine triphosphatases
HEPES	- 4-(2-hydroxyethyl)-1-piperazineethanesulfonic acid
HRP	- Horseradish peroxidase
LGMD	- Limb-girdle muscular dystrophy
MAP	- Mitogen-activated protein
MEB	- Muscle-eye-brain disease
MEK	- MAP kinase kinase
MMP	- Matrix metalloproteinase
MTOC	- Microtubule organising centre
NBT	- Nitro blue tetrazolium chloride
NMJ	- Neuromuscular junction
PBS	- Phosphate buffered saline
PCR	- Polymerase chain reaction
PVDF	- Polyvinylidene fluoride
RISC	- RNA-induced silencing complex
RNA	- Ribonucleic acid
RNAi	- RNA interference
ROCK	- Rho kinase
RT-PCR	- Reverse transcription polymerase chain reaction
SDS-PAGE	- Sodium dodecyl (lauryl) sulfate-polyacrylamide gel electrophoresis
shRNA	- Short hairpin RNA
siRNA	- Small interfering RNA
TBST	- Tris-buffered saline/Tween 20
WWB	- Walker-Warburg syndrome

Chapter 1: Introduction

Chapter 1

Introduction

1.1 Introduction

Dystroglycan is a widely expressed transmembrane cell adhesion molecule that links the actin cytoskeleton to the extracellular matrix (Ervasti and Campbell, 1993). The dystroglycan gene is highly conserved in many different species, indicative that its product has a fundamentally important function. Much of the early research into dystroglycan was focussed on its role in the pathogenesis of neuromuscular diseases, however it is now known to be a highly versatile receptor influencing multiple cellular functions including early development, epithelial morphogenesis, signal transduction, cytoskeletal remodelling and cancer progression. The focus of this chapter will be current understanding of dystroglycan biosynthesis, structure and function.

1.2 The dystrophin-glycoprotein complex

Dystroglycan, or the dystrophin-associated glycoprotein (DAG), is a heterodimeric glycoprotein that was first identified in skeletal muscle as a constituent of the dystrophin-glycoprotein complex (DGC) (Ervasti et al., 1990). This complex is found on the sarcolemma and acts as a link between the cell cytoskeleton and the extracellular matrix (ECM) (Ervasti and Campbell, 1993). The DGC in muscle is a large multimeric protein complex consisting of the dystroglycan complex, sarcoglycan complex and sarcospan, which are transmembrane proteins, associating with dystrophin, syntrophins and dystrobrevin which are located on the inner surface of the sarcolemma.

The importance of dystroglycan arose from its association with dystrophin, the protein encoded by the Duchenne muscular dystrophy (DMD) gene. DMD is an X-linked genetic disease that causes progressive muscle wasting and eventually death due to cardiac

or respiratory failure. Dystrophin associates with actin in the cytoskeleton, and is missing or defective in DMD patients (Hoffman et al., 1987). To try to understand the molecular pathogenesis of muscular dystrophy, proteins associated with dystrophin were isolated and included a glycoprotein component which was found to be depleted in dystrophic muscle and *mdx* mice (which lack dystrophin) (Ervasti et al., 1990); this was later named dystroglycan (Ibraghimov-Beskrovnaya et al., 1992). The loss of one or more proteins from the DGC disrupts the link between the actin cytoskeleton and the ECM, which is essential for maintaining the structural integrity of the cell membrane. One function of dystroglycan in muscle cells is thought to be as a transmembrane linker that strengthens the sarcolemma as the muscle alternately contracts and relaxes (Ervasti and Campbell, 1993) and it is also thought to be involved in modulating muscle cell signalling (Batchelor and Winder, 2006).

1.3 Dystroglycan complex in non-muscle cells

Shortly after dystroglycan was cloned from skeletal muscle, a study into a laminin-binding protein found in the brain, called cranin, was shown to have identical sequence homology to dystroglycan (Smalheiser and Kim, 1995). It is now well established that dystroglycan is widely expressed and has been found in every vertebrate tissue and cell type studied (Durbeej et al., 1998). Since dystrophin expression is restricted to muscle and neuronal tissue, dystroglycan binds to truncated forms of dystrophin or dystrophin homologues in non-muscle cells. Several truncated forms of dystrophin exist; these are alternatively spliced isoforms of dystrophin (Sadoulet-Puccio and Kunkel, 1996). Dystrophin also associates with utrophin, a dystrophin homologue sharing approximately 69% sequence homology. Utrophin was identified soon after dystrophin was sequenced, because its cDNA sequence was found to be very similar to the dystrophin gene. Utrophin was

originally called dystrophin-related protein (DRP) (Love et al., 1991), but was renamed after it was cloned and sequenced to reflect its ubiquitous expression (Tinsley et al., 1992). Utrophin was also shown to associate with dystroglycan in cells that did not contain dystrophin (James et al., 1996).

The dystroglycan complex in non-muscle cells is similar to the DGC in muscle cells in that it provides a link between the ECM and the actin cytoskeleton, however, the membrane complex itself contains fewer proteins (Durbeej and Campbell, 1999; Winder, 1997).

1.4 Dystroglycan biosynthesis and protein structure

1.4.1 Dystroglycan gene

Dystroglycan was initially cloned and sequenced from rabbit skeletal muscle in 1992 and was shown to be a heterodimer consisting of α and β subunits. α -Dystroglycan is a laminin receptor at its N-terminus and binds β -dystroglycan at its C-terminus through a non-covalent interaction. β -Dystroglycan is a transmembrane protein that binds α -dystroglycan at its N-terminus and dystrophin or utrophin at its C-terminus (Figure 1.1). The primary sequence of the gene encoding α and β dystroglycan was elucidated using complimentary DNA cloning (Ibraghimov-Beskrovnaya et al., 1992). This revealed that both subunits are encoded by a single gene, DAG1, containing two exons, separated by a large intron. Cloning of human dystroglycan followed a short time later and was found to have 93% sequence homology to the rabbit gene (Ibraghimov-Beskrovnaya et al., 1993). Dystroglycan has since been cloned from a variety of other species including mouse (Gorecki et al., 1994), *Torpedo* (Bowe et al., 1994), zebrafish (Parsons et al., 2002), *Caenorhabditis elegans* (Grisoni et al., 2002) and *Drosophila melanogaster* (Deng et al.,

2003). Sequence analysis has shown that the dystroglycan gene is highly conserved among vertebrates, which may reflect a fundamental conserved role for this protein.

1.4.2 Pro-peptide biosynthesis and processing

DAG1 encodes a single 5.8 kb mRNA transcript, which is translated into a 160kDa precursor propeptide (Holt et al., 2000) and proteolytically cleaved after residue 653 by an unknown protease to form α and β dystroglycan (Deyst et al., 1995; Smalheiser and Kim, 1995) (Figure 1.1 A). Prior to cleavage, the dystroglycan propeptide is glycosylated within the endoplasmic reticulum and golgi. The importance of glycosylation at this stage is not clear since separate studies have led to conflicting results as to whether glycosylation is required for cleavage and targeting of the precursor propeptide. One group showed that glycosylation was not required for cleavage but was required for membrane localisation, whereas a different study has shown the opposite result whereby glycosylation was required for cleavage but did not completely abolish membrane localisation (Esapa et al., 2003; Holt et al., 2000).

1.4.3 Structure of α -dystroglycan

The large dystroglycan subunit, α -dystroglycan, is a heavily glycosylated peripheral membrane protein that associates with components of the extracellular matrix via carbohydrate moieties and β -dystroglycan through a non-covalent interaction at its C-terminus (Figure 1.1 B). The predicted molecular weight from the primary sequence of α -dystroglycan is 72 kDa, however its actual molecular weight ranges from 120 - 156 kDa in different tissues due to tissue specific glycosylation (Durbeej et al., 1998). α -Dystroglycan has been shown to consist of two globular domains containing several sites for *N*-linked

glycosylation and glycosaminoglycan addition, connected by a central mucin-like region that is highly *O*-glycosylated (Brancaccio et al., 1995; Brancaccio et al., 1997).

1.4.4 Structure of β -dystroglycan

β -Dystroglycan is a 43 kDa type I transmembrane glycoprotein containing an N-terminal extracellular domain, a short transmembrane region and an unstructured C-terminal cytoplasmic tail (Figure 1.1 B). The N-terminal extracellular region forms a strong non-covalent interaction with α -dystroglycan. This region has been shown to have a random coil structure and is capable of binding α -dystroglycan in the absence of carbohydrate groups (Di Stasio et al., 1999). The extracellular domain of β -dystroglycan was found to contain one potential *N*-linked glycosylation site and three putative *O*-linked glycosylation sites in mouse, although two of these sites are not conserved in other mammals (Di Stasio et al., 1999; Henry and Campbell, 1996). Intracellularly, β -dystroglycan has an unstructured proline-rich cytoplasmic tail containing multiple binding sites for interacting proteins.

1.5 Dystroglycan binding partners

A multitude of interacting partners for dystroglycan have been identified and the list is still growing, emphasising the complexity of dystroglycan functions. These interactions do not all occur at the same time, in fact many share the same binding region (Figure 1.1 B), therefore binding to dystroglycan is likely to be highly regulated by tissue-specific expression and post-translational protein modifications.

1.5.1 α -Dystroglycan interactions

α -Dystroglycan is a receptor for a number of extracellular matrix components, such as laminin (Yamada et al., 1996) agrin (Yamada et al., 1996), perlecan (Peng et al., 1998), neuexins (Sugita et al., 2001) and biglycan (Bowe et al., 2000). These interactions do not all occur together; rather they are regulated by both tissue-specific expression of the ECM components and differential glycosylation of α -dystroglycan. Laminin (α 1 and α 2 chain), agrin, perlecan and neuexins bind to the carbohydrate moieties of sialylated *O*-linked oligosaccharides that are located on the α -dystroglycan mucin-like region (Chiba et al., 1997). These interactions are mediated by laminin G domain modules on the glycoproteins and are calcium-dependent (Hohenester et al., 1999; Tisi et al., 2000). Biglycan binds to the N-terminal globular region and this interaction is not dependent upon glycosylation. A binding domain contained within the C-terminal globular domain of α -Dystroglycan associates with the extracellular N-terminal region of β -dystroglycan through a tight non-covalent interaction that is not dependent upon glycosylation of either subunit (Bozzi et al., 2003; Di Stasio et al., 1999; Sciandra et al., 2001).

1.5.2 β -Dystroglycan interactions

1.5.2.1 Dystrophin and utrophin

The β -dystroglycan cytoplasmic tail contains motifs capable of interacting with a plethora of cytoskeletal and cytosolic proteins due to its proline-rich sequence. In particular, a binding motif at the extreme C-terminus of the cytoplasmic tail can interact with WW domain containing proteins, such as dystrophin and utrophin (Jung et al., 1995; Tommasi di Vignano et al., 2000). Dystrophin and utrophin contain a single type II WW domain in their cysteine-rich region. This is a globular region of ~38-40 amino acids with two highly conserved tryptophan residues spaced 20-22 residues apart (Sudol, 1996). Type II WW

domains recognise ligands with a P-P-x-Y motif (where x is any amino acid) (Chen et al., 1997). Type II WW domains have been likened to SH3 domains since they both bind to polyproline ligands. The cytoplasmic tail of β -dystroglycan contains two of these motifs, one starting at residue 828 (P-P-E-Y) and another at residue 889 (P-P-P-Y) (Ilsley et al., 2002). The latter of these two motifs, which is located in the last 10-15 amino acids of the cytoplasmic tail, was shown to be necessary but not sufficient for interaction with dystrophin (Jung et al., 1995). This interaction also requires an EF-hand motif of dystrophin to bind to β -dystroglycan (Rentschler et al., 1999). The crystal structure of the WW domain-containing fragment of dystrophin interacting with β -dystroglycan helped to explain the role of the EF-hand region. This showed that the dystrophin WW domain is embedded between two EF-hand regions and one of these is required to stabilise the N-terminal of the P-P-P-Y motif (Huang et al., 2000). A closer analysis of the dystrophin (Ilsley et al., 2001) and utrophin (James et al., 2000) β -dystroglycan binding region showed that the ZZ domain, a zinc finger region, (Ponting et al., 1996) close to the EF-hand is also required for the interaction.

1.5.2.2 Caveolin-3

Caveolin-3, the main protein component of caveolae membranes in muscle cells, contains a WW-domain and associates with β -dystroglycan by binding to the same P-P-P-Y motif as dystrophin. Caveolin-3 competes with dystrophin for this binding site and the function of this may be to regulate the recruitment of dystrophin to the sarcolemma (Sotgia et al., 2000). Unlike dystrophin, caveolin-3 can interact with β -dystroglycan when the P-P-P-Y is tyrosine phosphorylated. This phosphorylation event could switch the binding partner of β -dystroglycan from dystrophin to caveolin-3 (Ilsley et al., 2001). Mutations in the caveolin-3 gene result in a form of limb-girdle muscular dystrophy (LGMD1C) (Minetti et

al., 1998). When investigating the function of caveolin-3, it was found that overexpression in mice gives a DMD phenotype, this supports the theory that caveolin-3 competes for the dystrophin binding site (Galbiati et al., 2000).

1.5.2.3 GRB2

β -Dystroglycan directly interacts with GRB2 (Growth factor receptor bound protein 2), which is an adaptor protein involved in the initiation of the Ras-MAP kinase signal transduction cascade and the control of cytoskeletal organisation. This protein is composed of an SH2 domain sandwiched in between two SH3 domains (Lowenstein et al., 1992). In 1995, Yang et al showed that in brain and skeletal muscle, β -dystroglycan interacts with an SH3 domain of GRB2 via its C-terminal proline-rich region (Yang et al., 1995). Closer examination of the β -dystroglycan-GRB2 interaction using a range of binding assays identified the region of β -dystroglycan that binds to the SH3 domain of GRB2 as residues 891-894 (P-Y-V-P), which overlaps with the P-P-P-Y dystrophin/utrophin binding motif (Russo et al., 2000).

1.5.2.4 Other proteins

β -Dystroglycan interacts with components of the ERK-MAP kinase signaling pathway through poly-proline rich motifs (Spence et al., 2004b). Furthermore, β -dystroglycan associates with the cytoskeletal linker protein, ezrin through a binding motif located at the juxtamembrane region of the β -dystroglycan cytoplasmic tail (Spence et al., 2004a). The cytoplasmic protein rapsyn associates with dystroglycan via a binding motif also in the juxtamembrane position (Bartoli et al., 2001; Cartaud et al., 1998). The β -dystroglycan cytoplasmic tail has also been shown to contain binding sites capable of interacting directly with F-actin (Chen et al., 2003). Two other proteins, dystrobrevin and DRP2,

associate with dystroglycan since their C-terminal regions share substantial sequence homology with the dystroglycan-binding region of dystrophin. These are products of distinct genes, but their functions are poorly understood (Blake et al., 1996; Chung and Campanelli, 1999; Roberts et al., 1996).

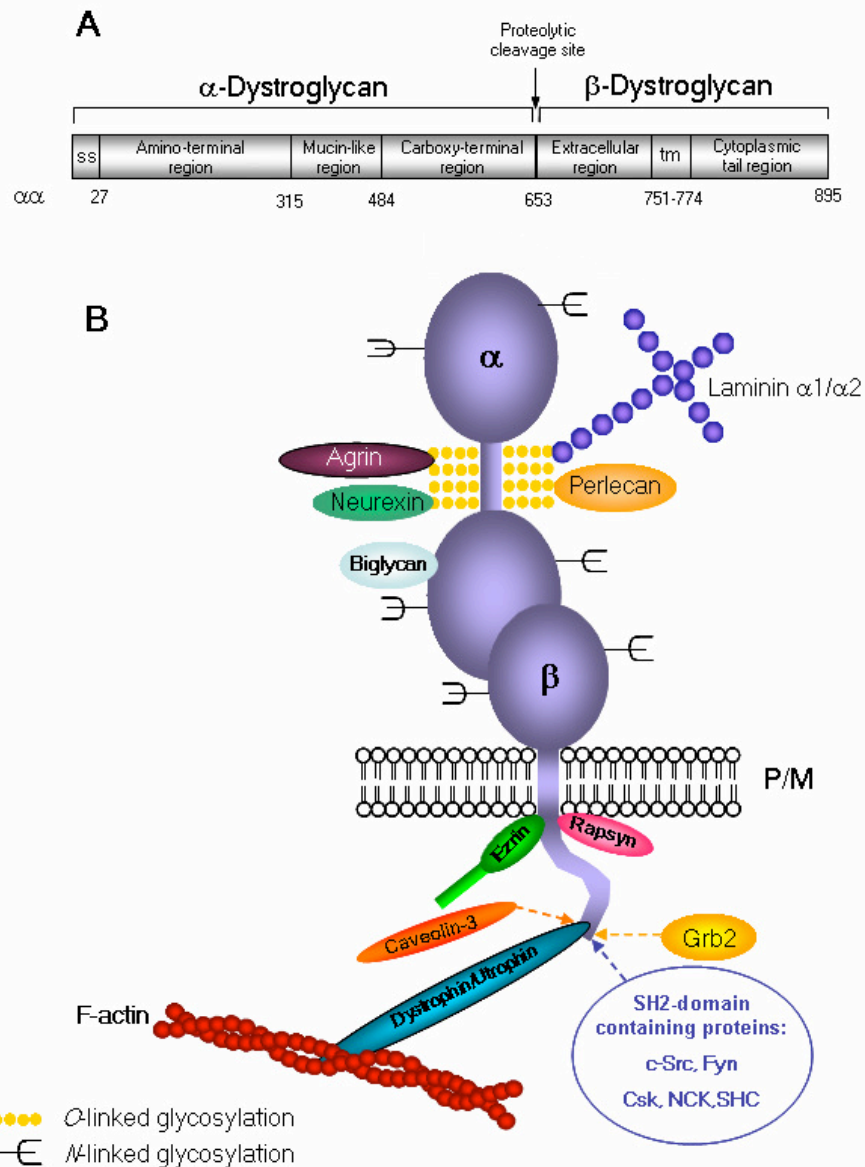


Figure 1.1 Dystroglycan structure and binding partners. **A:** Structure of dystroglycan pro-peptide. $\alpha\alpha$ = amino acid residue number; SS = signal sequence. **B:** Schematic representation of the dystroglycan complex at the plasma membrane (P/M). α -Dystroglycan is a dumbbell-shaped peripheral membrane protein that is highly decorated with carbohydrate residues (O- and N-linked glycosylation) that binds to ECM components and β -dystroglycan. β -Dystroglycan is an integral membrane protein with a proline-rich cytoplasmic tail containing binding sites for a multitude of cytoskeletal and cytosolic binding partners. The dystroglycan interacting proteins illustrated are unlikely to all bind dystroglycan at the same time; in fact several compete for the same binding region. Binding is regulated by tissue-specific expression and protein modifications, such as differential glycosylation of α -dystroglycan or phosphorylation of β -dystroglycan.

1.5.3 Dystroglycan phosphorylation

In non-muscle cells, tyrosine phosphorylation of the β -dystroglycan P-P-x-Y motif in response to cell adhesion breaks the link between β -dystroglycan and utrophin. This in turn releases the dystroglycan complex from the underlying cytoskeleton, which may be important for processes such as cell adhesion, migration, proliferation and differentiation (James et al., 2000). The adhesion-dependent phosphorylation of dystroglycan has not yet been demonstrated in muscle cells (Ilsley et al., 2002), but dystroglycan was shown to be tyrosine phosphorylated using the tyrosine phosphatase inhibitor, peroxyvanadate (Ilsley et al., 2001).

The interaction between β -dystroglycan and the WW domain of dystrophin or utrophin is regulated by phosphorylation of tyrosine 892 in the P-P-P-Y motif. When this tyrosine is phosphorylated, β -dystroglycan cannot interact with the WW domain of dystrophin (Ilsley et al., 2001) or utrophin (James et al., 2000). The reason for the effect of phosphorylation can be explained using the crystal structure of dystrophin bound to β -dystroglycan. In this structure, the extreme C-terminus of the cytoplasmic tail fits into a hydrophobic pocket produced by the EF-hand domains (Huang et al., 2000). Following phosphorylation of the tyrosine residue contained within the P-P-P-Y motif, the bulky phosphate group prevents the motif from entering this pocket and an essential hydrogen bond cannot be formed (James et al., 2000).

In v-Src transformed cells, it was discovered that the tyrosine-phosphorylation of β -dystroglycan was constitutively elevated. This was reconstituted *in vivo* by transiently co-expressing wild type c-Src with a fusion protein containing β -dystroglycan. This experiment showed that Src-induced tyrosine phosphorylation occurred on the P-P-x-Y motif of β -dystroglycan. Using a GST- β -dystroglycan fusion protein, five different SH2 domain-containing proteins that interact with β -dystroglycan in a phosphorylation-

dependent manner were identified. These proteins were c-Src, Fyn, Csk, NCK and SHC (Sotgia et al., 2001). Adhesion-dependent tyrosine phosphorylation of the P-P-x-Y motif may act as a binary regulatory switch to inhibit the binding of certain WW-domain containing proteins, for example dystrophin, and promote the recruitment of other WW-domain containing proteins or SH2 and SH3 domain-containing proteins. This dynamic regulation of the DGC is not fully understood, but is undoubtedly very important for normal tissue function, since the loss of several different components have been shown to result in a muscular dystrophy phenotype (Sotgia et al., 2001). In a recent study, Sotgia and colleagues have shown that tyrosine phosphorylation of β -dystroglycan causes it to be internalised into intracellular vesicles, which were shown to be recycling endosomes. This suggests a mechanism by which dystroglycan function at the membrane might be regulated (Sotgia et al., 2003).

1.6 Development

1.6.1 Basement membrane formation

A dystroglycan knockout mouse (DAG1 null) model was generated in order to gain further understanding of the function of dystroglycan in development. The mice were found to be embryonic lethal, due to the failure to produce an early basement membrane (Reichert's membrane) (Williamson et al., 1997). The basement membrane is an ordered lattice of extracellular matrix proteins that lies in direct contact with cell surfaces. α -Dystroglycan is a receptor for laminin-1, a major component of basement membranes (Ervasti and Campbell, 1993). The role of dystroglycan in basement membrane assembly was further investigated using DAG1 null embryonic stem (ES) cells and embryoid bodies derived from them. Dystroglycan was found to be required for initiating the self-assembly of the ECM by organising laminin on the surface of the cell. One study found that in DAG1 null

embryoid bodies, the basement membrane was severely disrupted and in undifferentiated DAG1 null ES cells, laminin-1 did not form clusters on the cell surface as seen in wild-type ES cells. Re-introduction of dystroglycan rescued the ability of the DAG1 null embryoid bodies to form a basement membrane and DAG1 null ES cells to bind soluble laminin and organise it on the cell surface (Henry and Campbell, 1998). This study was, however, disputed by a separate investigation into basement membrane assembly in DAG1 null embryoid bodies. In the later study, dystroglycan was not found to be essential for the development of the embryonal basement membrane adjacent to the epiblast, as had been reported earlier (Li et al., 2002). This later study did not, however, contradict the finding that the DAG1 knockout mouse could not form the Reichert's membrane, since this occurs at an earlier stage of development (Williamson et al., 1997). Conditional deletion of dystroglycan in mouse brain resulted in partial disruption of the pial basement membrane (Moore et al., 2002), whereas conditional deletion of dystroglycan in skeletal muscle of mice did not affect basement membrane formation (Cote et al., 1999). The importance of dystroglycan to basement membrane assembly is therefore still under question.

1.6.2 Muscle

Due to the embryonic lethality of the DAG1 knockout mouse, further investigation into dystroglycan deficiency in muscle was undertaken using different methods to deplete dystroglycan expression. Cote *et al* used DAG1 null ES cells to generate chimaeric mice that had skeletal muscle lacking dystroglycan. These mice exhibited a muscular dystrophy phenotype and disrupted neuromuscular synapses, but dystroglycan was not found to be required for basement membrane formation in skeletal muscle (Cote et al., 1999). Another study in which dystroglycan was selectively deleted from mouse skeletal muscle produced mice with a surprisingly mild dystrophic phenotype. This was found to be due to the

partial regeneration of muscle tissue by satellite cells still expressing dystroglycan. Satellite cells are quiescent adult stem cells of myogenic lineage that lie adjacent to the muscle fibre sarcolemma beneath the basal lamina. These cells are triggered to proliferate and differentiate into myoblasts in order to repair muscle fibres in response to injury. The results obtained from this study suggested that dystroglycan is important for muscle cell regeneration (Cohn et al., 2002). Reduction of dystroglycan in mouse myotubes by RNAi resulted in a reduced ability of the cells to bind laminin accompanied by a gradual loss of cells caused by an increase in apoptosis (Montanaro et al., 1999) and a study in which α -dystroglycan was prevented from binding to laminin by antibody interference induced a muscular dystrophy phenotype in primary mouse muscle cell cultures (Brown et al., 1999).

1.6.3 Neuromuscular Junction

Dystroglycan is found abundantly at the neuromuscular junction (NMJ) where it is important during synaptogenesis for the formation of the basement membrane and also for the maintenance of acetylcholine receptor aggregates (Jacobson et al., 2001; Jacobson et al., 1998). Dystroglycan associates with agrin (Gee et al., 1994; Sugiyama et al., 1994), a proteoglycan component of the ECM that is important during embryogenesis for the development of the NMJ and the aggregation of acetylcholine receptors (AChR) during synaptogenesis (Nitkin et al., 1987). Intracellularly, β -dystroglycan associates with rapsyn (Apel et al., 1995; Bartoli et al., 2001; Cartaud et al., 1998), which is involved in agrin-induced AChR clustering via muscle-specific kinase (MuSK), a receptor tyrosine kinase. The importance of dystroglycan at the NMJ has been exemplified in studies investigating dystroglycan-deficient muscle cells, which were unable to aggregate AChR (Jacobson et al., 2001) and in the dystroglycan-deficient mouse which had disrupted neuromuscular synapses (Cote et al., 1999).

1.6.4 Epithelial Morphogenesis

Dystroglycan expression was found to be elevated during branching epithelial morphogenesis of the developing mouse kidney, salivary gland and lung (Durbeej et al., 1995). This process involves the differentiation of mesenchymal cells into epithelial cells and requires close interaction between the cell and the basement membrane in order to allow for the developing epithelial cell to polarise correctly. Binding of dystroglycan to laminin-1 was found to be crucial because inhibition of this interaction, since using antibodies to block the laminin-1 binding site on α -dystroglycan inhibited the process (Durbeej et al., 1995; Durbeej et al., 2001). Furthermore, dystroglycan expression was found to increase during lactogenesis of mammary epithelial cells and reduction of dystroglycan by RNAi inhibited differentiation (Sgambato et al., 2006).

1.6.5 Central and peripheral nervous system

Selective deletion of the dystroglycan gene in mouse brain led to severe brain malformations resembling those caused by congenital muscular dystrophies (CMD) such as Fukuyama CMD (FCMD), muscle-eye-brain disease (MEB) and Walker-Warburg syndrome (Moore et al., 2002). The mutations causing these diseases are thought to be in genes encoding glycosyltransferases, which are required for the correct glycosylation of α -dystroglycan.

Dystroglycan function has also been shown to extend to the peripheral nerve system in a study in which dystroglycan was selectively deleted in Schwann cells, which are responsible for creating the myelin sheaths surrounding axons. Dystroglycan localises to the outer membrane of Schwann cells, opposing the basal lamina, where it associates with laminin and agrin in the ECM (Yamada et al., 1996). Loss of dystroglycan in Schwann cells caused there to be a decrease in nerve conduction and abnormal myelination

accompanied by a reduction in Na⁺ channel density and disorganised microvilli at the nodes of Ranvier (Saito et al., 2003).

1.7 Dystroglycan depletion in model organisms

Dystroglycan homologues have been identified in a number of different species and loss of function studies in several model organisms have provided further insight into dystroglycan function. Removal of dystroglycan expression in zebrafish using antisense morpholino oligonucleotides showed that it was not required for early embryogenesis, in contrast to the phenotype seen in the mouse model. Unlike mice, zebrafish do not require early basement membrane formation, this is only important once organogenesis is underway. At later stages of development, however, a muscular dystrophy phenotype emerged, manifested by loss of muscle integrity and cell death by necrosis and apoptosis (Parsons et al., 2002).

Dystroglycan deficiency has also been studied in the model organism, *Drosophila melanogaster* using RNAi and mosaic analysis to knock down dystroglycan expression. The focus of this research was to investigate the role of dystroglycan in polarity determination. Dystroglycan expression was depleted in follicle and imaginal disc epithelial cells and was found to disrupt apicobasal polarity, shown by the mislocalisation of polarity markers. At early stages of drosophila embryogenesis, anteroposterior polarity is essential for the correct development of the drosophila oocyte and involved extensive cytoskeletal rearrangements. In the early oocyte, the microtubule organising centre (MTOC) is located at the anterior of the oocyte, which moves to a posterior position as development progresses. Dystroglycan depletion in the early oocyte disrupted this rearrangement suggesting that it is involved in the maintenance of anteroposterior polarity in the developing drosophila oocyte. Moreover, dystroglycan depletion in follicle cell

epithelium was found to result in the disruption of cortical F-actin in neighbouring wild-type cells, suggesting that dystroglycan also contributes to cell-cell communication (Deng et al., 2003).

Dystroglycan depletion in the retina of *Xenopus laevis* using antisense morpholino oligonucleotides highlighted the importance of dystroglycan during eye development. Dystroglycan depletion resulted in a decrease in the overall size of the eye, which was found to be a result of increased apoptosis, disruptions to the basement membrane and eye malformations similar to those seen in CMD (Lunardi et al., 2006).

1.8 Signal transduction

In addition to its structural role, dystroglycan is now thought to play an important role in signal transduction. Due to its wide expression pattern and abundance of interacting proteins, dystroglycan is likely to function at the intersection of multiple cell signalling pathways.

1.8.1 SH2 and SH3 domain containing signalling molecules

There is evidence that β -dystroglycan, in association with GRB2, recruits the non-receptor tyrosine kinase, FAK (focal adhesion kinase). FAK is involved in regulating focal adhesion assembly, which are areas of close contact between the cytoskeleton and the ECM allowing for signal transduction to occur between the cell and its surroundings influencing cell motility and cytoskeletal reorganisation. In bovine brain synaptosomes, GRB2 bound to FAK, was isolated together with the dystroglycan complex. There was no evidence of a direct interaction between β -dystroglycan and FAK, suggesting that GRB2 links FAK to the dystroglycan complex (Cavaldesi et al., 1999). Interestingly, dystroglycan and utrophin have both been shown to localise to focal adhesions, suggesting that dystroglycan may be important for mediating signal transduction through focal

adhesion complexes in a manner similar to integrins (Belkin and Burridge, 1995; Belkin and Burridge, 1995; Belkin and Smalheiser, 1996; James et al., 1996; James et al., 2000; Khurana et al., 1995; Spence et al., 2004b).

The β -dystroglycan cytoplasmic tail has also been shown to interact with the SH2-domain containing signalling molecules c-Src, Fyn, Csk, NCK and SHC in a phosphorylation-dependent manner but consequences of these interactions have not yet been elucidated (Sotgia et al., 2001).

1.8.2 ERK-MAP kinase signalling

Dystroglycan has been implicated in modulating the ERK-MAP kinase signalling cascade, a pivotal signal transduction pathway that regulates diverse cellular functions, such as gene expression, mitosis, differentiation and cell survival. Dystroglycan was found to have an inhibitory effect on the $\alpha 6 \beta 1$ integrin-mediated activation of the ERK-MAP kinase pathway following laminin binding in epithelial cells, suggesting that dystroglycan is involved in regulating ERK-MAP kinase signalling in response to cell adhesion (Ferletta et al., 2003). The involvement of dystroglycan in ERK-MAP kinase signalling was further substantiated with the finding that the cytoplasmic tail of β -dystroglycan directly associates with two of its components, MEK2 (MAP kinase kinase 2) and the activated form of its downstream effector, ERK. Dystroglycan was not found to be a substrate for ERK and did not affect the activity of MEK on ERK; rather its function appears to be to act as a membrane scaffold for these proteins. Interestingly, dystroglycan was found to localise with MEK and ERK in different cellular structures: dystroglycan localised with active ERK to focal adhesions and with MEK to membrane ruffles. This suggests a possible mechanism for how dystroglycan may be involved in regulating the activation of ERK-MAP kinase signalling, whereby sequestration by dystroglycan of MEK and ERK to

separate cellular compartments may serve to activate the MAP kinase cascade under different circumstances (Spence et al., 2004b). A separate study, looking at the effects of mechanical stretch on lung epithelia found that, upon the induction of cyclic stretch, dystroglycan binding to laminin-6 transduced a mechanical signal that activated MAP-kinase signalling. Furthermore, depletion of dystroglycan by RNAi or perturbation of the dystroglycan-laminin interaction by antibody binding significantly reduced MAP-kinase activation in rat alveolar epithelial cells (Jones et al., 2005). A separate study in which dystroglycan was downregulated by RNAi in mouse mammary epithelial cells reported an increase in phosphorylated ERK and MEK compared to control cells (Sgambato et al., 2006). Research into the role that dystroglycan plays in mediating ERK-MAP kinase signalling is still in its infancy, nonetheless it is clear that dystroglycan serves an important function in regulating this complex pathway.

1.8.3 PI3K/AKT signalling

Dystroglycan has been implicated in the regulation of the phosphoinositide 3-kinase (PI3K)/protein kinase B (AKT) pathway, which mediates a number of cellular processes including cell proliferation, motility and survival. No direct interaction between dystroglycan and components of this pathway have been identified, however, perturbation of the dystroglycan-laminin interaction in myoblasts was found to disrupt PI3K/AKT signalling resulting in increased apoptosis (Langenbach and Rando, 2002). Knockdown of dystroglycan expression in several different cell types has also been shown to result in increased apoptosis (Lunardi et al., 2006; Montanaro et al., 1999; Parsons et al., 2002; Sgambato et al., 2006).

1.8.4 ERM proteins and Rho GTPase signalling

Dystroglycan has recently been found to interact with the ERM (ezrin-radixin-moesin) family member, ezrin, via a juxtamembrane binding motif (Spence et al., 2004a). The ERM proteins are cytoskeletal linkers that connect the actin cytoskeleton to membrane-bound proteins and are involved in the mediation of cell signalling (Tsukita and Yonemura, 1999). The interaction between dystroglycan and ezrin was shown to be important for the formation of filopodia, previously reported to be induced upon dystroglycan overexpression (Chen et al., 2003). This filopodia phenotype was also found to be dependent upon the activity of the Rho-GTPase family member, Cdc42 (Spence et al., 2004a). Rho, Rac and Cdc42 are members of the Ras-related superfamily of small GTPases (guanosine triphosphatases) and link membrane receptors to signal transduction pathways that induce changes in the actin cytoskeleton (Nobes and Hall, 1995). A recent study into the mechanism by which dystroglycan induces filopodia formation showed that the cytoplasmic tail of β -dystroglycan bound to ezrin recruits the GEF (GDP/GTP exchange factor), Dbl, an upstream activator of Cdc42 and Rho, which can then drive localised Cdc42 activation leading to the induction of filopodial protrusions on the membrane surface (Batchelor et al., 2007). Concurrent with this study, dystroglycan was shown to co-localise with moesin in microvilli structures in the nodes of Ranvier, found in Schwann cells of the peripheral nerve, and selective deletion of dystroglycan caused the microvilli to be disrupted (Saito et al., 2003). This is another example of dystroglycan functioning as a scaffold molecule for the recruitment of signalling molecules to the membrane, where they can exert their effects.

A study looking at the effects of cellular signalling upon reduction of the DGC in muscle atrophy supports the theory that there is a link between dystroglycan and Rho GTPase signalling. In rat skeletal muscle atrophy, members of the DGC, including β -

dystroglycan, were found to be reduced with a simultaneous reduction in the activity of the small GTPases (Chockalingam et al., 2002).

1.9 Dystroglycan and disease

1.9.1 Duchenne muscular dystrophy and secondary dystroglycanopathies

Duchenne muscular dystrophy is caused by mutations in the dystrophin gene and disassembly of the DGC including loss of dystroglycan from the sarcolemma occurs as a consequence (Hoffman et al., 1987; Ibraghimov-Beskrovnaya et al., 1992).

There have been no human diseases identified that are caused by primary mutations in the dystroglycan gene, however defective post-translational processing of dystroglycan implicates it in the pathogenesis of several forms of human congenital muscular dystrophies. These diseases are caused by mutations in genes encoding known or putative glycosyltransferases whose function is to *O*-glycosylate α -dystroglycan during post-translational processing. In the disease state, α -dystroglycan is hypoglycosylated and as a result loses its ability to bind components of the ECM, such as laminin, perlecan, agrin and neurexins which normally associate with its heavily *O*-glycosylated mucin-like region. Fukuyama CMD (FCMD), muscle-eye-brain disease (MEB), Walker-Warburg syndrome (WWS) and congenital muscular dystrophies types 1C and 1D (MDC1C and MDC1D) are all congenital muscular dystrophies caused by mutations in glycosyltransferases such as POMT1, POMT2, POMGnT1, LARGE or putative glycosyltransferases fukutin and FKRP (Beltran-Valero de Bernabe et al., 2002; Brockington et al., 2001; Kobayashi et al., 1998; Longman et al., 2003; Yoshida et al., 2001). Although the pathology of the disease is caused by α -dystroglycan loss of function, these diseases are sometimes referred to as secondary dystroglycanopathies since the mutations are not contained within the dystroglycan gene itself (Michele et al., 2002). The Large^{myd} mouse has a spontaneous

mutation in the gene encoding LARGE and is a useful model system for studying the human disease, MDC1D (Grewal et al., 2001). Recently, it has been found that overexpression of LARGE rescues the dystrophic phenotype in Large^{myd} mice. Moreover, overexpression of LARGE in cells from patients with CMD caused by mutations in other glycosyltransferases also resulted in a functional hyperglycosylated α -dystroglycan capable of binding extracellular ligands (Barresi et al., 2004). This has led to the suggestion that LARGE could be a potential therapeutic target for dystroglycanopathies and research into this area is ongoing.

1.9.2 Cancer

Aside from its involvement in the pathogenesis of neuromuscular disease, dystroglycan has also been implicated in the development of epithelial cancers. Adhesion molecules such as dystroglycan and integrins mediate cell-cell and cell-ECM interactions and correct control of these interactions is vital for maintaining tissue integrity. Adhesion molecules not only tether the cell to the surrounding matrix, but also act as modulators of the cytoskeleton and signalling cascades affecting growth and differentiation of the cell. Deregulation of cell-ECM interactions is a hallmark of cancer progression and promotes tumour cell metastasis. As previously discussed, dystroglycan is important in determining polarity, morphogenesis and basement membrane interactions in epithelial cells (Sections 1.6-1.7). Recently, several groups have reported that dystroglycan expression is reduced or lost in a number of cancer cell lines and primary tumours (Henry et al., 2001; Jing et al., 2004; Losasso et al., 2000; Muschler et al., 2002; Sgambato et al., 2003; Sgambato et al., 2006). Furthermore, dystroglycan expression has been shown to be elevated in vascular endothelial cells during formation of new blood vessels (angiogenesis) in malignant tumours compared to vascular endothelial cells in normal tissue, but the significance of this and the molecular mechanisms involved are not yet understood (Hosokawa et al., 2002).

Immunohistochemical staining of tissue sections obtained from breast and prostate primary tumours revealed a marked reduction in dystroglycan expression (Henry et al., 2001). Biochemical analysis of dystroglycan expression in a variety of cancer cell lines and tumours from breast, prostate, colon, cervix and oral squamous cell carcinomas revealed that α -dystroglycan protein expression was undetectable in the majority, resulting in the loss of laminin-binding (Jing et al., 2004; Losasso et al., 2000; Muschler et al., 2002; Sgambato et al., 2003; Sgambato et al., 2006). Reduction of β -dystroglycan protein expression has also been reported following western analysis of both tumour samples and cancer cell lines. The reduced expression of 43 kDa β -dystroglycan was often accompanied by the increased incidence of a ~30 kDa β -dystroglycan band (Jing et al., 2004; Losasso et al., 2000; Muschler et al., 2002; Sgambato et al., 2003). RT-PCR analysis showed that dystroglycan mRNA levels did not reflect the reduction in protein expression (Jing et al., 2004; Sgambato et al., 2003) and there was no evidence of alternative spliced forms of β -dystroglycan, concluding that production of the ~30 kDa β -dystroglycan must occur at the post-transcriptional level (Losasso et al., 2000). The ~30 kDa β -dystroglycan peptide was found to be the proteolytic product of membrane-associated matrix metalloproteinases (MMPs), which cleave the extracellular portion of β -dystroglycan leaving the transmembrane and cytoplasmic regions intact (Losasso et al., 2000; Yamada et al., 2001). A study using specific inhibitors to investigate this proteolytic event identified MMP-2 and MMP-9 as being important for β -dystroglycan cleavage (Zhong et al., 2006) and treatment of cell lines with MMP inhibitors decreased the appearance of ~30 kDa β -dystroglycan (Herzog et al., 2004). The loss of the extracellular portion of β -dystroglycan causes the disintegration of the dystroglycan complex by simultaneously releasing α -dystroglycan from the cell surface and, therefore, disrupting the link with the ECM. This would be an attractive mechanism for the apparent

disappearance of α -dystroglycan in cancer cells, however since the proportions of 43 kDa and ~30 kDa β -dystroglycan are highly variable, whereas α -dystroglycan is consistently reduced it is likely that aberrant glycosylation is also a factor as this would decrease the immunoreactivity of α -dystroglycan (Singh et al., 2004).

The most pronounced reduction of dystroglycan protein expression was found in high grade tumours (Henry et al., 2001; Sgambato et al., 2003) and has been linked to a decrease in patient survival (Sgambato et al., 2003). A study carried out using different breast cancer cell lines found that those expressing the lowest levels were unable to polarise correctly, were not contact inhibited in response to basement membrane components and were highly invasive. Over-expression of dystroglycan in a breast carcinoma cell line, expressing low levels of endogenous dystroglycan, rescued the cells ability to polarise and form growth-restricted epithelial structures, thus reducing their tumourigenic potential (Muschler et al., 2002). A separate study also reported the reduction in tumourigenicity of a human breast cancer cell line in response to overexpression of dystroglycan cDNA. This study, however, found that although β -dystroglycan was overexpressed, they were unable to increase α -dystroglycan expression due to its continued release from the membrane due to proteolysis (Sgambato et al., 2004).

A study looking at the significance of reduced dystroglycan expression in breast cancer cells utilised RNAi in order to diminish dystroglycan expression in non-tumourigenic mouse mammary epithelial cells. Interestingly, dystroglycan knockdown resulted in the accumulation of cells in S-phase and an increase in apoptotic cell death while also affecting crucial cell signalling pathways (Sgambato et al., 2006). While appearing paradoxical with respect to the previous findings in cancer cells, which undergo uncontrolled cell proliferation, these results highlight the complexity with which dystroglycan may be functioning during cancer progression. As previously discussed,

proteolytic processing cleaves the extracellular domain of β -dystroglycan, resulting in the release of α -dystroglycan, whilst preserving the cytoplasmic domain of β -dystroglycan (Losasso et al., 2000; Yamada et al., 2001). Since this cytoplasmic tail region binds to components of several different cell signalling pathways, perhaps in the absence of extracellular communication these proteins are retained at the membrane, resulting in aberrant signalling that may affect cell proliferation and apoptotic pathways.

1.9.3 Viral infection

Dystroglycan is the cellular receptor for several viral pathogens such as the arenaviruses, including LCMV (lymphocytic choriomeningitis virus) and the species that causes Lassa fever (Cao et al., 1998). This binding was found to be dependent upon *O*-linked glycosylation in the mucin-like region of α -dystroglycan (Kunz et al., 2005). α -Dystroglycan in association with the $\alpha 2$ chain of laminin is also a receptor for *Mycobacterium Leprae*, the pathogen that causes leprosy (Rambukkana et al., 1998). These infectious agents use dystroglycan to gain entry into the host cell.

1.10 Summary and aims

Dystroglycan is a highly versatile adhesion molecule with multiple biological functions. With its wide expression pattern and ability to bind many different proteins, dystroglycan has been implicated in diverse functions ranging from early development and muscle stability to cellular signalling and cancer progression.

α -Dystroglycan is a cell surface receptor for several components of the ECM and these interactions are crucial for its correct functionality. Binding of ECM components, such as laminin, agrin and perlecan, to α -dystroglycan is dependent upon correct glycosylation of the α -dystroglycan mucin-like region and perturbation by antibody

interference or mutations in glycosylation enzymes result in the inhibition of dystroglycan function. The ramifications of incorrect dystroglycan glycosylation in the pathogenesis of neuromuscular disease and cancer progression are the current focus of many research groups.

Comparatively speaking, while much research has focussed on the handful of interactions associated with α -dystroglycan, relatively little is known about the interactions that occur at the cytoplasmic domain of β -dystroglycan, which associates with a whole host of binding partners. The extreme C-terminus of the β -dystroglycan cytoplasmic tail contains binding sites for a variety of signalling and signal-adaptor proteins, but our understanding of the regulation of these interactions and the consequent implications on cellular function is still at the early stages. Furthermore, the association of β -dystroglycan with cytoskeletal components, such as the ERM family member ezrin and the discovery of a direct interaction between β -dystroglycan and F-actin suggests that dystroglycan may be intimately involved in actin cytoskeletal dynamics. Clearly, there is much scope for research into the intracellular functions of β -dystroglycan since many questions remain to be answered. For example: How does β -dystroglycan regulate binding to different proteins? In what intracellular processes does dystroglycan function?

Dystroglycan has not been extensively studied in relation to its influence on the reorganisation of the actin cytoskeleton, however emerging evidence links it to a Rho GTPase signalling pathway resulting in dramatic actin cytoskeleton rearrangements in cultured fibroblasts (Batchelor et al., 2007; Chen et al., 2003; Spence et al., 2004a). Fibroblasts are cells of mesenchymal origin that are a useful *in vitro* model system for studying the actin cytoskeleton as they are relatively easy to maintain and manipulate in cell culture and exhibit dynamic cytoskeletal rearrangements. This study aims to further develop our current understanding of dystroglycan function at the cellular level, with

particular emphasis on the cytoskeleton, by investigating the effects of dystroglycan deficiency in cultured fibroblasts.

Chapter 2: Materials and Methods

Chapter 2

Materials and Methods

2.1 Materials

2.1.1 Molecular biology reagents

Restrictions enzymes were obtained from New England Biolabs Inc. (75-77 Knowl Piece, Wilbury Way, Hitchin, Hertfordshire, SG4 OTY). Pfu DNA polymerase was bought from Promega (Delta House, Enterprise Road, Chilworth Research Centre, Southampton SO1 7NS) and the Rapid DNA ligation kit was manufactured by Fermentas Inc. (7520 Connelley Drive, Hanover, MD 21076, USA).

Absolutely RNA RT-PCR miniprep kit was purchased from Stratagene Inc. (11011 N. Torrey Pines Road La Jolla, CA 92037, USA) and the Titan One-Tube RT-PCR System was obtained from Roche Applied Science Ltd. (Bell Lane, Lewes, East Sussex BN7 1LG). DEPC was bought from Sigma-Aldrich Company Ltd. (Fancy Road, Poole, Dorset, BH17 7NH) and RNase ZAP from Ambion Ltd. (Ermine Business Park, Spitfire Close, Huntingdon, Cambridgeshire, PE29 6XY).

The DNeasy Tissue Kit, QIAprep Spin Miniprep kit, QIAprep Spin Maxiprep kit and QIAquick Gel Extraction kit were bought from Qiagen Ltd. (Fleming Way Crawley, West Sussex RH10 9NQ). The DIG Northern Starter Kit was purchased from Roche Applied Science, Ltd.

Electrophoresis grade, high gel strength agarose was bought from Melford Laboratories (Bideston Road, Chelsworth, Ipswich IP7 7LE) and ethidium bromide from VWR International (Hunter Boulevard, Magna Park, Lutterworth, Leicestershire LE17 4XN). DNA Hyperladder I and dNTPs were both purchased from Bionline Ltd. (16 The Edge Business Centre, Humber Road, London NW2 6EW). Oligonucleotides were purchased from MWG Biotech UK Ltd. (Waterside House, Peartree Bridge, Milton

Keynes, MK6 3BY) or Operon Biotechnologies GmbH (Nattermannallee 1 D- 50829 Cologne, Germany). DNA sequencing was carried out by The Sequencing Service, University of Dundee (School of Life Sciences, MSI/WTB Complex, University of Dundee, Dundee DD1 5EH).

Agarose gels were run using the Mini Sub Cell GT electrophoresis tank from Bio-Rad Laboratories Ltd. (Bio-Rad House, Maxted Road, Hemel Hempstead, Hertfordshire, HP2 7DX) and visualised with a gel documentation system comprising a transilluminator (BST-15.M), camera, viewer and video copy processor (Mitsubishi P91), all of which were obtained from UVITEC Ltd. (Avebury House, 36a Union Lane, Cambridge, CB4 1QB).

The pEGFP-N3 vector and the RNAi ready pSIREN-RetroQ vector kit were obtained from BD Biosciences-Clontech (21 Between Towns Road, Cowley, Oxford OX4 3LY). Plasmid maps and details of cloning strategies are detailed in Appendix I. Other DNA constructs used in this study are detailed in Appendix II.

PCR was carried out using either a Biometra Uno II or Biometra T-Gradient Thermocycler both manufactured by Biometra GmbH (Rudolf-Wissell-Straße 30, 37079 Goettingen, Germany).

2.1.2 Cells, cell culture vessels and reagents

Cells used in this study and their source are detailed in Appendix III. All reagents used in the culture and maintenance of cell lines are detailed below.

Dulbecco's Minimum Essential Medium (DMEM), RPMI-1640 Medium, OptiMEM, foetal bovine serum (FBS), penicillin/streptomycin, Fungizone, Lipofectamine reagent and Annexin V Vybrant Apoptosis Assay Kit #2 (Alexa Fluor 448 annexin V/propidium iodide) were all purchased from Invitrogen Life Technologies Ltd. 0.25%

Trypsin/EDTA, Mitomycin C, Sequabrene (Hexadimethrine Bromide), sterile DMSO, gelatin and puromycin were obtained from Sigma-Aldrich Company Ltd. ESGRO was purchased from Chemicon Ltd. (The Science Centre, Eagle Close, Chandlers Ford, Hampshire, SO53 4NF).

All plastic ware, including tissue culture flasks, round dishes and multi-well dishes, were purchased from Griener Bio-One Ltd. (Brunel Way, Stroudwater Business Park, Stonehouse, Gloucestershire, GL10 3SX). The haemocytometer was bought from Weber Scientific International Ltd. (Marlborough Road, Lancing Business Park, West Sussex BN15 8TN). Cryoware cryogenic vials and the Cryofreezing container were manufactured by Nalgene and obtained from Fisher Scientific UK Ltd. Glass coverslips and slides were purchased from VWR International. 0.2 μ m and 0.45 μ m Minisart syringe filters were from Sartorius Ltd. (Longmead Business Centre, Blenheim Road, Epsom, KT19 9QQ) and BD Microlance from BD Biosciences.

Cells in culture were visualised using a Ceti Versus inverted brightfield microscope obtained from Wolf Laboratories Ltd. (Wolf House, 80 Market Street, Pocklington, York, YO42 2AB). Fluorescence microscopy was carried out using a Leica DM IRE2 inverted fluorescence microscope in conjunction with a 1.3 megapixel CCD camera (DC 350F) from Leica Microsystems (UK) Ltd. (Davy Avenue, Knowlhill, Milton Keynes, MK5 8LB). The THD 60-16 heated stage and MC60 controller used for live-cell imaging were manufactured by Linkam Scientific Instruments (No. 8 Epsom Downs Metro Center, Waterfield, Tadworth, Surrey KT20 5HT).

2.1.3 SDS-PAGE, Western blotting and detection reagents

The Mini-PROTEAN II gel system, Trans-Blot SD Semi-Dry Transfer Cell, PVDF and Coomassie Brilliant Blue R-250 were all purchased from Bio-Rad Laboratories Ltd. Nupage Transfer buffer was bought from Invitrogen Life Technologies Ltd. Acrylamide:bisacrylamide (37.5:1) was bought from GeneFlow Ltd. (Fradley Business Centre, Wood End Lane, Fradley, Staffordshire, WS13 8NF) and Broad-range prestained protein molecular weight markers were purchased from New England Biolabs Inc. The Micro BCA Protein Assay Kit was obtained from Perbio Science UK Ltd. (Unit 9, Atley Way, North Nelson Industrial Estate, Cramlington, Northumberland, NE23 1WA). Protease inhibitors, TEMED, BCIP and NBT were all purchased from Sigma-Aldrich Company Ltd. Marvel non-fat dry milk powder was purchased from a local supermarket.

Kodak MXB film was purchased from Xograph Imaging Systems Ltd. (Xograph House, Hampton Street, Tetbury, Gloucestershire, GL8 8LD). Films were fixed in Kodak RP X-OMAT LO, developed in Kodak X-OMAT EX II, both purchased from VWR International, using an Optimax 1170 film processor from IGP UK Ltd. (1/5 Cutlers Road, South Woodham Ferrers, Chelmsford, Essex, CM3 5WD). Scanned images were obtained using a UMAX Powerlook 1000 transmissive scanner.

2.1.4 Antisera

Sources and details of working dilutions of primary and secondary antisera are detailed in Appendices IV and V respectively. Rhodamine phalloidin and DAPI were both obtained from Invitrogen Life Technologies Ltd. Hydromount mounting medium was manufactured by National Diagnostics and purchased from Fisher Scientific UK Ltd. (Bishop Meadow Road, Loughborough, Leicestershire, LE11 5RG).

All other chemicals used were of standard or AnalaR reagent grade and purchased from Sigma-Aldrich Company or VWR International.

2.1.5 Miscellaneous lab equipment

The Cyan ADP flow cytometer used in this study was obtained from Dakocytomation (4850 Innovation Drive, Fort Collins, Colorado 80525, USA) and run with Dakocytomation Summit Software (Version 4.1).

The centrifuges used were Beckman Coulter Optima MAX Ultracentrifuge (Beckman TLA-100 rotor), Sigma 4K15, Sigma 12169-H, Sigma 12256, Sigma 1-15K (Sigma Nr.12132-H rotor) and Sigma 204 (Sigma 11030 rotor) bench top centrifuges. All centrifuges were manufactured by Beckman Coulter (U.K.) Ltd. (Oakley Court, Kingsmead Business Park, London Road, High Wycombe, Buckinghamshire, HP11 1JU) or Sigma-Aldrich Company.

2.2 Methods

Methods for all of the protocols used in this study are detailed in this section. The recipes for stock solutions, buffers and media compositions are listed in Appendix VI.

2.2.1 Molecular biology techniques

All standard molecular biology techniques such as restriction digests, cloning, bacterial transformation and agarose gel electrophoresis were carried out as described in Sambrook *et al* (Sambrook *et al.*, 1989).

The Rapid DNA ligation kit was used according to the standard protocol supplied by the manufacturer. Plasmid purification by mini- or maxi-prep kits and genomic DNA extraction using the DNeasy tissue kit were all carried out according to the manufacturer's

instructions. In circumstances where the purification of linear DNA was required, the QIAquick PCR Purification kit and QIAGEN gel extraction kit were used according to the manufacturer's instructions.

DNA concentration was determined by measuring absorbance at 260 nm using a spectrophotometer and calculated as follows:

DNA concentration ($\mu\text{g/ml}$) = $(\text{OD}_{260}) \times (\text{dilution factor}) \times (50 \mu\text{g DNA/ml}) / (1 \text{ OD}_{260} \text{ unit})$.

RNA extraction was achieved using the Stratagene Absolutely RNA Miniprep kit using the protocol supplied, and RNA was eluted in 2 x 25 μl elution buffer. RNA concentration was quantified by absorbance at 260 nm and calculated as follows:

RNA concentration ($\mu\text{g/ml}$) = $(\text{OD}_{260}) \times (\text{dilution factor}) \times (40 \mu\text{g RNA/ml}) / (1 \text{ OD}_{260} \text{ unit})$

2.2.2 Polymerase chain reaction

Polymerase chain reaction (PCR) was typically carried out using 1-10 ng of template DNA, which was either double stranded DNA from a large-scale plasmid preparation in a 100 μl reaction volume or 250 μg genomic DNA in a 50 μl reaction. The reaction also contained 100 pmol of each of the forward and reverse primers, 200 μM dNTPs (comprising equimolar concentrations of each of the four bases), 1 unit of Pfu DNA polymerase and 10 μl of enzyme buffer (supplied by the manufacturer).

The following PCR conditions were typically used when amplifying from plasmid DNA: 95°C for 3 minutes; 30 cycles of 95°C for 30 seconds (denaturation), 55-60°C for 30 seconds (primer annealing) and 70°C for 90 seconds (elongation); and, finally, 72°C for 5 minutes. Amplification of genomic DNA was carried out under the following conditions: 94°C for 60 seconds; 30 cycles of 94°C for 15 seconds, 60-65°C for 30 seconds, 72°C for 3 minutes; and, finally, 72°C for 5 minutes. Annealing temperatures

varied depending upon the melting temperature of the primers used; typically a temperature 5°C below the lowest melting temperature of the two primers was chosen. On completion of the reaction, PCR products were analysed by agarose gel electrophoresis (1% (w/v) agarose gel) containing 80 ng/ml ethidium bromide and photographed using a UV transilluminator.

2.2.3 RT-PCR

Reverse transcription polymerase chain reaction (RT-PCR) was carried out using the Titan One-Tube RT-PCR System (Roche), according to the manufacturer's protocol. Total RNA (0.5-1 µg) was used as a template in all reactions in a 50 µl reaction volume. The following reaction conditions were typically used: 50°C for 30 minutes (reverse transcription); followed by 30 cycles of 94°C for 10 seconds (denaturation), 55-65°C for 30 seconds (primer annealing) , 68°C for 45 seconds (elongation); and, finally, 72°C for 5 minutes. PCR products were analysed by agarose gel electrophoresis (1% (w/v) agarose gel) containing 80 ng/ml ethidium bromide and photographed using a UV transilluminator.

2.2.4 Northern blotting

The presence of mouse dystroglycan mRNA in dystroglycan null-derived fibroblasts was detected by northern blot analysis using the DIG Northern Starter kit (Roche) according to the manufacturer's instructions. A DIG (digoxigenin)-labelled, single stranded RNA probe was generated by *in vitro* transcription of template DNA complimentary to the terminal 366 bp of mouse DAG1 in the presence of digoxigenin-UTP using T7 RNA polymerase. Isolated total RNA (~1.5 µg) from dystroglycan null-derived fibroblasts was separated by electrophoresis through an agarose/formaldehyde gel (see Section 2.2.1). RNA was transferred onto a positively charged nylon membrane by standard northern blot procedure (Sambrook et al., 1989) and crosslinked onto the membrane using a Stratalinker UV

crosslinker at 120 mJ. Mouse DAG1 mRNA was detected by hybridisation using the DIG-labelled probe followed by immunological detection using anti-digoxigenin-AP antisera and visualisation with CDP-Star chemiluminescent reagent. All procedures were carried out under RNase-free conditions.

2.2.5 Growth and maintenance of mammalian tissue culture cells

All cells used in this study were grown at 37°C under 5% CO₂. Cos-7, Ref52, Swiss 3T3 and immortalised DAG1^{-/-} derived fibroblast cell lines were cultured in DMEM medium supplemented with 10% FBS (fetal bovine serum). HeLa and CHO-K1 cell lines were cultured in RPMI supplemented with 10% FBS. Cells were sub-cultured by rinsing once in PBS (phosphate buffered saline) and then incubated in 0.25% Trypsin-EDTA (ethylenediaminetetraacetic acid) at 37°C to detach the cells from the dish. Cells were resuspended in DMEM/RPMI supplemented with 10% FBS (working medium) and seeded into tissue culture flasks (between 1:2 and 1:10 dilution depending on cell line) to maintain the cells.

2.2.6 Maintenance and differentiation of embryonic stem cells

DAG^{-/-} embryonic stem (ES) cells (a generous gift from S. Carbonetto (Cote et al., 1999)) were maintained in on a feeder cell layer (STO fibroblasts) that had been pre-treated with 10 µg/ml mitomycin C for 4 hours to inhibit proliferation. Cells were differentiated into embryoid bodies using a method adapted from Drab et al (Drab et al., 1997). Briefly, ~1000 cells in 20 µl medium were placed on the lids of petri dishes filled with PBS and cultivated in hanging drops for 2 days. Embryoid bodies were transferred into petri dishes containing the same medium and cultured for 4 days. Embryoid bodies were then transferred to individual wells of a 0.1% (w/v) gelatine-coated 24-well plate in

differentiation medium containing 10^{-8} M retinoic acid and 0.5 mM dibutyryl-cAMP to induce differentiation and maintained in culture for 2 days. Medium was changed to differentiation medium without retinoic acid and dibutyryl-cAMP, and cells were cultured for a further 2 days. Spontaneously contracting smooth muscle cells began to appear after approximately 10 days, and these were maintained in culture until they had lost all smooth muscle characteristics and reverted to fibroblasts. Clonal fibroblast populations were generated by limiting dilution. This was achieved by diluting cells in suspension to such a degree that, when seeded into a 96-well plate, each well contained ~1 cell/well. Dystroglycan null-derived fibroblasts were continually passaged until they had by-passed the Hayflick limit (Hayflick and Moorhead, 1961), to produce an immortal fibroblast cell line.

2.2.7 Generation of stable dystroglycan RNAi knockdown cells

SiRNA target sequences that were highly specific for dystroglycan were identified using the 'RNAi target sequence prediction' tool on the BBSRC Chick EST database (<http://www.chick.umist.ac.uk/>) and cross-checked using BLAST to ensure that there was no significant sequence homology to any other gene. The four sequences selected for cloning were: DAG1 185 GGTGGCATTCCAGACGGTAC 205, DAG 1 1298 AACGCCTTCAACTGATTCGTC 1318, DAG1 1319 AACTACCACAACCTCGGAGGCC 1340, DAG1 1569 AATGAGGATACCACTACCGAC 1589. These sequences were modified into antisense short hairpin RNA oligonucleotides (shRNA) using the siRNA Hairpin Oligonucleotide Sequence Designer, in order to generate 73mer siRNA constructs containing the target sequence in forward and reverse orientation separated by a TTCAAGAGA hairpin loop with BamH 1 and EcoR 1 overhangs (<http://bioinfo.clontech.com/rnaidesigner/oligoDesigner.do>). These oligonucleotides were

ligated into the RNAi-Ready pSIREN RetroQ (Clontech) retroviral vector (see map in Appendix I) as detailed in the Clontech “Knockout RNAi Systems User Manual”. The 21mer sequence selected for generating dystroglycan knockdown fibroblasts was mouse DAG1 1319 AACTACCACAACCTCGGAGGCC 1340. The ‘sense’ control siRNA was generated using the complimentary strand of the chosen antisense siRNA sequence to generate a siRNA hairpin that produced a sense-oriented strand that could not anneal to the target sequence in DAG1 mRNA. Constructs were sequenced and shown to be correct before they were stably transfected into a PT67 packaging cell line. Retrovirus containing the dystroglycan shRNA construct was produced according to instruction in the Clontech “Retroviral Gene Transfer and Expression User Manual”. Swiss 3T3 fibroblasts were exposed to two rounds of retroviral infection, followed by puromycin selection to identify cells expressing the shRNA construct. Clonal populations were generated by limiting dilution as previously described in Section 2.2.6.

2.2.8 Cryogenic preservation and storage

Confluent cells in a T175 flask were harvested by trypsinisation and centrifuged at 1000 x g for 5 minutes. The cell pellet was resuspended in 4 ml freezing media and 1 ml of this cell suspension was transferred to a 2 ml cryovial. Cryovials were frozen in a Nalgene 1°C cryofreezer jacketed with isopropanol at -80°C overnight before being transferred to liquid nitrogen for long-term storage.

2.2.9 LipofectAMINE transfection

Cells were seeded on sterile glass coverslips in 35mm tissue culture dishes to approximately 50-70% confluency the day prior to transfection. 2 µg of DNA (4µg for HeLa transfections) and 100 µl OptiMEM were mixed gently by pipetting in a sterile

Eppendorf tube. 6 μ l LipofectAMINE (10 μ l for HeLa transfections) and 100 μ l Opti-MEM were mixed in a second Eppendorf tube. The two solutions were combined and incubated at room temperature for 30 minutes, after which 600 μ l Opti-MEM was added. Cells were rinsed once in Opti-MEM and incubated with the transfection solution for 5 hours at 37°C, under 5% CO₂. The transfection solution was then aspirated off, and cells were incubated in fresh growth media overnight.

2.2.10 Generation of stable transfected cell lines

Cells were seeded into 35 mm tissue culture dishes and transfected using lipofectamine reagent or retroviral infection as previously described in Section 2.2.9. At 48 hours post-transfection, cells were re-plated into a T25 cell culture flask to which antibiotic selection medium, specific for the resistance gene present in transfected vector, was added. Antibiotic selection of transfected PT67 cells and infected Swiss 3T3 fibroblasts was carried out using 10 μ g/ml puromycin. Cells were cultured in antibiotic selection medium for ~21 days, during which the medium was changed every 1-2 days.

2.2.11 Cell fixation

Cells were washed once with PBS and then fixed by incubation with 3.7% (v/v) paraformaldehyde/PBS (500 μ l in 35 mm tissue culture dish) for 10 minutes at room temperature. Cells were then washed three times in PBS. Alternatively, cell were washed once in PBS and then incubated in 100% methanol chilled to -20°C. In the case of methanol fixation, cells were incubated at -20°C for 4 minutes and then washed three times in PBS.

2.2.12 Immunocytochemistry

Cells were seeded on sterile round glass coverslips, either 13 mm or 22 mm in diameter, and all incubations were carried out at room temperature in a humidified container. Fixed cells were permeabilised by incubating in permeabilising buffer (see Appendix VI) for five minutes and then blocked in blocking buffer (see Appendix VI) for one hour. Primary antibodies were diluted in blocking buffer at the appropriate concentration (Appendix IV), and the cells were incubated in primary antibody solutions for one hour before being washed once in blocking buffer followed by 3 x 5 minute washes in PBS. For indirect immunofluorescence, cells were incubated with secondary antibodies diluted according to manufacturer's specifications (detailed in Appendix V) in blocking buffer for one hour. Filamentous actin (F-actin) was stained using Rhodamine phalloidin, which was added to the secondary antibody solution. Cells were then washed for 3 x 5 minutes in PBS and then mounted onto glass slides using Hydrmount mounting medium containing DAPI (4',6-Diamidino-2-phenylindole). Images were obtained with a Leica DMIRE2 inverted fluorescent microscope, collected with Leica QFluoro software and processed using Adobe Photoshop v.6.0.

2.2.13 Morphological analysis

Cell morphology was assessed using immunofluorescence images of cells stained with cortactin (for area and circularity) or vinculin (focal adhesion quantification).

2.2.13.1 Area and circularity quantification

Quantification of the area and circularity of cells was carried out using Image J software (<http://rsb.info.nih.gov/ij/>). Area was determined by setting the threshold level to generate

a silhouette image of each cell and calculating the number of square pixels in the selection and converting this into the calibrated units i.e. μm^2 .

Circularity was calculated using the area and perimeter measurements of each cell according to the following equation:

$$\text{Circularity} = 4\pi \left(\frac{A}{P^2} \right)$$

Where A is area (μm^2) and P is perimeter (μm). A circularity value of 1.0 indicates a perfect circle, whereas values approaching 0 indicate an increasingly elongated polygon. The area and circularities of 100 cells were determined per sample.

2.2.13.2 Focal adhesion quantification

Immunofluorescence images of cells stained for the general focal adhesion marker, vinculin, were processed using Adobe Photoshop v.6.0. Cell area was determined as previously described (see Section 2.2.13.1) and the number of focal adhesions per μm was calculated. Focal adhesions were counted and categorised according to size by comparison with a calibrated paintbrush tool that was $2 \mu\text{m}$ in diameter. Adhesions that were $< 2 \mu\text{m}$ were categorised as focal contacts, those $> 2 \mu\text{m}$ as focal adhesions and those that were $> 2 \mu\text{m}$ and elongated as fibrillar adhesions, which are usually centrally located and not peripheral.

2.2.14 Cell proliferation assay

The proliferation rate of cultured cells was determined by cell counting over a five day period. Cells were seeded into 5 x T25 cell culture flasks on Day 0 at ~50% confluency, such that each flask contained the approximately the same number of cells. On Day 1 – Day 5, cells were trypsinised and resuspended in an appropriate volume of media,

dependent upon the cell density. Typically, cells were diluted 1:10-1:20 v/v prior to analysis. Cells were counted using a haemocytometer as described in Spector *et al* (Spector et al., 1998) and number of cells/ml was calculated.

2.2.15 BrdU (5-bromo-2-deoxyuridine) incorporation

Cells were seeded onto glass coverslips, grown to semiconfluence and then treated with 20 μ M BrdU for 45 minutes at 37°C, 5% CO₂. Cells were washed in PBS (3 x 5 minutes) and fixed in absolute ethanol (pre-chilled to -20°C) for 10 minutes at -20°C. Fixative was removed by aspiration, and the cells were left to air dry for a few minutes at room temperature. Cells were rehydrated by immersion in PBS for 3 minutes before treatment with 2 N HCl for 15 minutes at room temperature to denature the DNA. HCl was neutralised by addition of 0.1 M Borate buffer pH 8.5, which was changed twice over a 10 minute period followed by 3 x 5 min washes in PBS. BrdU incorporation was visualised by staining cells with anti-BrdU antisera, followed by indirect immunofluorescence. Mitotic index was determined by counting ~1000 cells per experiment (visualised by DAPI staining) and calculating the percentage of cells counterstained with FITC-BrdU. Three independent experiments per cell line were carried out.

2.2.16 Cell synchronisation methods

2.2.16.1 Double thymidine block and transfection

HeLa cells were cultured to semiconfluence in RPMI supplemented with 10% FBS. Cells were trypsinised and 1/20 of the culture seeded on a new 10 cm culture dish. After 1 day, cells were synchronised in S phase by culturing in RPMI, containing 10% FBS and 10 mM thymidine for 15 h. Cells were then washed twice in serum-free media and incubated in fresh media containing 10% FBS for 9 h. A second thymidine block was then added for 3

h, replaced with serum-free Opti-MEM and transfected with 4 μg DNA using LipofectAMINE for 3 h as previously described. After transfection, the cells were cultured again in the thymidine-containing medium for another 9 h. The cells were then washed twice with serum-free media and cultured in fresh media containing 10% FBS. After 6 h, nocodazole was added to a final concentration of 40 ng/ml, and the culture was continued for another 6 h. Round mitotic cells were further purified by shake-off procedure and suspended in fresh media containing 10% FBS to release from the nocodazole arrest. This protocol was adapted from Kimura *et al* (Kimura et al., 2000).

2.2.16.2 Cell Synchronisation by double block with thymidine and mimosine

Swiss 3T3 fibroblasts were plated on 10 cm dishes to a cell density of $\sim 2 \times 10^5$ cells/ml ($\sim 50\%$ confluence) in DMEM containing 10% FBS. The following day, the medium was replaced with DMEM containing 2 mM thymidine and incubated for 12 h. The cells were then washed with PBS and grown in fresh media for 13 h to recover. The cells were blocked for a second time by incubation with DMEM, 10% FBS, and 200 μM mimosine for 12 h. The cells were washed twice with PBS and released from the block by incubating with fresh medium. This was taken as time 0 for the time course. Samples were taken at 0, 2, 4, 6, 8, 12 and 24 h. At each time point, cells from each dish were trypsinised and transferred to a 15 ml Falcon, centrifuged at $100 \times g$ in Sigma 204 benchtop centrifuge (Sigma 11030 rotor) for 3 minutes and washed twice in PBS. The cells were fixed by drop-wise addition of ice-cold 70% ethanol, while mixing on a vortex. A further 10 ml of ethanol was added at this stage. An asynchronous population of cells was also collected. The fixed cells were pelleted and washed once in 10 ml PBS and then resuspended in 300 μl PBS. To this, 20 μl propidium iodide (1 mg/ml stock) and 16 μl RNase I (from 10 mg/ml stock) were added before incubating at 37°C for 30 minutes. The cells were

transferred to a flow cytometry tube and analysed using a CyAn ADP cytometer. Data analysis was performed using Summit software v.4.1 and the MODfit LT v.3.0 program which uses a Gaussian Curve to mathematically model phases G1 and G2/M. The S-phase limits were taken from G1 and G2/M positions. This protocol was adapted from Spector *et al* (Spector et al., 1998).

2.2.17 Time-lapse microscopy

Time-lapse live cell images were acquired by seeding cells onto glass coverslips and placing them in 35 mm tissue culture dishes prior to transfection. Dishes were placed onto a pre-warmed stage heated to 37°C, which was mounted on a Leica DMIRE2 inverted fluorescent microscope. Fluorescence images of live cells were collected at 1 minute intervals. Movie images were collected using Leica QFluoro Software and processed using Adobe Photoshop v.6.0.

2.2.18 Wound healing assays

Cells were seeded onto coverslips and grown to confluence. A wound was made by scraping the cell monolayer with a sterile micropipette tip. The width of the wound was ~200-300 μm . For determining MTOC (microtubule organising centre) position, cells were fixed 3 hours post-wounding and stained for α -tubulin. DNA was stained with DAPI. Wound edges were analysed using a fluorescent microscope and images were captured on a 63 x objective lens, which facilitated MTOC localisation. The position of the MTOC was determined in 100 cells on each wound edge (200 cells per experiment).

2.2.19 Annexin V apoptosis assay

Apoptotic cells were detected using the Vybrant Apoptosis Assay Kit #2 (Alexa Fluor 448 annexin V/propidium iodide) according to the manufacturer's instructions. Semiconfluent cells were harvested with trypsin and washed in cold PBS before incubation with Alexa Fluor 448 annexin V and propidium iodide in annexin V binding buffer. Positive controls were pre-treated with 1 μ M staurosporine for 5 hours to induce apoptosis. Negative control cells were treated with annexin V binding buffer alone. Stained cells were analysed by flow cytometry at 520 nm (Alexa Fluor 448 annexin v) and 670 nm (propidium iodide) using a CyAn ADP cytometer, and results were plotted as annexin V 448 vs. propidium iodide using Summit software v 4.1. Apoptotic cells were identified as only emitting green fluorescence, dead (necrotic) cells were identified as emitting both red and green fluorescence, and live cells could be distinguished based upon their emission of very low levels of green fluorescence. Gates were set to define the three cell populations were applied identically to every plot, allowing for direct comparison of the proportion of apoptotic cells in each sample.

2.2.20 Actin fractionation

Semi-confluent cells in 10 cm diameter cell culture dishes were washed once in PBS and lysed by addition of 200 μ l actin fractionation buffer. Pools of globular actin (G-actin) and filamentous actin (F-actin) were separated from lysed cells by ultracentrifugation at 386,000 x g for 30 minutes using a TL100 rotor in a Beckman ultracentrifuge. The supernatant was transferred to a new Eppendorf tube and the pellet was resuspended in 200 μ l modified sample buffer, sonicated briefly, and incubated on ice for 30 minutes to solubilise further. Equivalent volumes of supernatant (G-actin) and pellet (F-actin) were

loaded on a gel and probed for α -actin by western blot and enhanced chemiluminescence (ECL) development. Western blots were scanned at 300 dpi on a UMAX Powerlook 1000 scanner using Adobe Photoshop 6 and the UMAX Magic Scan software interface. The proportions of G- and F-actin were determined by measuring the intensity (integrated density) of the actin bands using the Image J software (<http://rsb.info.nih.gov/ij/>).

2.2.21 Total cell lysates

Adherent cells were rinsed in PBS prior to lysis in modified sample buffer. Cells were harvested using a cell scraper, transferred to an Eppendorf tube and then sonicated on ice. Protein concentration was determined using the Micro BCA assay kit and adjusting solution was added to the samples prior to boiling and loading onto SDS-PAGE gels.

2.2.22 Determination of protein concentration

Protein concentrations were determined using the Micro BCA Protein Assay kit according to the manufacturer's instructions. Briefly, the sample or the lysis buffer only control was diluted in 500 μ l distilled H₂O (dilutions ranged between 1:20 and 1:500 (v/v) depending on the sample) and incubated at 60°C for one hour with 500 μ l Micro BCA reaction solution. Samples were allowed to cool to room temperature, after which the absorbance was measured at a wavelength of 562 nm, using the control reaction as a reference. Protein concentration was determined using a standard curve, which was produced using known concentrations (in the range 1-20 μ g/ml) of BSA (bovine serum albumin) in the relevant sample buffer.

2.2.23 SDS-polyacrylamide gel electrophoresis

Protein samples were prepared by addition of 2 x sample buffer and denatured by boiling for 5 minutes. SDS-PAGE (sodium dodecyl (lauryl) sulfate-polyacrylamide gel electrophoresis) was carried out according to Laemmli (Laemmli, 1970) in the Mini-Protean II system (Bio-Rad) with 1mm spacers. Proteins were resolved using 10% or 12% polyacrylamide gels. Electrophoresis was carried out at 120 V for ~1 hour. Resolved protein bands were stained using Coomassie blue stain followed by incubation in destain solution until protein bands were clearly visible. Otherwise, gels were used unstained for western analysis.

2.2.24 Western analysis

Protein transfer from polyacrylamide gel to PVDF (polyvinylidene fluoride) membrane was performed using a semi-dry blotter (Bio-Rad Trans-Blot SD Semi-Dry Transfer Cell) in transfer buffer at 150 mA, 25 V for 30-45 minutes depending on protein size. The membrane was then blocked in 2.5% (w/v) Marvel dried skimmed milk powder in TBST (Tris-buffered saline/Tween 20) for 1 hour before incubation in primary antisera in 2.5% (w/v) Marvel/TBST for either 2 hours at room temperature or overnight at 4°C. Primary antibody dilutions are detailed in Appendix IV. Membranes were then washed for 3 x 10 minutes in TBST and incubated in secondary antisera diluted in 2.5% Marvel/TBST (detailed in Appendix V) for 1 hour at room temperature. After a second wash step, immunoreactive bands were detected either by ECL or alkaline phosphatase chromogenic detection.

2.2.25 Western blot detection

2.2.25.1 ECL detection

Western blots probed with HRP (horseradish peroxidase)-conjugated secondary antisera were developed by enhanced chemiluminescence (ECL). Equal volumes of ECL solution I and II (see Appendix VI) were mixed and the membrane was incubated in this reaction mixture for 1 minute. The membrane was subsequently transferred to an autoradiography cassette and exposed to Kodak MXB X-ray film. Film was developed in a Kodak X-OMAT film processor.

2.2.25.2 Alkaline phosphatase detection

Western blots probed with AP-conjugated secondary antisera were developed by chromogenic detection. 132 μ l NBT (nitro blue tetrazolium chloride) stock solution and 66 μ l BCIP (5-Bromo-4-chloro-3'-indolyphosphate p-Toluidine salt) stock solution were added to 10 ml alkaline phosphatase buffer, mixed and added to membrane. Membrane was gently agitated until the colour developed and bands were visible. The reaction was stopped by immersing the membrane in distilled H₂O.

Chapter 3: Isolation and analysis of dystroglycan null-derived fibroblasts

Chapter 3

Isolation and analysis of dystroglycan null-derived fibroblasts

3.1 Introduction

The cell adhesion molecule dystroglycan is the central component of a multiprotein membrane complex that links the actin cytoskeleton to the extracellular matrix (Ibraghimov-Beskrovnaya et al., 1993). In muscle and neuronal tissue, dystroglycan forms part of the dystrophin-glycoprotein complex and mutations in components of this complex leads to severe neuromuscular diseases (Durbeej and Campbell, 2002), however no diseases have been attributed to mutations in the dystroglycan gene, suggesting that it plays a vital role within the cell. Several studies have previously been undertaken to investigate the outcome of dystroglycan deletion in different tissues. The dystroglycan knockout mouse was found to be embryonic lethal. This was thought to be due to the embryos inability to form a basement membrane because an interaction between dystroglycan and laminin initiates the process (Williamson et al., 1997). However, this fundamental role in embryogenesis has been disputed since deletion of dystroglycan in zebrafish had no effect on early development, but did induce a dystrophic muscle phenotype at later stages (Parsons et al., 2002). Dystroglycan does appear to be essential for later stages of development in mammals too since chimaeric mice deficient in dystroglycan developed a muscular dystrophy phenotype and had disrupted neuromuscular synapses (Cote et al., 1999) and selective deletion in differentiated striated muscle resulted in a mild dystrophic phenotype, thought to be partially compensated by satellite cells expressing dystroglycan (Cohn et al., 2002). Moreover, deletion of dystroglycan in peripheral nerve caused abnormal myelination and neurological defects (Saito et al., 2003) and brain selective deletion of dystroglycan in mice resulted in the development of congenital muscular dystrophy-like malformations (Moore et al., 2002). These studies

have focussed primarily on the interaction between α -dystroglycan and extracellular matrix components, which occurs on the outer surface of the cell. Intracellularly, β -dystroglycan plays intricate roles in cell signalling pathways in addition to its function as a tether to the actin cytoskeleton via dystrophin or utrophin (Spence et al., 2004a; Spence et al., 2004b) and the effects of dystroglycan deletion on these intracellular processes have not yet been fully investigated.

The aim of the present research was to examine the effect of dystroglycan deficiency at the cellular level by characterising dystroglycan null fibroblasts. These fibroblasts were derived from the same DG $-/-$ ES cells that were used to generate the dystroglycan chimaeric mice (Cote et al., 1999). Initial observations of the cells suggested that they had a late cytokinetic defect due to the appearance of multinucleate cells and persistent intercellular connections. However, the discovery that the cells were actually expressing dystroglycan and did not contain the gene disrupting cassettes halted their characterisation and they were deemed unsuitable for further research.

3.2 Results

3.2.1 Generation of fibroblasts from dystroglycan null embryonic stem cells

Dystroglycan null (DG $-/-$) mouse embryonic stem (ES) cells (Figure 3.1 A), produced by targeted gene disruption of the DAG1 gene (Cote et al., 1999), were used to generate DG $-/-$ fibroblasts. The methods used to differentiate and isolate DG $-/-$ fibroblasts were adapted from Drab *et al* (Drab et al., 1997) and are detailed in Section 2.2.6. Briefly, ES cells were differentiated into embryoid bodies in hanging drop cultures, which were then grown on 0.1% gelatin-coated tissue culture dishes and allowed to spread (Figure 3.1 B). After ~10 days, spontaneously contracting smooth muscle cells began to appear and these were maintained in culture until they had lost all smooth muscle characteristics and reverted to fibroblast-like cells. Four different DG $-/-$ derived clonal cell lines were established from these cells by limiting dilution, and will be referred to as DG $-/-$ A, B, C and D. These clones were sub-cultured until they were calculated to have passed the Hayflick Limit (Hayflick and Moorhead, 1961) to produce immortal cell lines.

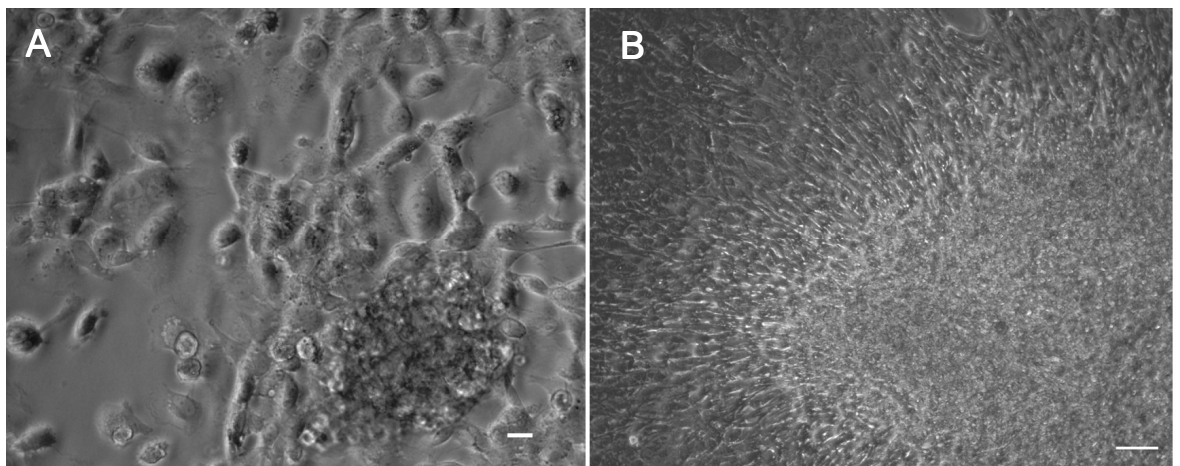


Figure 3.1: Phase contrast images of DG $-/-$ embryonic stem cells cultured on a fibroblast feeder layer (A) and a differentiating embryoid body (B). A: Scale bar = 40 μm . B: Scale bar = 100 μm .

3.2.2 Characterisation of DG $-/-$ cell clones

As previously described, DG $-/-$ derived clones were differentiated from pluripotent embryonic stem cells which are capable of differentiation into any cell type leading to the formation of epithelial, connective, muscle and nerve tissues. Consequently, prior to further investigation into dystroglycan deficiency, isolated DG $-/-$ clones were characterised to study their morphology and if possible ascertain their cell lineage.

3.2.2.1 DG $-/-$ cells displayed typical fibroblast morphology

Firstly, cells were seeded onto uncoated glass coverslips and their overall morphology analysed under a light microscope. All cells exhibited classic, elongated spindle shaped morphology, which is characteristic of fibroblasts (Figure 3.2). Interestingly, DG $-/-$ B, C and D had a mesenchymal character, whereas DG $-/-$ A grew in clusters reminiscent of epithelial cells, despite having a fibroblastic morphology (Figure 3.2, left panel).

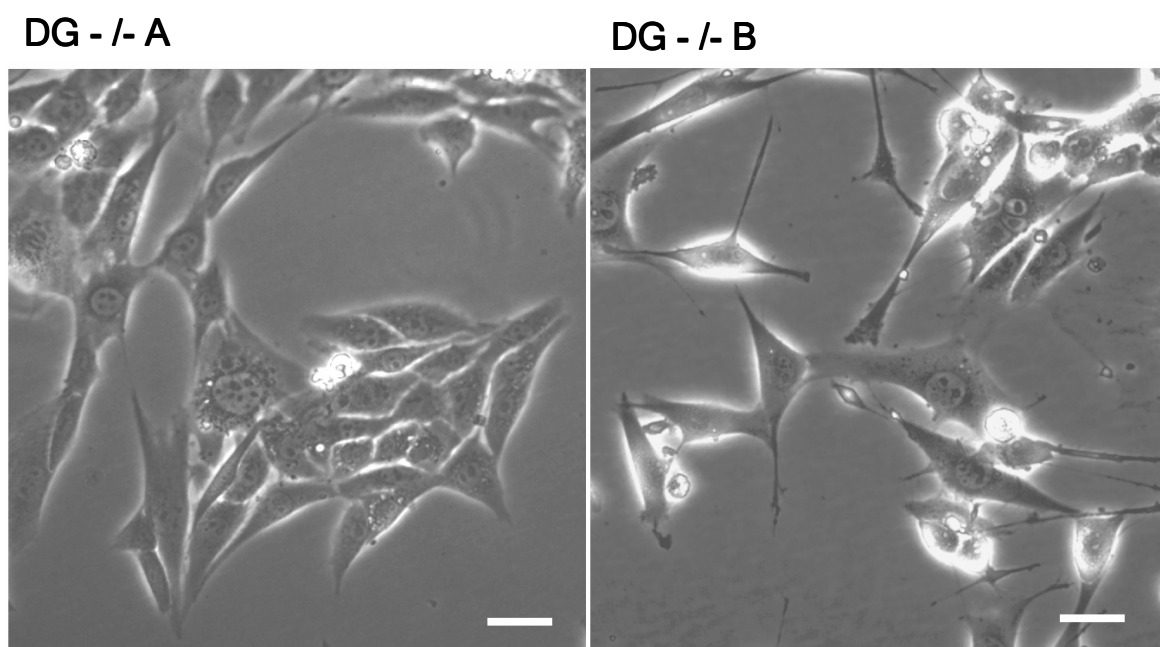


Figure 3.2: Cellular morphology of DG $-/-$ clones. Example phase contrast images of clones DG $-/-$ A and DG $-/-$ B. All clones displayed typical elongated spindle-shaped fibroblastic morphology. DG $-/-$ B, C and D cells grew happily as single cells after migrating away from each other (right panel), whereas DG $-/-$ A cells grew in epithelial-like clusters (left panel). Scale bar = 20 μ m.

3.2.2.2 Determination of DG ^{-/-} cell lineage

Subsequently, the lineage of the DG ^{-/-} clones was investigated by preparing total cell lysates and determining the presence or absence of different intermediate filaments by western analysis. Fibroblasts are cells of mesenchymal origin and express the intermediate filament, vimentin. Desmin, however, is expressed only in cells of myogenic origin such as smooth muscle cells. The expression of keratin is a marker for epithelial cells. The results show that all four DG ^{-/-} clones were vimentin positive but desmin and keratin negative (Figure 3.3). Together, these results suggest that DG ^{-/-} cells were fibroblasts since they expressed the mesenchymal marker, vimentin, and had a typical fibroblastic morphology.

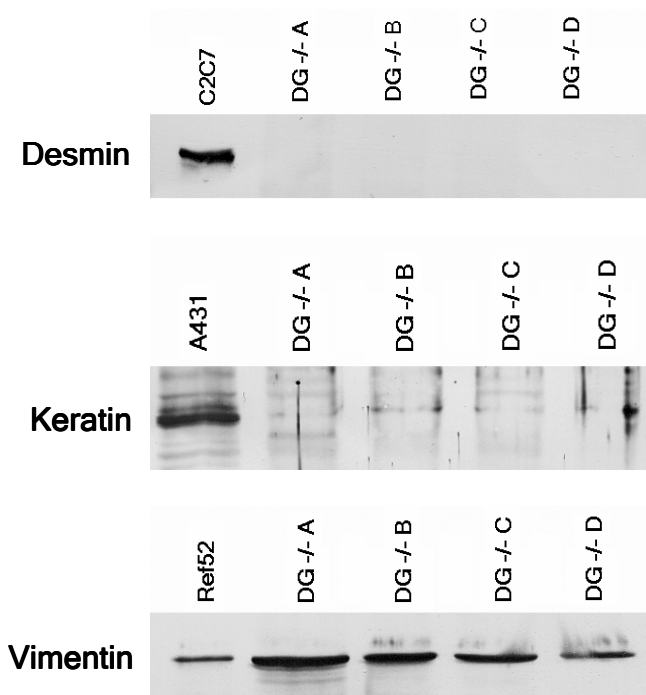


Figure 3.3: Determination of cell lineage. Cell lysates from all four DG ^{-/-} cell clones were subjected to western analysis with specific antisera for different intermediate filaments. Lysates of C2C7 myoblasts, A431 and Ref52 functioned as positive controls for desmin, keratin and vimentin respectively. All four DG ^{-/-} clones contained only vimentin, which confirmed that they were of mesenchymal origin and therefore likely to be fibroblasts.

3.2.2.3 DG $-/-$ cells exhibited a multinucleate phenotype

Analysis by fluorescence microscopy revealed that many cells were multinucleated or alternatively, maintained long thin connections between other cells, despite being some distance apart (Figure 3.4). Thus, the microtubule organisation of DG $-/-$ fibroblasts was investigated by immunostaining for α -tubulin. The presence of these connections between two well-spread cells suggests that these cells may have a late cytokinetic defect, since daughter cells appear to be unable to completely sever their connection.

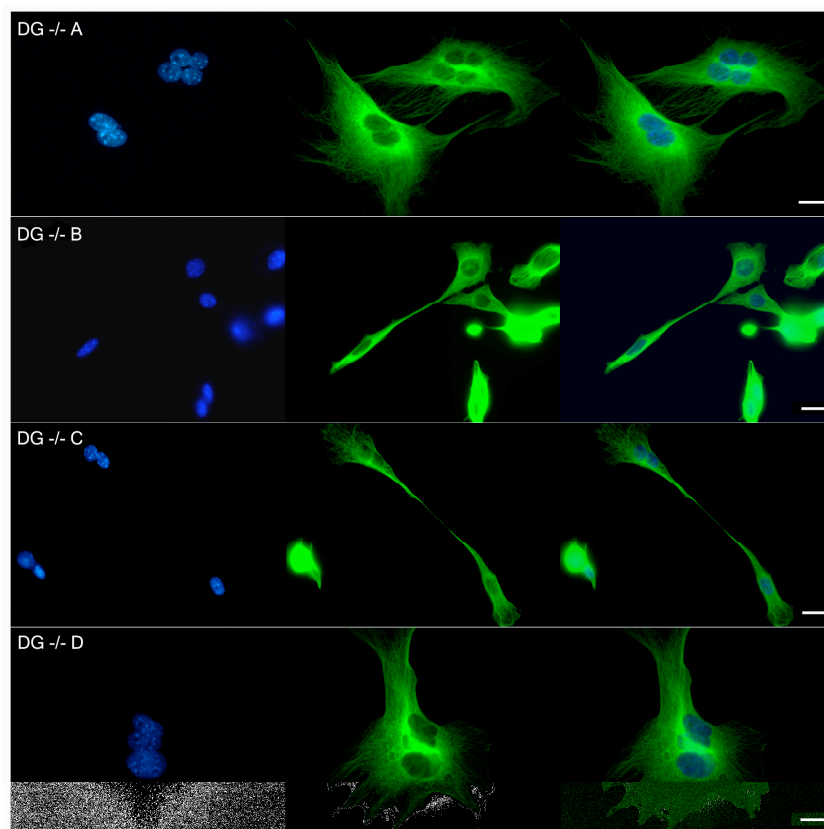


Figure 3.4: Immunofluorescence staining of DG $-/-$ fibroblasts. α -Tubulin (green) and DNA (blue). Many of the cells were found to be multinucleate and maintained long thin extensions despite being some distance apart. Scale bar = 20 μ m.

3.2.3 DG $-/-$ derived cells expressed dystroglycan

Cell lysates were prepared from DG $-/-$ derived fibroblasts and control cell lines and subjected to western analysis using specific antisera against β -dystroglycan as verification that they were, indeed, dystroglycan null. Unexpectedly, however, the cells were found to

express β -dystroglycan and this was shown using three different anti- β -dystroglycan antisera (Figure 3.5). All of the anti- β -dystroglycan antisera used in this study have been thoroughly characterised in other studies and have been shown to recognise the C-terminus of β -dystroglycan with high specificity (Cullen et al., 1994; Hnia et al., 2007; Ilsley et al., 2001; James et al., 2000; Pereboev et al., 2001). In addition to the 43 kDa band corresponding to β -dystroglycan, two other bands could sometimes be detected (Figure 3.5 A and B). The ~30 kDa band is a proteolytic product of β -dystroglycan previously reported in other cell lines (Durbeej and Campbell, 1999; Durbeej et al., 1998; Losasso et al., 2000; Saito et al., 1999; Sgambato et al., 2006; Sgambato et al., 2003; Yamada et al., 1996; Yamada et al., 2001). The third band is an intermediate, which has been previously reported and may also result from proteolytic events (Losasso et al., 2000) (Driss et al., 2006). Thus, β -dystroglycan was found to be present in all four DG^{-/-} fibroblast cell lines.

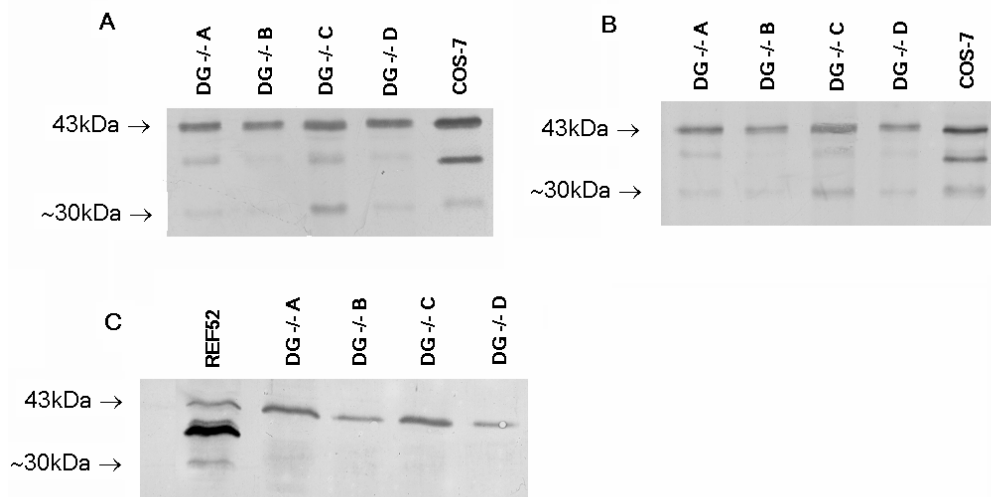


Figure 3.5: DG^{-/-} cells expressed dystroglycan. Cell lysates from DG^{-/-} fibroblasts were subjected to western analysis using specific antisera directed against β -dystroglycan. A: Cell lysates probed with anti- β -dystroglycan 43DAG/8D5 monoclonal antisera. B: Cell lysates probed with anti- β -dystroglycan MANDAG2 monoclonal antisera. C: Cell lysates probed with anti- β -dystroglycan 1709 and 1710 polyclonal antisera (50:50 each) Lysates from COS-7 and Ref52 cells served as positive controls.

3.2.4 Proposed re-initiation of dystroglycan expression

Further to the previous finding that DG *-/-* fibroblasts were in fact expressing dystroglycan, possible reasons as to how this could be possible were explored. The DAG1 gene was disrupted by the incorporation of neomycin and hygromycin resistance gene cassettes prior to exon 2 (Cote et al., 1999). Close analysis of the DAG1 sequence using the Database of Transcriptional Start Sites (<http://dbtss.hgc.jp/>) revealed that there is a potential intraexonic transcriptional start site located in exon 2 in the region after the gene targeting cassette (Figure 3.6). Furthermore, a Kozak sequence and start codon were located shortly downstream from this site. This led to the hypothesis that, perhaps, a truncated form of the dystroglycan pro-protein was being expressed in DG *-/-* cells due to the re-initiation of transcription after the site of gene disruption. Since the anti- β -dystroglycan antisera used for western analysis all target the extreme C-terminus of the β -dystroglycan cytoplasmic tail, perhaps expression of a truncated dystroglycan product would still allow a complete β -dystroglycan to be expressed and therefore it would be detected by β -dystroglycan western analysis.

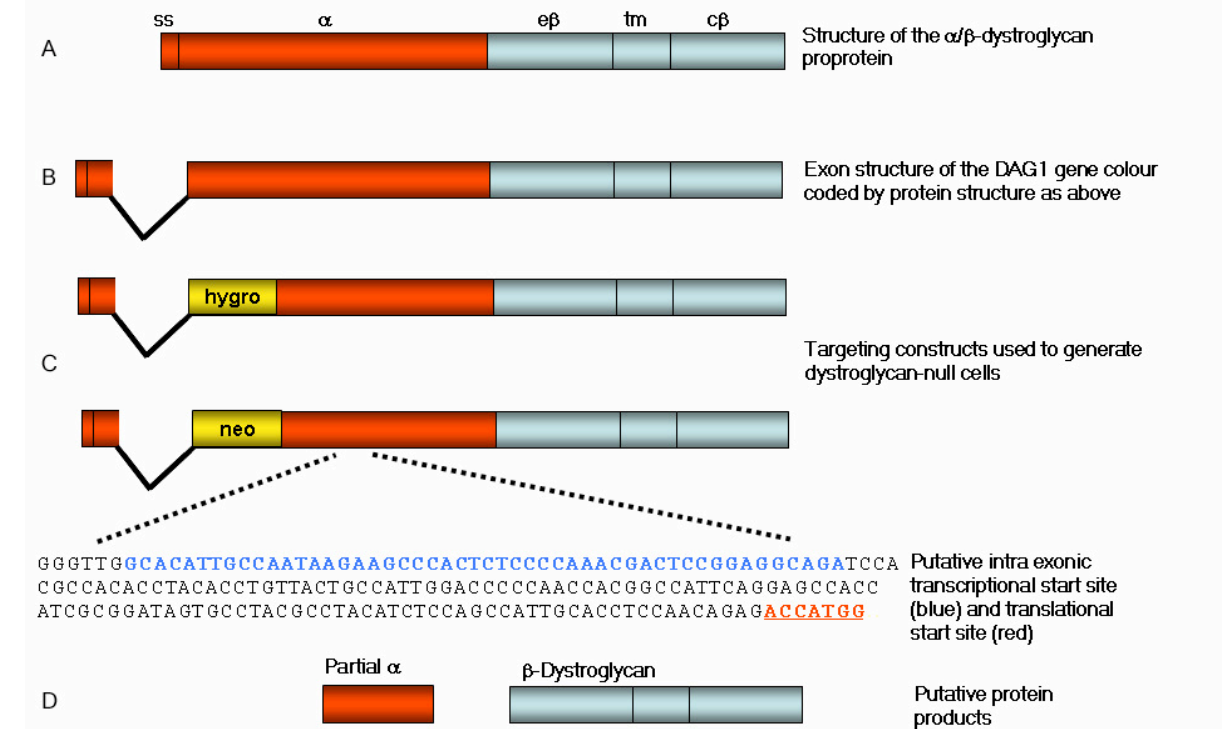


Figure 3.6: Potential re-initiation of dystroglycan expression. A: Schematic representation of the dystroglycan pro-protein. B: Exon structure of DAG1 gene. C: Schematic diagrams of disrupted DAG1 alleles containing either a hygromycin or neomycin gene cassette showing potential intra-exonic re-initiation site in region after cassette (blue text) followed by a Kozak sequence and start codon (red text). D: Proposed truncated dystroglycan product.

3.2.4.1 RT-PCR analysis

To investigate this re-initiation of transcription theory, total RNA was isolated from all four DG $-/-$ fibroblasts and the presence of dystroglycan mRNA was determined by RT-PCR. Specifically designed primers were used to amplify DAG1 mRNA sequences before and after the proposed transcriptional re-initiation site (primer sequences are detailed in Appendix VII). The location of each primer pair relative to the hygromycin/neomycin resistance cassette and proposed transcriptional re-initiation site on the DAG1 gene are illustrated in Figure 3.7 A. Primer pair (a) amplifies a region occurring prior to the proposed re-initiation site, therefore if the gene has been disrupted in these cells we would not expect to see a product. Primer pair (b) amplifies a region occurring after the proposed re-initiation site but still within the α -dystroglycan coding region. Therefore, if a product

is amplified it may mean that a truncated form of the dystroglycan pro-protein is being expressed. Primer pair (c) amplifies the first half of the β -dystroglycan gene and a product using these primers would tell us whether β -dystroglycan is expressed in DG $-/-$ fibroblasts. Finally, primer pair (d) recognise the first part of the α -dystroglycan gene, and a product would not be expected if the gene is disrupted as the reverse primer anneals to a sequence that is deleted by the incorporation of the hygromycin/neomycin cassette. The mouse myoblast cell line, C2 C4, was used as a positive control and amplification of the ubiquitously expressed glyceraldehyde phosphate dehydrogenase (GAPDH) gene was used as an internal positive control in all samples. As shown in Figure 3.7 B, DG $-/-$ cells were found to express all of the mRNA sequences recognised by these primers. These results disagree with the re-initiation hypothesis since primers recognising sequences prior to the proposed re-initiation site still amplified a product. Furthermore, these findings suggest that DG $-/-$ fibroblasts did not contain the hygromycin/neomycin resistance cassettes since primers that recognised sequences that are disrupted by these cassettes were still capable of amplifying a product. Since the primers used in this experiment collectively encompass the majority of the DAG1 gene, we can conclude that these cells in fact express full length dystroglycan and are therefore are invalid as a model for investigating dystroglycan deficiency.

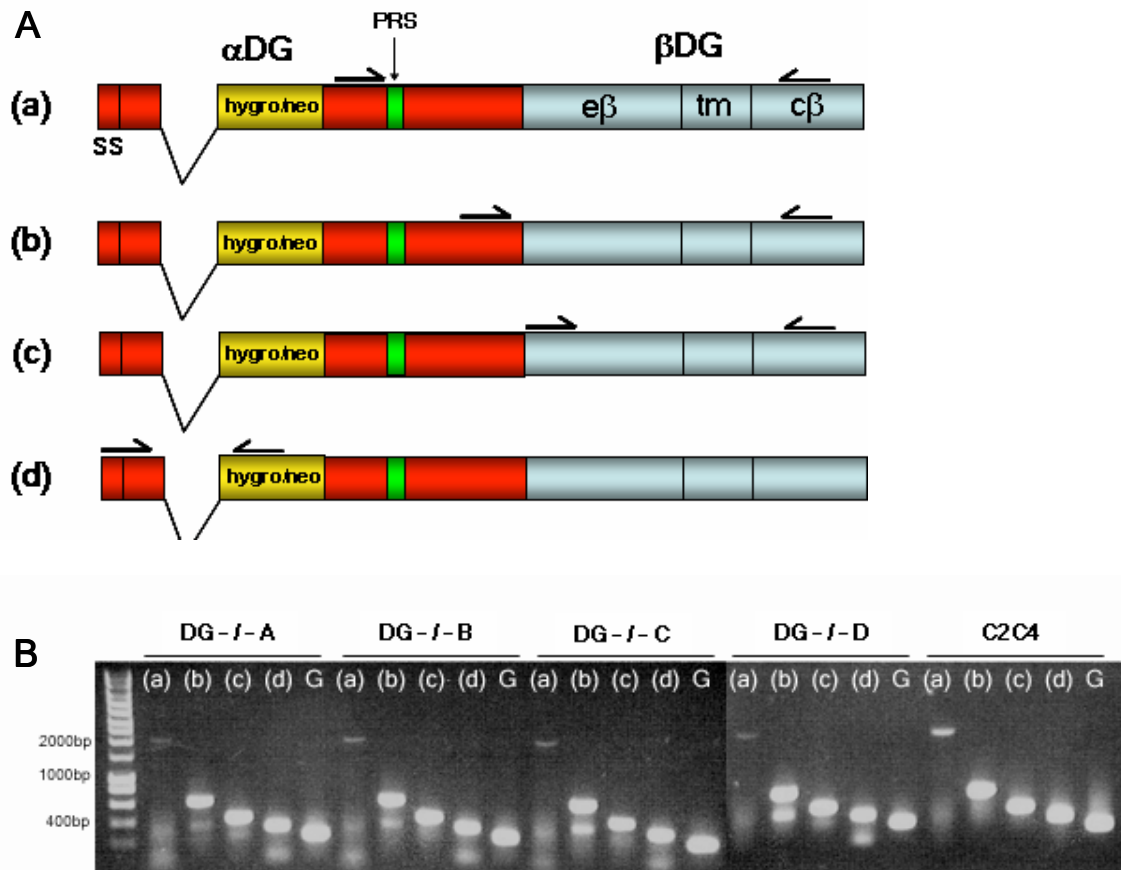


Figure 3.7: RT-PCR analysis of DG $-/-$ cells. A: Schematic diagram illustrating location of each primer pair on the DAG1 gene. PRS = Proposed re-initiation site. B: Agarose gel of RT-PCR products from each of the primer pairs. DG $-/-$ Cells G = GAPDH positive internal control.

3.2.4.2 DG $-/-$ cells express full-length DAG1 mRNA

To confirm the presence of DAG1 mRNA in DG $-/-$ cells, total RNA was analysed by northern blotting using a specifically designed RNA probe targeted to the cytoplasmic tail of β -dystroglycan. The RNA probe was DIG (digoxigenin)-labelled and following hybridisation to total mRNA were immunodetected with anti-digoxigenin-AP antisera followed by chemiluminescent development. The results, shown in Figure 3.8, confirm the presence of DAG1 mRNA in DG $-/-$ derived cells. In the absence of DNA markers, the size of the DAG1 band was determined relative to the 18s and 28s ribosomal subunits which are 1.9 kb and 4.8 kb respectively. DAG1 mRNA is 5.8 kb (Ibraghimov-

Beskrovnaya et al., 1992) and a band corresponding to this full length DAG1 transcript was observed (Figure 3.8) confirming the expression of dystroglycan in DG $-/-$ derived fibroblasts.

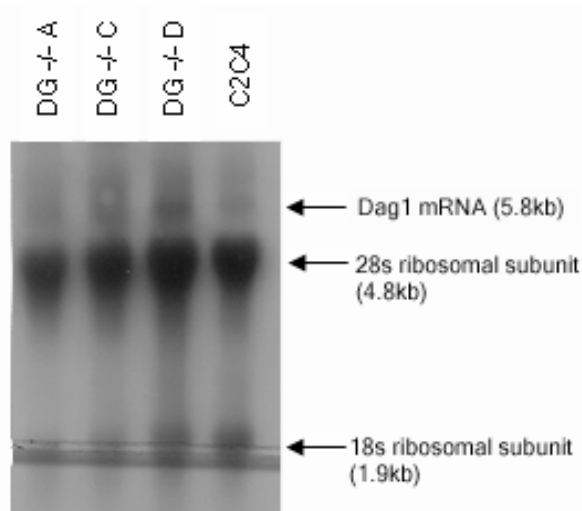


Figure 3.8: Northern blot of DAG1 mRNA. Total RNA was isolated from DG $-/-$ fibroblasts A, C, D and subjected to northern blotting using a DIG-labelled probe that targeted the cytoplasmic tail of β -dystroglycan. C2 C4 mouse myoblasts were used as a positive control for dystroglycan expression.

3.2.5 3C12 epithelial-like DG $-/-$ derived cells expressed dystroglycan

The fibroblasts generated using DG $-/-$ embryonic stem cells were found to express dystroglycan and were therefore unsuitable for further study into dystroglycan deficiency. Consequently, an epithelial-like cell line derived from the same DG $-/-$ ES cells was obtained in order to continue the investigation into dystroglycan deficiency. This cell line will be referred to as 3C12. In addition to this, a positive control cell line (R1) was also obtained, which had a wild type genotype (Zhan et al., 2005). Unfortunately, the R1 cells did not survive the thawing process and could not be cultured. 3C12 cells also had a low rate of survival following thawing, however after a period of recovery, some the expansion of some cell colonies allowed for their analysis. Cell lysates were prepared from 3C12 cells and subjected to western analysis for β -dystroglycan to confirm that they were

dystroglycan null. As shown in Figure 3.9, however, 3C12 cells were found to contain β -dystroglycan and therefore could not be used for further study.

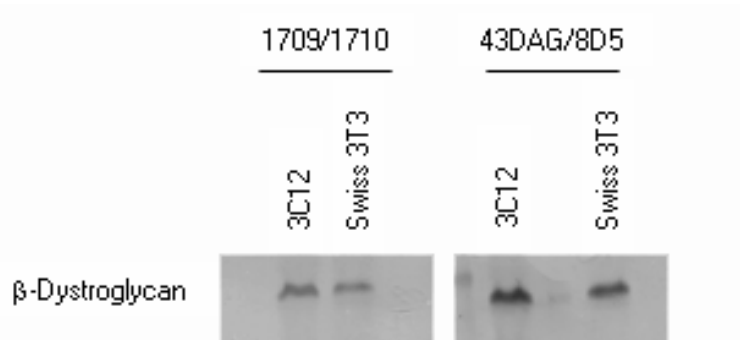


Figure 3.9: Detection of β -dystroglycan in 3C12 cells. Cell lysates from 3C12 were probed for the presence of β -dystroglycan using polyclonal (1709/1710) and monoclonal antisera (43DAG/8D5). Cell lysates from Swiss 3T3 cells were also analysed as a positive control. 3C12 cells were found to express β -dystroglycan, shown using two different anti- β -dystroglycan antisera.

3.2.6 *DG*^{-/-} fibroblasts and 3C12 cells did not contain gene disrupting cassette sequences

To further confirm that the cells obtained in this study had a wild-type genotype and did not contain the hygromycin and neomycin resistance cassette sequences used to disrupt the *DAG1* gene, specific primers were used to detect the presence of these sequences by genomic PCR. Total genomic DNA was isolated from *DG*^{-/-} fibroblasts and 3C12 cells to determine the presence of the targeted gene cassettes using specifically designed primer pairs, illustrated in Figure 3.10 A (primer sequences are detailed in Appendix VIII). Primers DG001/DG006 and primers DG001/DG002 determine the presence of the hygromycin and neomycin resistance cassettes respectively, since their reverse primers are located in the cassette sequences. DG003/DG004 primers act as a diagnostic tool to decipher between wild-type and *DG*^{-/-} cells since the primers are targeted on either side of the neomycin resistance cassette. These primers amplify a 350 bp fragment in wild-type cells and a 1500 bp fragment in dystroglycan null cells since they contain the neomycin resistance gene. The DG003 primer site is deleted in the hygromycin allele and therefore

does not give information about that allele, however, will identify cells contain the neomycin resistance cassette. The results of this PCR, shown in Figure 3.10 B, show that all DG *-/-* cell clones and 3C12 cells do not contain the hygromycin or neomycin resistance cassettes. This is concluded because primers DG001/DG002 and DG001/DG006 did not amplify a PCR product, indicating that these cells do not contain the sequences that the reverse primers anneal to, which are within the resistance genes. Further verification is provided by the fact that primers DG003/DG004 amplified a 350 bp fragment in all of the samples, which is indicative that the neomycin gene cassette is not present because these primers anneal to sequences located on either side of the neomycin resistance cassette and a product of this size is expected in wild-type cells. The results obtained from this analysis confirm that DG *-/-* derived cell clones A, B, C and D and the previously published DG null 3C12 cells all contain dystroglycan and are unsuitable for further study into dystroglycan deficiency.

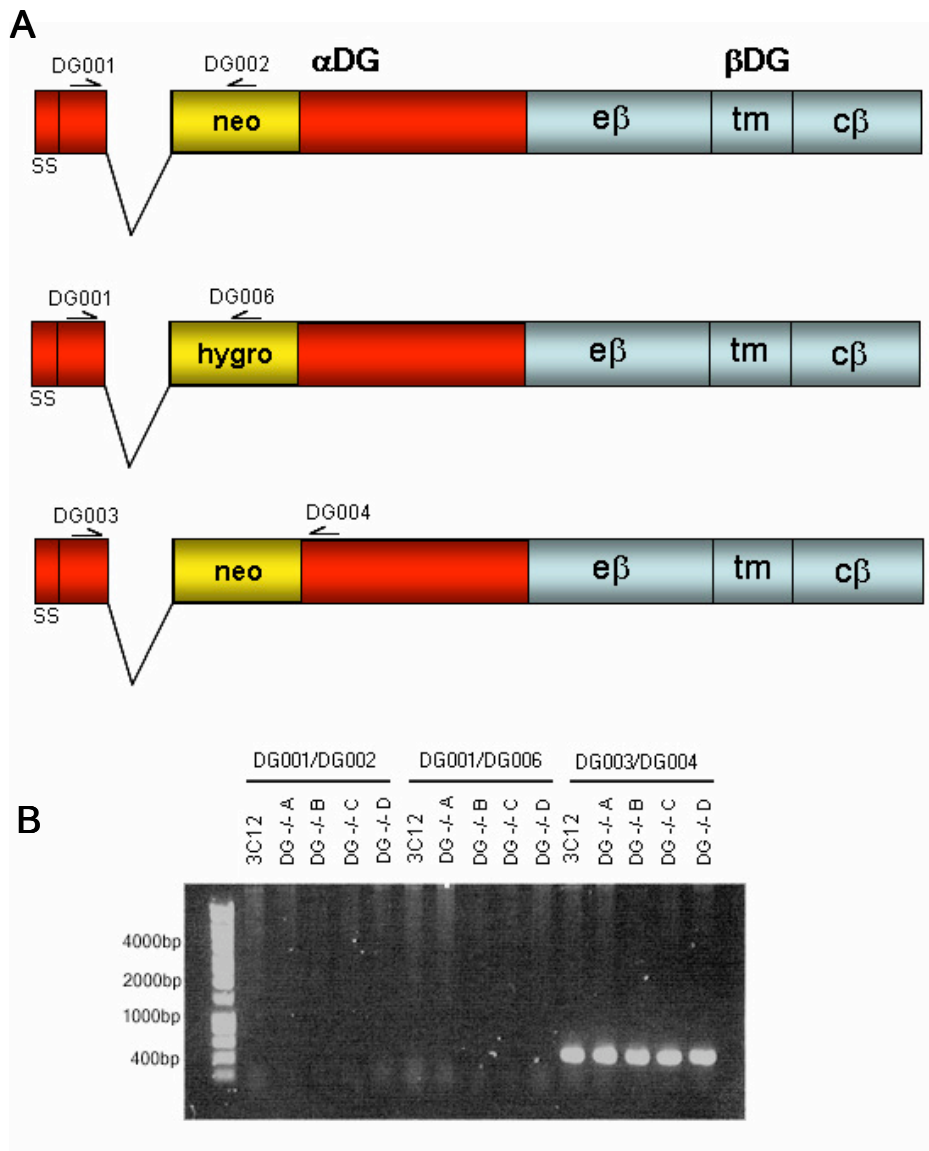


Figure 3.10: Genomic PCR of DG ^{-/-} and 3C12 cells. A: Schematic diagram illustrating the targets of the primer pairs used to determine the presence of disrupting gene cassettes. B: Genomic PCR products of diagnostic primers showing that DG ^{-/-} cells and 3C12 cells did not contain the hygromycin or neomycin resistance cassettes.

3.3 Discussion

In the present study, four fibroblast clones were produced by differentiation of DG *-/-* ES cells in order to investigate the effect of dystroglycan deficiency at the cellular level (Section 3.2.1). The cells used in this study were generated using DG *-/-* mouse embryonic stem cells that were produced by targeted gene disruption of both DAG1 alleles, which were previously used to generate the chimaeric mouse (Cote et al., 1999). Confirmation that the isolated cells were, indeed, fibroblasts, was undertaken by firstly examining the overall cell shape, which were found to have a classic elongated and spindle-shaped fibroblastic morphology (Section 3.2.2.1) and secondly, the specific immunoblotting of DG *-/-* cell lysates for vimentin, an intermediate filament present in cells of mesenchymal origin (Section 3.2.2.2).

Initial observations carried out by immunofluorescence microscopy of DG *-/-* derived fibroblasts stained for α -tubulin and DNA revealed that many cells were multinucleated and/or retained thin intercellular connections despite being well spread and some distance apart (see Section 3.2.2.3). This is indicative of a late cytokinetic defect as it suggests that the cells have failed to separate completely.

Considering that the main objective was to develop and study DG *-/-* fibroblasts, cell lysates were prepared and subjected to western analysis for β -dystroglycan to ensure that they were definitely null. Astonishingly, the cells were found to express β -dystroglycan at similar levels to wild-type cell lines and this was shown using three different anti- β -dystroglycan antisera (Section 3.2.3). All of the anti- β -dystroglycan antisera used in this study have previously been thoroughly characterised and have been shown to be highly specific for the C-terminus of β -dystroglycan (Cullen et al., 1994; Hnia et al., 2007; Ilsley et al., 2001; James et al., 2000; Pereboev et al., 2001). The possibility that these cell lines had been contaminated at some point with different cells is highly

unlikely for several reasons. Firstly, utmost care was taken during the differentiation, isolation and culture of these cells to reduce the risk of cross-contamination, each individual clone having its own separate stock of growth medium. Besides this, the cells did not resemble any other cell line used within the laboratory. Furthermore, considering that each clone was isolated very early on and maintained separately, the risk of cross-contamination of all four clones is highly improbable. Clearly, these cells were deemed unsuitable for further research into dystroglycan deficiency; however, several more investigative steps were undertaken in an attempt to understand why these cells were expressing dystroglycan.

The DG null ES cells used in this study were developed by the incorporation of antibiotic resistance gene cassettes into the coding sequence of DAG1 by homologous recombination. Both DAG1 alleles were targeted with different cassettes encoding either hygromycin or neomycin resistance (Cote et al., 1999). Close examination of the coding sequences following the gene cassette revealed the existence of a possible intra exonic transcriptional re-initiation site (Section 3.2.4), suggesting perhaps that expression of dystroglycan could recommence following disruption by the gene cassette. The predicted re-initiation site lies within exon 2 of DAG1 and the expected protein product would be a truncated α -dystroglycan and full-length β -dystroglycan. Since western analysis was carried out using only anti- β -dystroglycan antisera, the resultant band of the correct size for full-length β -dystroglycan is consistent with this theory. All western analyses carried out using anti- α -dystroglycan antisera were unsuccessful in both DG $-/-$ -derived cell lines and control cell lines, therefore no evidence can be presented to show the existence of a truncated α -dystroglycan protein product. A possible reason for this may be that α -dystroglycan was constitutively shed from the membrane due to proteolytic activity of MMPs, which have previously been reported to act upon dystroglycan (Herzog et al.,

2004; Yamada et al., 2001). However, since α - and β -dystroglycan are expressed as a single polypeptide and post-translationally cleaved, the existence of β -dystroglycan leads to the assumption that α -dystroglycan was also expressed, albeit possibly in a truncated form.

The re-initiation hypothesis was, however, disproved by amplification of specific DAG1 mRNA sequences by RT-PCR (see Section 3.2.4.1). Primers designed to recognise β -dystroglycan and a region encompassing the latter portion of α -dystroglycan and the early portion of β -dystroglycan amplified RT-PCR products from total RNA isolated from DG $-/-$ derived fibroblasts (Figure 3.7 (b) and (c)). The results also showed that regions existing prior to the putative re-initiation site were amplified by primers recognising these regions, suggesting that a complete DAG1 mRNA transcript was, in fact, being expressed in DG $-/-$ cells (Figure 3.7 (a) and (d)). This data strongly suggests that the DG $-/-$ clonal fibroblasts had somehow lost the hygromycin and neomycin gene cassettes that were incorporated into the ES cells from which they were derived.

To confirm the expression of the complete DAG1 mRNA transcript in DG $-/-$ cells, total RNA was isolated and subjected to northern blot analysis for the detection of dystroglycan mRNA (Section 3.2.4.2). The DAG1 gene encodes a 5.8kb mRNA transcript (Ibraghimov-Beskrovnaya et al., 1992) and a band of this size was identified (Figure 3.8), thus further substantiating the evidence to suggest that the DAG1 gene was not disrupted in DG $-/-$ cells.

Consequently, new epithelial-like cells (3C12) derived from DG $-/-$ ES cells (a gift from S. Carbonetto (Zhan et al., 2005)) were cultured as an alternative to the DG $-/-$ fibroblasts. There was, however, a low survival rate following thawing of 3C12 cells and when eventually the cells did recover, allowing for their analysis, they too were found to

express β -dystroglycan (Section 3.2.5) and were therefore unsuitable for further investigation.

Conclusive evidence to show that the DG null ES-derived cell lines did not contain the hygromycin and neomycin gene targeting cassette was achieved by genomic PCR (Section 3.2.6). Primers designed to recognise sequences within the gene targeting cassettes did not amplify a product. Moreover, the amplification of a specific DNA sequence using primers that exist on either side of the neomycin cassette produced a 350 bp product, which confirms their wild-type genotype since a product of 1500 bp would be expected if the neomycin cassette was present. Although every effort was made in this study to minimise cross-contamination, it is possible that the targeted embryonic stem cell clones that were originally sent may have contained contaminating *wt* embryonic stem cells and these may have been favourably selected by limiting dilution. Other than contamination from another cell line, another explanation is the possibility that the incorporation of the gene targeting cassettes was unstable and they were subsequently lost by further homologous recombination events. It is now clear that by verifying the resistance of the DAG *-/-* derived cells to hygromycin and neomycin early on in their analysis would have given a clear indication as to whether the cells were indeed correctly targeted.

In conclusion, the four clonal fibroblast cell lines derived from DG *-/-* ES cells were all found to express dystroglycan and did not carry the targeted gene cassettes that were originally incorporated into both alleles of the DAG1 gene of the ES cells. Possible reasons for this unexpected expression have been explored but the mystery as to how these cells came to express dystroglycan remains to be solved. Consequently, another approach was undertaken to generate dystroglycan deficient fibroblasts and this will be addressed in Chapter 4.

Chapter 4: Investigation of dystroglycan-deficiency in fibroblasts

Chapter 4

Investigation of dystroglycan deficiency in fibroblasts

4.1 Introduction

The aim of this research was to gain further understanding of the role dystroglycan plays in the cell using a loss of function approach. The rationale behind loss of function studies is to learn more about a chosen protein by characterising the phenotype resulting from complete loss or knockdown of its expression. One method of doing this is to generate a knockout animal, such as a null mouse. However, as described in Chapter 3, the dystroglycan null-derived mouse fibroblasts used in this study were found to express dystroglycan, and therefore could not be used as a model for dystroglycan deficiency. Consequently, stable dystroglycan knockdown fibroblasts were generated by RNA interference (RNAi) to investigate the phenotype caused by sustained dystroglycan deficiency.

RNAi exploits a cells inherent post-transcriptional gene silencing mechanism in response to double-stranded RNA in order to knockdown the expression of a target gene (Fire et al., 1998). The dsRNA is cleaved into 21-23 nucleotide small interfering RNA molecules (siRNA) which bind to a nuclease complex to form an RNA-induced silencing complex (RISC) that binds and cleaves target mRNA transcripts (Hutvagner and Zamore, 2002; Nykanen et al., 2001). RNAi is an effective method for gene silencing since it is highly specific, inexpensive and relatively straightforward to accomplish. In the present study, a DNA construct expressing hairpin siRNA molecules (shRNA) specific for mouse DAG1 was introduced to Swiss 3T3 mouse fibroblasts. This construct uses the cell's own RNA polymerase III to transcribe antisense siRNA targeted to the DAG1 gene using the human U6 promoter, which induces a high level of expression (Kunkel and Pederson, 1989). The construct was integrated into the cells genome by retroviral infection to

maximise the expression efficiency and promote permanent and stable shRNA gene expression. A stable knockdown cell line system was preferentially used in this study because transient transfection is only short-lived and to achieve full characterisation of the phenotype long-term stable knockdown of dystroglycan gene expression was required.

Previous studies investigating dystroglycan knockdown have focussed on its function in development and disease in animal model systems. The aim of this study was to investigate the effect of dystroglycan deficiency in fibroblasts in order to gain insight into the fundamental functions of dystroglycan at the cellular level.

4.2 Results

4.2.1 Establishment of stable dystroglycan knockdown fibroblasts

4.2.1.1 shRNA knockdown

In this study, stable dystroglycan knockdown Swiss 3T3 fibroblasts were generated by RNAi. Several potential sequences were chosen for their specificity to mouse DAG1 and suitability for RNAi using the 'RNAi target sequence prediction' tool on the BBSRC Chick EST database (<http://www.chick.umist.ac.uk/>). Four sequences were selected and used to generate constructs encoding antisense siRNA hairpin oligonucleotides (shRNA), which act as RNA interference molecules that suppressed the expression of dystroglycan. Sequences were chosen for their suitability for RNAi based on several criteria including GC content, T_m of sense/antisense duplex and the differential stability of the sequence ends and ranked depending on their similarities to the optimal values (details at <http://bioinfo.clontech.com/rnaidesigner/>). Each of the four dystroglycan shRNA pSIREN constructs were stably transfected into the packaging cell line, PT67, which produces a non-replicative retrovirus carrying the shRNA vector. A preliminary analysis of the transfected PT67 cell lines was carried out as an indication of the dystroglycan knockdown efficiency of each of the shRNA sequences since the shRNA sequences are designed to target the mouse DAG1 gene and PT67 cells are derived from a mouse fibroblast (NIH 3T3) cell line. Cell lysates from transfected PT67 cells were prepared and analysed for dystroglycan expression by western analysis. As shown in Figure 4.1, all of the shRNA sequences induced a reduction in β -dystroglycan expression in PT67 cells compared to cells transfected with a control construct. Ultimately, shRNA 1319 (mouse DAG1 1319 AACTACCACA ACTCGGAGGCC 1340) was selected to generate knockdown cells because overall it was the highest scoring sequence according to the criteria set for effective RNAi. Swiss 3T3 cells were exposed to two rounds of retroviral infection and a

clonal stable cell line was established by antibiotic selection followed by limiting dilution. A stable knockdown cell line system was preferentially used because transient transfection is only short-lived and to achieve full characterisation of the phenotype long-term stable knockdown of gene expression was required. Ideally, dystroglycan knockdown cells derived using several shRNA targeting different DAG1 sequences would have been generated, which would address any non-specific effects of one particular sequence. In addition to this, it would be beneficial to examine several different clones generated from each shRNA to check for off target effects of the shRNA and/or effects of the retroviral insertion site. In this study, the dystroglycan knockdown Swiss 3T3 fibroblast cell line will be referred to as DG - cells.

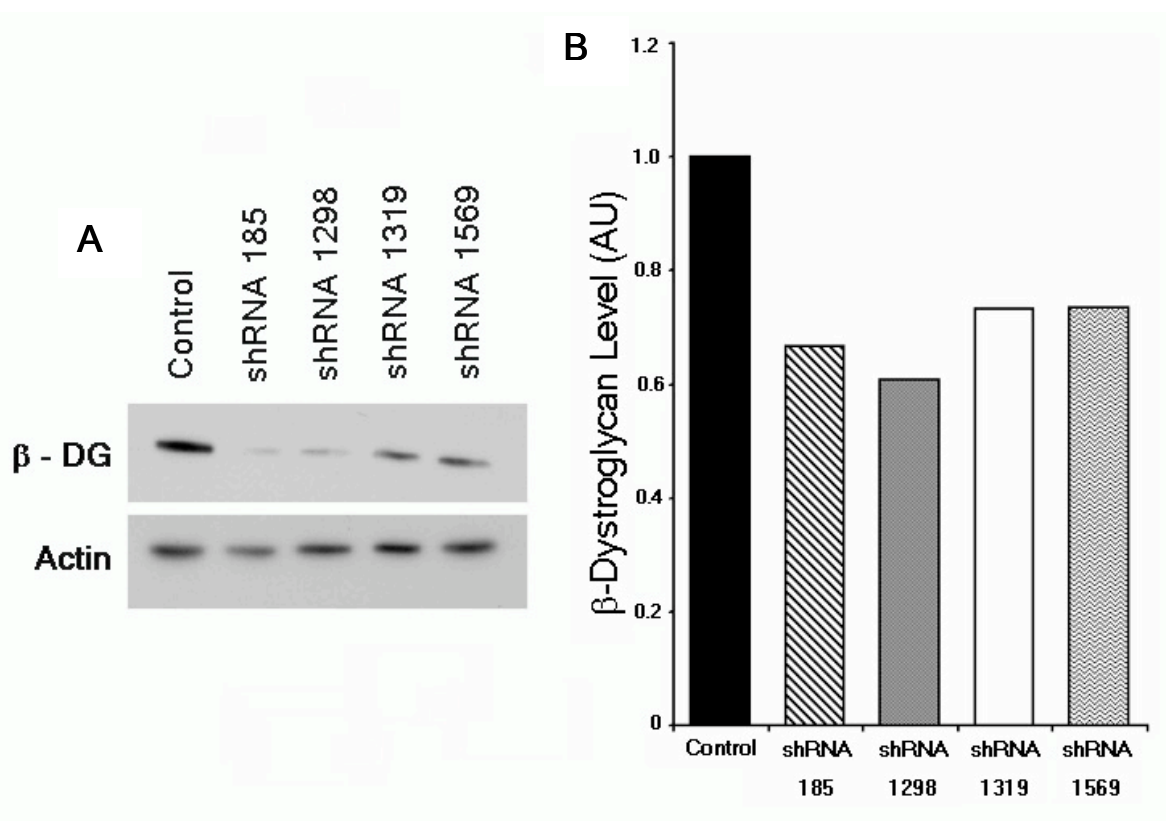


Figure 4.1: Four different shRNA sequences specific for dystroglycan induced a reduction in dystroglycan expression when stably transfected into PT67 packaging cells. A: β -Dystroglycan protein expression levels in cell lysates prepared from shRNA transfected PT67 packaging cell lines were compared by western blotting relative to an actin loading control. B: β -Dystroglycan expression levels were quantified by measuring integrated density of the resultant bands using NIH Image and are expressed as β -dystroglycan/actin.

4.2.1.2 shRNA control

For the purpose of this study, a negative control cell line was generated alongside the DG - cells in order to control for any side-effects caused by either the shRNA vector or retroviral infection. In order to generate such a negative control, Swiss 3T3 cells were infected with an RNAi vector expressing an oligonucleotide with no homology to mouse DAG1. Initially, the sense strand of the luciferase gene was used, however, after creating a stable cell line, there was an increase in the abundance of senescent cells which may have been a result of non-specific effects of this sequence (Figure 4.2), for this reason these cells were discarded. Consequently, an alternative negative control was generated using the sense strand complimentary to the chosen antisense DAG1 shRNA sequence (GTTGATGGTGTGAGCCTCCG), which had no homology to any other sequences in the mouse genome. The resultant Swiss 3T3 cell line was indistinguishable from wild-type Swiss 3T3 fibroblasts and will henceforth be referred to as DG + cells.

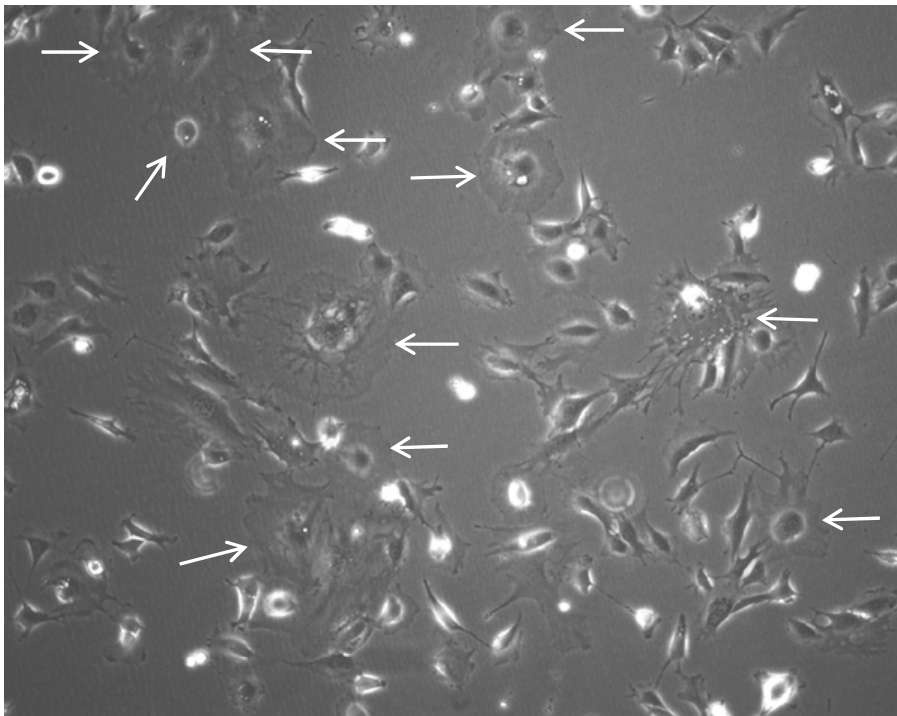


Figure 4.2: Phase contrast image of negative control generated by retroviral infection of a construct containing the sense strand of the luciferase gene. Following cloning out by limiting dilution, many cells appeared large and senescent (arrows).

4.2.2 Quantification of dystroglycan knockdown

In order to determine the efficiency of dystroglycan knockdown, the dystroglycan protein expression level was determined in DG + and DG - cells. Semi-confluent cells were lysed directly in their cell culture vessels and analysed by immunoblotting using monoclonal β -dystroglycan antisera. In order to quantify dystroglycan expression, the intensity of the dystroglycan bands was measured using NIH Image and normalised against an α -tubulin loading control. A clone with ~60% decrease in dystroglycan expression was chosen for further characterisation (see Figure 4.3). The highest level of dystroglycan knockdown achieved was ~80% in non-clonal transfected cells, however, this could not be maintained in a permanent stable cell line, possibly because a limiting threshold level of dystroglycan is required for cell survival.

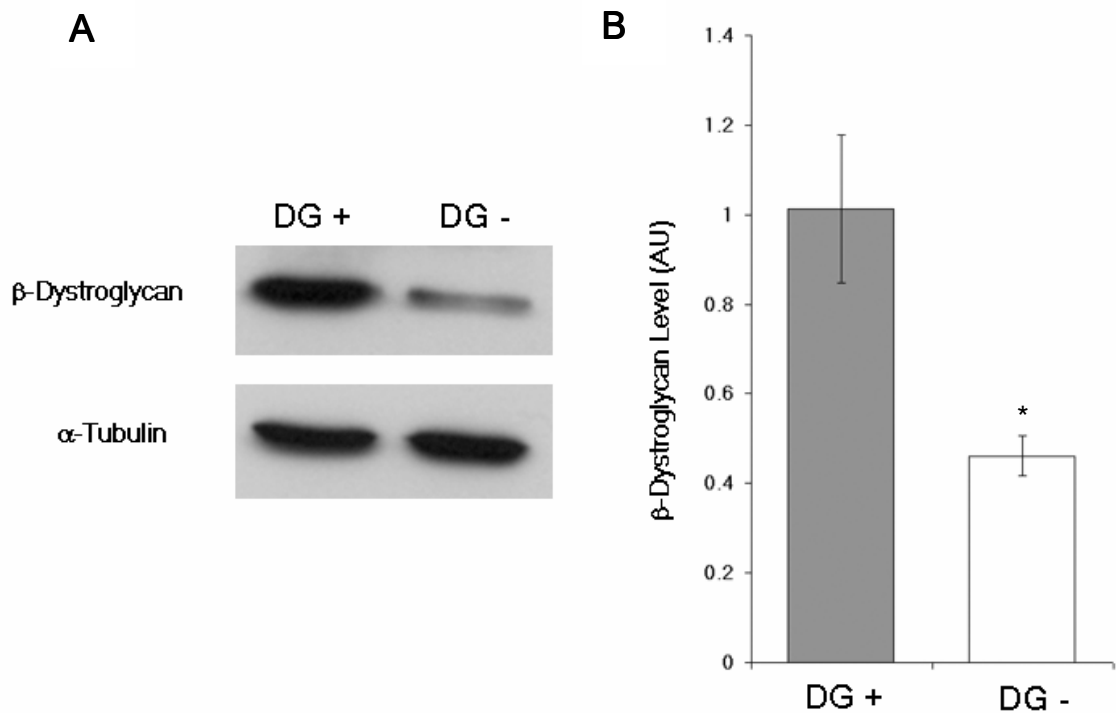


Figure 4.3: Quantification of dystroglycan expression following shRNA knockdown. A: β -Dystroglycan protein expression levels in DG + and DG - cells were compared by western blotting relative to an α -tubulin loading control. B: Expression levels were quantified by measuring integrated density of the resultant bands using NIH Image. β -dystroglycan expression levels are expressed as β -dystroglycan/ α -tubulin. The values attributed to dystroglycan expression level are represented in arbitrary units (\pm SE, $n = 3$, * $p < 0.05$).

4.2.3 *DG - fibroblasts have a reduced cell area and are less rounded than control*

Following the generation of stable dystroglycan knockdown fibroblasts, cell morphology was characterised and compared with that of the control. Dystroglycan has multiple binding partners and is involved in numerous cell signalling pathways (see Chapter 1), therefore we would expect to see morphological changes in DG - cells that reflect the importance of this protein within the cell.

Initially, overall morphology was investigated by immunofluorescence microscopy. Semi-confluent cells were stained with rhodamine phalloidin to visualise F-actin and probed with specific monoclonal antisera to visualize cortactin by indirect immunofluorescence (Figure 4.4 A). Cortactin is an F-actin binding protein that is abundant in the cell cortex (Wu and Parsons, 1993) and was used in this experiment to discern the periphery of the cell in order to analyse cell size and shape. After visualisation of the actin cytoskeleton, total cell area and circularity were determined using Image J software. As is evident from Figure 4.4, DG - cells have a significantly decreased cell area compared to that of DG + cells (Figure 4.4 B). Since dystroglycan is an adhesion molecule, this may reflect the cell's inability to spread completely as a result of decreased dystroglycan expression.

During culture, it was observed that DG + cells appeared more rounded than DG - cells. In order to determine if this was a real difference in cell morphology attributable to dystroglycan deficiency, the overall circularity of both cell types was calculated, as described in Section 2.2.9, whereby a value of 1.0 designates a perfect circle. According to Figure 4.4 there was a highly significant difference in cell morphology between the two samples; DG - cells exhibited a much more elongated and jagged morphology whereas control cells were relatively uniformly spread (Figure 4.4 C). Following on from the previous observation that overall cell area is decreased, the less rounded morphology

exhibited by DG - cells is possibly also the result of reduced cell spreading, perhaps owing to a reduction in the number of cell-substrate adhesions.

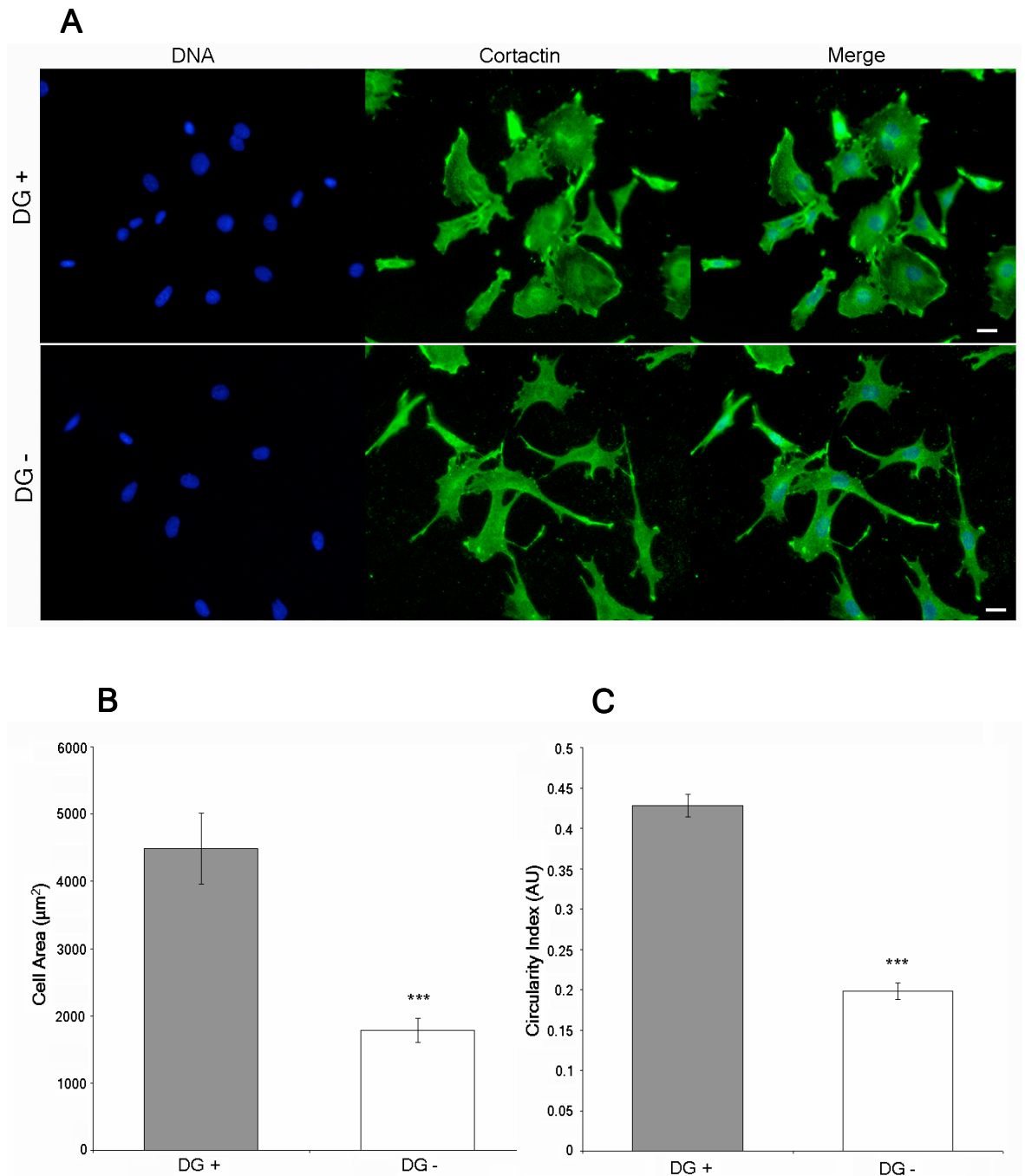


Figure 4.4: Effect of dystroglycan depletion on size and shape of Swiss 3T3 fibroblasts. Cells were stained for cortactin, imaged by immunofluorescence and their area and circularity measured using Image J software. A: DG + and DG - cells stained for cortactin (green) and DNA (blue). Scale bar = 20 μm . B: The mean area (μm^2) of DG + and DG - fibroblasts is shown. C: The overall circularity of DG + and DG - fibroblasts was calculated using Image J software as described in Section 2.2.9. The area and circularity of 100 cells were measured per sample and graphs represent a mean of these results ($\pm\text{SE}$, *** $p < 0.001$).

4.2.4 Focal adhesions are reduced in DG - cells

The results obtained from measuring the area and circularity of DG - cells indicated that they are more spindle shaped than DG + cells. Since dystroglycan is a cell adhesion molecule, a possible explanation of this may be that DG - cells have a reduced number of cell-substrate adhesions, otherwise known as focal adhesions. In order to address this possibility, DG + and DG - cells were seeded onto glass coverslips, fixed and stained for the universal adhesion marker, vinculin (Geiger et al., 1980). Immunofluorescence images of both samples were captured (Figure 4.5 A) and used to compare the quantity and size of focal adhesions in each cell line (Figure 4.5 B-C). In this study, the term “focal adhesion” will refer to all types of cell-substrate adhesions.

As mentioned previously (see Section 4.2.3), DG - cells were found to be markedly smaller than the control. Hence, the observable difference in the quantity of focal adhesions per cell may be misleading since smaller cells are likely to have less adhesions overall. To take this into consideration and to determine whether there was an actual reduction in focal adhesions irrespective of cell size, the number of adhesions per cell area was calculated. The results, shown in Figure 4.5 (B), indicate that DG - fibroblasts have significantly fewer focal adhesions per μm^2 than DG + cells, which supports the hypothesis that their smaller size may be due to an inability to spread due to less contacts with the substrate or due to fewer stress fibres as a result of downregulation of Rho.

From visual inspection of vinculin staining by immunofluorescence, it is not only apparent that DG - cells have a decreased number of focal adhesions, but the adhesions themselves also appear smaller than those found in DG + cells (Figure 4.5 A). In order to quantify this observation, focal adhesions visualised by vinculin staining were counted and broadly categorised according to their size ($< 2 \mu\text{m}$, $> 2 \mu\text{m}$ and $>2 \mu\text{m}$ elongated). According to Figure 4.5 C, DG - cells and DG + cells contained similar proportions of

small adhesions ($< 2 \mu\text{m}$) and adhesions that were $> 2 \mu\text{m}$. However, DG - cells did have a significantly lesser proportion of large elongated adhesions ($> 2 \mu\text{m}$ elongated); which suggests that dystroglycan may also be involved in the establishment of larger, more mature adhesions.

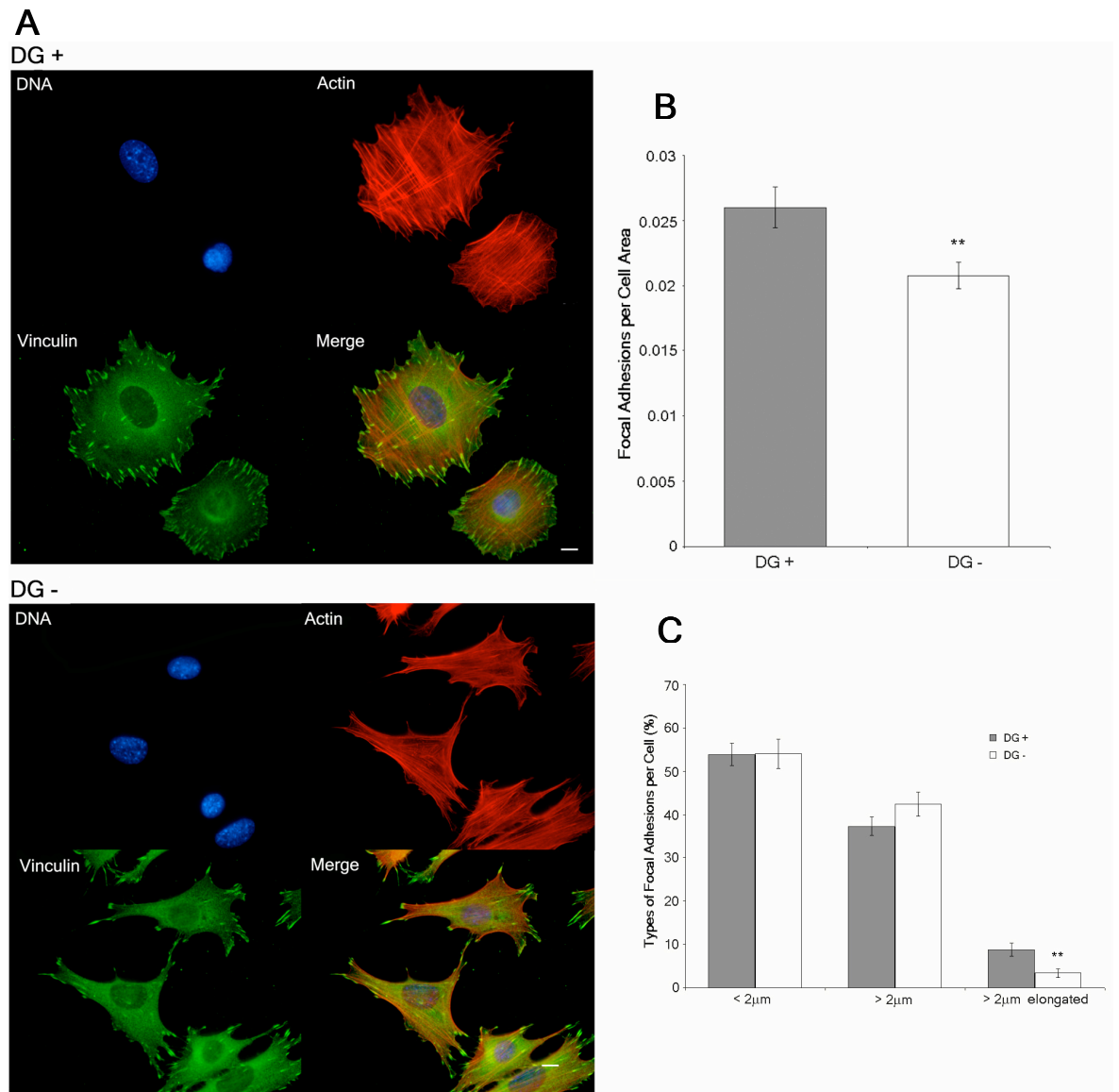


Figure 4.5: Effect of dystroglycan knockdown on number and size of focal adhesion complexes. A: Immunofluorescence staining of DG + and DG - cells stained for vinculin (green), F-actin (red) and DNA (blue). Scale bar = $10 \mu\text{m}$. B: Quantification of focal adhesions per cell area. Focal adhesions were manually counted in vinculin-stained DG - and DG + cells and normalised to total cell area, as determined (in μm^2) using Image J software. Data is represented as the mean number of focal adhesions per cell area ($\pm\text{SE}$, $n = 35$). C: Categorisation of focal adhesion size. The relative proportions of focal adhesions were calculated for each cell line ($\pm\text{SE}$, $n = 36$, ** $p < 0.01$).

4.2.5 DG - cells have weak actin stress fibres but no decrease in F-actin content

Previous results have shown that DG - cells are generally smaller, more spindle-shaped and have a reduced number of focal adhesions when compared to DG + fibroblasts (Sections 4.2.3-4). Dystroglycan is not only an important extracellular cell adhesion molecule, but it has also been found to recruit proteins that modulate the actin cytoskeleton (Chen et al., 2003; Spence et al., 2004a). Therefore, depletion of endogenous dystroglycan may have adverse effects on actin cytoskeletal organisation. To investigate this hypothesis, DG - cells were stained for F-actin with rhodamine phalloidin and the actin cytoskeleton visualised by immunofluorescence. According to Figure 4.6 A, it appears that overall fluorescent intensity of F-actin in DG - cells is reduced in comparison to the control. In addition, the actin stress fibres appear spindly and fragile when compared to those in DG + cells.

To investigate the hypothesis that dystroglycan depletion disrupts F-actin production and/or stability, an actin fractionation assay was carried out in DG + and DG - cells to quantify the proportions of G- and F-actin. Cell lysates were harvested and subjected to ultracentrifugation, as described (see Section 2.2.20), resulting in soluble G-actin monomers in the supernatant and insoluble F-actin fractionated into the pellet. Following re-suspension of the pellet, equal volumes of each fraction were separated by SDS-PAGE and analysed by immunoblotting using anti-actin antisera. Percentages of actin in the supernatant and pellet fractions were quantified by measuring the integrated density of the actin bands using NIH Image software. The results of this fractionation represented in Figure 4.6 C as the percentage of F-actin content, show that there is a slight, but not significant, reduction in F-actin in DG - cells compared to the control. Fluorescence microscopy revealed a reduction in stress fibres, which was very noticeable visually,

however this does not necessarily correlate with a reduction in total F-actin content and the biochemical analysis showed this to be the case.

A possible explanation for the visual differences in phalloidin staining may be that there is a reduction in actin bundling in response to dystroglycan knockdown, thus making the stress fibres appear less robust by immunofluorescence imaging. Further investigation is required to understand the apparent alteration in F-actin morphology.

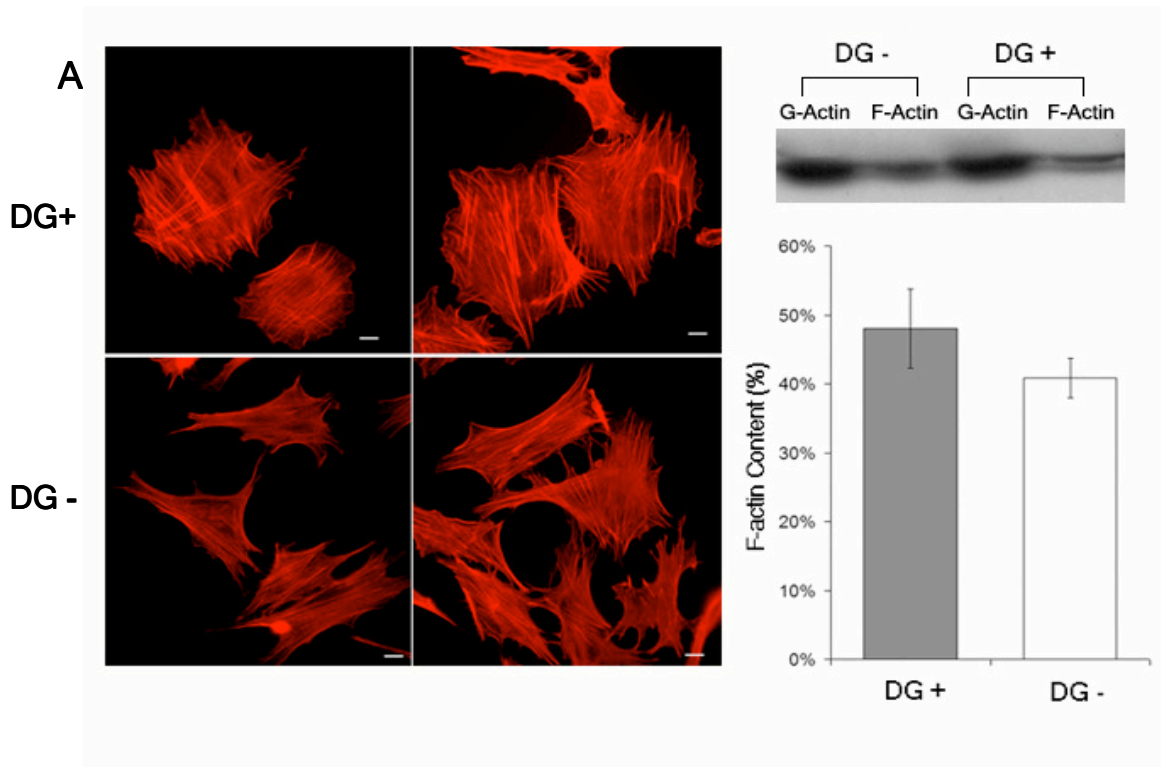
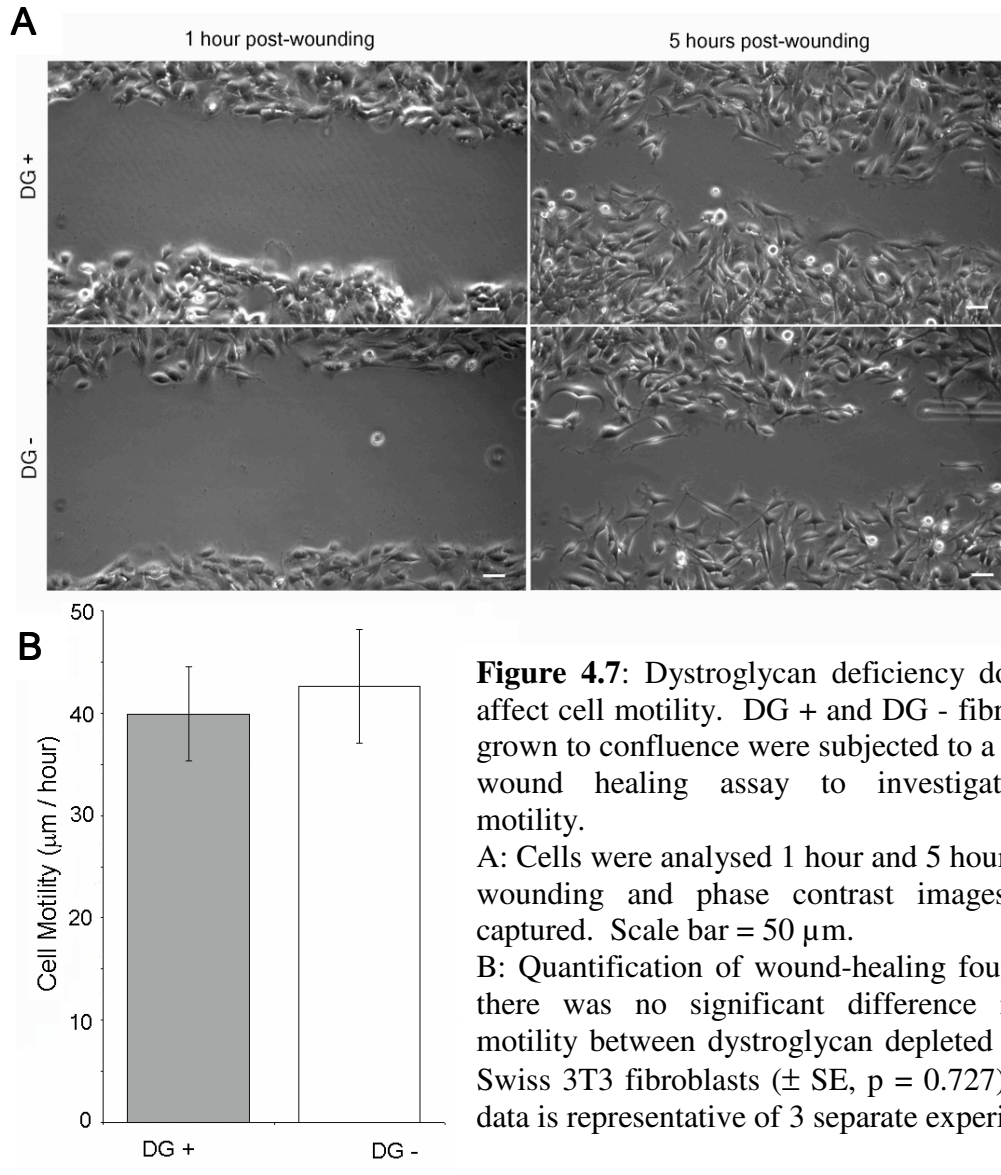


Figure 4.6: Quantification of F-actin content. A: Rhodamine phalloidin staining of DG - and DG + cells. DG - appear to have weaker actin stress fibres than DG +. Both images were taken at the same exposure. Scale bar = 10 μ m. B: DG + and DG - fibroblasts were lysed in actin fractionation buffer and subjected to ultracentrifugation to separate G- and F-actin. Samples were analysed by immunoblotting using anti-actin antisera and the intensities of the bands quantified using NIH image. C: Quantification of actin fractionation showed that there was no significant difference in F-actin content between DG + and DG - cells (\pm SE, n = 3, p = 0.306).

4.2.6 Dystroglycan deficiency does not affect cell motility

Recent evidence has suggested that dystroglycan is involved in modulating the actin cytoskeleton, particularly in the formation of filopodia (Spence et al., 2004a). Since cell motility is governed by the actin cytoskeleton, DG - cells were subjected to an *in vitro* scratch wound healing assay to investigate the effect of dystroglycan deficiency on cell motility. Cells were seeded into round tissue culture dishes and grown to confluence. Subsequently, a straight wound was made across the cell monolayer and the cells ability to move into the wound was observed over a 5 hour period. Cell motility was quantified by measuring the width of the wound at 1 hour and 5 hours post-wounding and calculating the distance the cells had migrated in $\mu\text{m}/\text{hour}$. The results show that DG - cells moved into the wound at approximately the same rate as DG + cells (Figure 4.7). This evidence suggests that dystroglycan is not essential for actin-based motility in fibroblasts, otherwise there was sufficient dystroglycan expression remaining in the DG - cells to allow for normal cell migration.



4.2.7 Dystroglycan deficiency does not affect cell polarity

Correct cytoskeletal organisation is vital for many cellular processes including cell polarity (Etienne-Manneville, 2004). RNAi studies carried out in drosophila have shown that dystroglycan knockdown disrupts epithelial cell polarity during oogenesis (Deng et al., 2003) and this has also been reported in the study of breast tumour epithelial cells in which dystroglycan expression is functionally diminished (Muschler et al., 2002). Because this is the first characterisation of the cytoskeleton in dystroglycan-deficient fibroblasts, this study utilized the scratch wound model to investigate the ability of fibroblasts to polarise and hence determine if dystroglycan is similarly involved cell polarity in this cell type.

The scratch wound model exploits the observation that, as fibroblasts migrate towards a wound, their microtubule organising centre (MTOC) reorientate forward of the nucleus in the direction of cell migration (Kupfer et al., 1982). In the present study, DG + and DG - cells were subjected to a wound healing assay followed by fixation and staining with anti- α -tubulin antisera before visualisation by immunofluorescence (Figure 4.8 A). To quantify cell polarity, cells at the wound edge were scored depending on the position of their MTOC relative to the wound edge. MTOC within 120° of the wound edge were scored positively for normal polarity as illustrated in Figure 4.8 B. The results indicate that DG + and DG - cells polarise towards the wound edge to the same extent (Figure 4.7 C). Consequently, it appears that the level of dystroglycan deficiency seen here does not disrupt cell polarity in Swiss 3T3 fibroblasts.

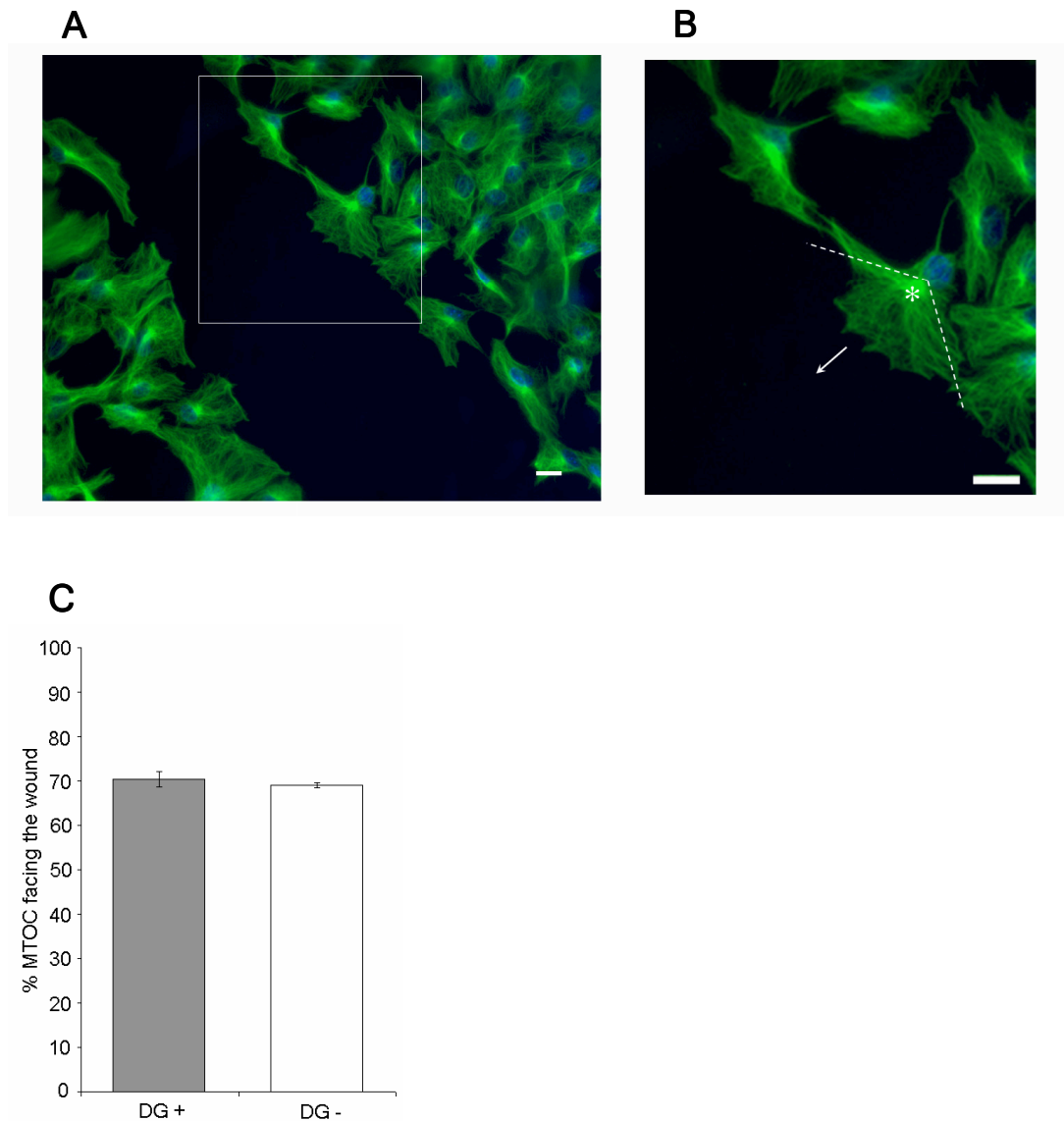


Figure 4.8: Dystroglycan deficiency does not affect cell polarity. **A:** Semi-confluent cells were wounded, fixed, stained for α -tubulin (green) and DNA (blue), and visualised by immunofluorescence. Scale bar = 20 μ m **B:** Cell polarity was determined by locating the position of the MTOC of cells on the edge of the wound in relation to the wound edge. If the MTOC (asterisk) was within 120° of the wound edge (dashed lines), cells were scored positively. Arrow indicates direction of cell migration into the wound. **C:** Quantification of wound edge polarity found that there was no significant difference between *wt* and dystroglycan deficient Swiss 3T3 fibroblasts ($p = 0.512$). Values are represented as mean percentage cells with correct cell polarity (\pm SE, $n = 3$). 100 cells were counted per experiment.

4.2.8 DG - cells exhibit a reduced proliferation rate

Observations made during the maintenance of DG - cells in culture, based upon frequency of passaging, suggested that they had a reduced proliferation rate compared to DG + cells. To determine whether DG - cells had a growth defect, a proliferation assay was carried out over a five day period. Briefly, DG + and DG - cells were each seeded at equal density ($\sim 3 \times 10^4$ cells per dish) into five tissue culture dishes on Day 0, harvested sequentially over a five day period and cell count determined using a haemocytometer. According to Figure 4.9, DG - cells have a markedly reduced proliferation rate compared to the control, suggesting that dystroglycan deficiency affects the cells ability to proliferate.

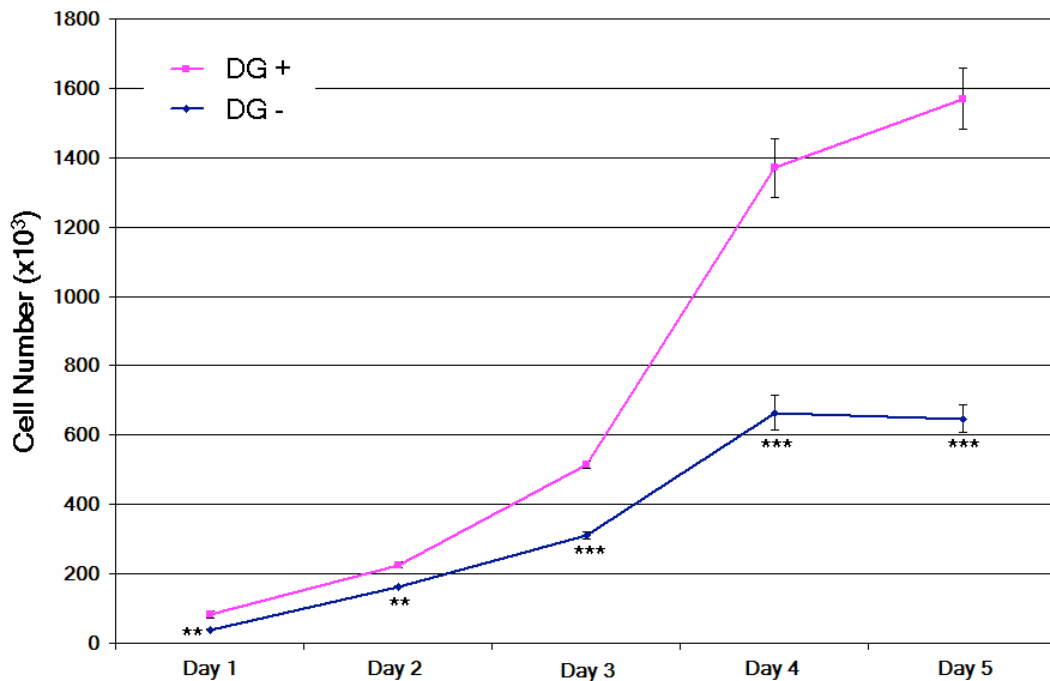


Figure 4.9: DG - cells have a reduced proliferation rate. Cells at approximately equal density (3×10^4 cells per dish) were seeded onto five tissue culture dishes on Day 0 and cell number calculated using a haemocytometer over a five day period. DG - cells had a reduced cell proliferation rate compared to the control (\pm SE, n = 3, *** p < 0.001)

4.2.9 DG - cells do not have reduced mitotic index

To further investigate the finding that DG - cells have a reduced proliferation rate compared to DG + cells, the mitotic indices of DG + and DG - cells were determined. Dystroglycan protein levels have previously been shown to fluctuate as cells pass through the cell cycle, whereby dystroglycan expression peaks during S-phase (Hosokawa et al., 2002; Sgambato et al., 2006). Therefore, if dystroglycan is essential for passage through the cell cycle, dystroglycan deficiency may be perturbing its progression. Consequently, this investigation aimed to establish if there was an accumulation of DG - cells in S-phase. To address this, cells were treated with BrdU before being fixed and stained with anti-BrdU antisera to highlight cells undergoing DNA replication. BrdU is a thymidine analogue that incorporates into newly synthesised DNA, allowing for the detection of actively proliferating cells. According to Figure 4.10, DG - cells appear to have a slight reduction in BrdU incorporation compared to DG + cells, but this was not found to be significant. Therefore, the reduced proliferation rate exhibited by DG - cells cannot be attributed to the inhibition of DNA replication.

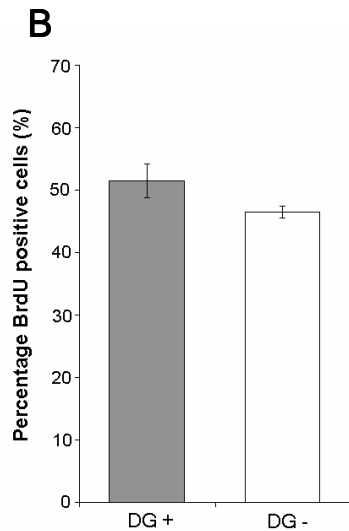
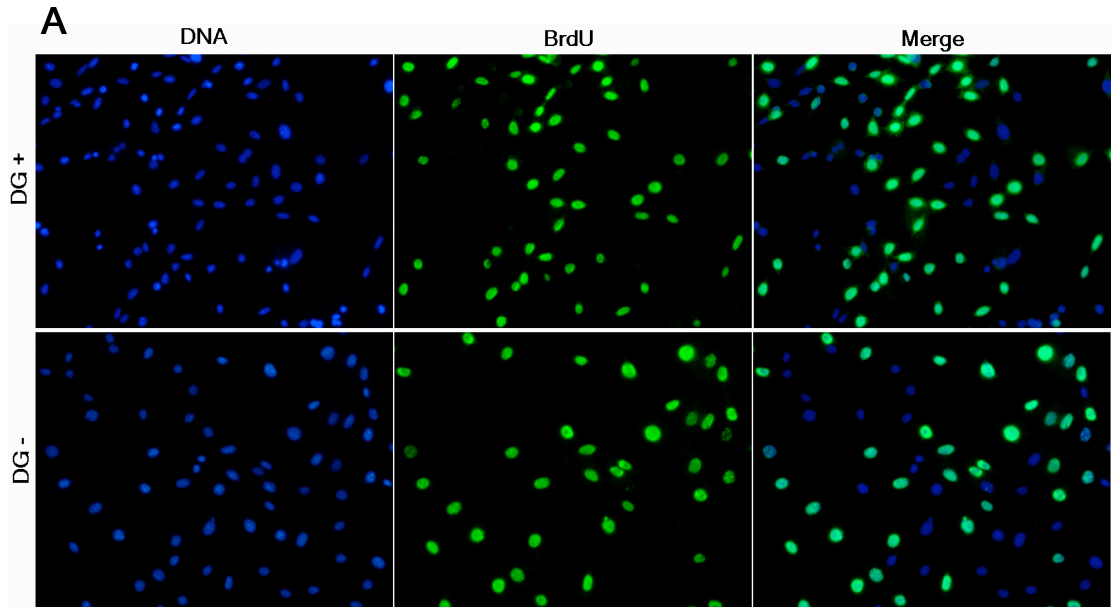


Figure 4.10: Effect of dystroglycan deficiency on mitotic index. Cells treated with BrdU for 45 minutes, followed by fixation and staining with anti-BrdU antisera were visualised by immunofluorescence (A) and the mitotic index was calculated as percentage mitotic cells. Cells were co-stained for DNA with DAPI to facilitate total cell count. There was found to be no significant difference in the mitotic index of *wt* and dystroglycan deficient Swiss 3T3 fibroblasts (\pm SE, $n = 3$, $p = 0.149$). ~1000 cells were counted per experiment.

4.2.10 DG - cells do not have a multinucleate phenotype

This study has previously shown DG - cells to have a slower proliferation rate, but a similar mitotic index, to that of the control (Sections 4.2.7-8). These observations may be explained by a possible defect in cytokinesis. To investigate this, the proportion of multinucleate cells in the cell population was determined. DNA was visualised using DAPI, and nuclear morphology was examined by fluorescent microscopy. Multinucleate cells are defined as those having two or more nuclei per cell and example images are shown in Figure 4.11 A. Following quantification (Figure 4.11 B), it became apparent that DG - cells do not have a multinucleate phenotype, since the number of multinucleate cells

calculated for both samples was at a low frequency and within the level normally expected in cultured cells.

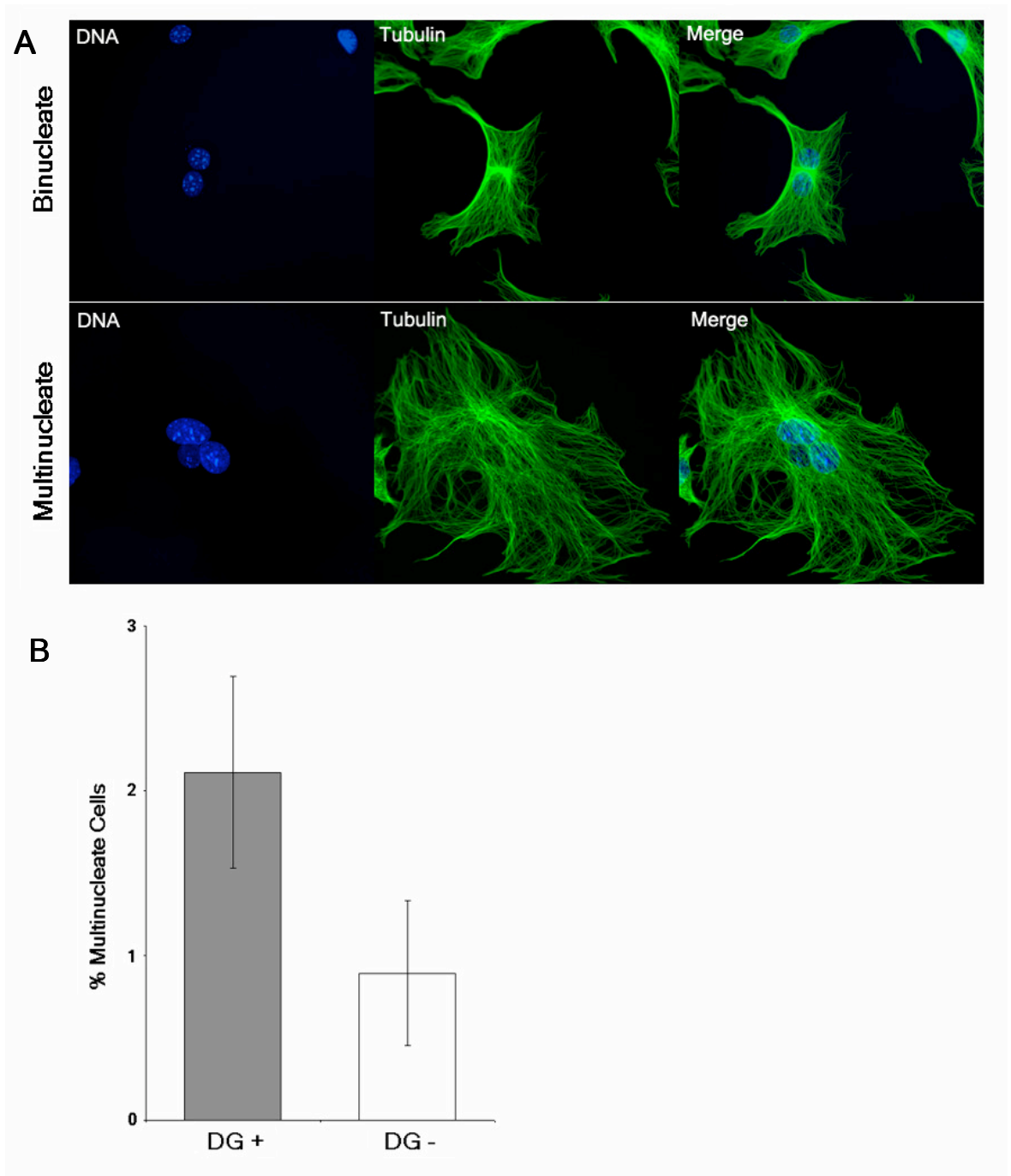


Figure 4.11: Effect of dystroglycan knockdown on the degree of multinucleation. A: Immunofluorescence images of binucleate and multinucleate morphologies present in the cell population. Cells were stained for α -tubulin (green) and DNA (blue). B: The percentage of multinucleate cells in DG + and DG - cells was calculated. There was found to be no significant difference in the number of mitotic cells between *wt* and dystroglycan deficient Swiss 3T3 fibroblasts (\pm SE, $n = 3$, $p = 0.17$). ~800 cells were counted per experiment.

4.2.11 DG - cells have an altered cell cycle profile

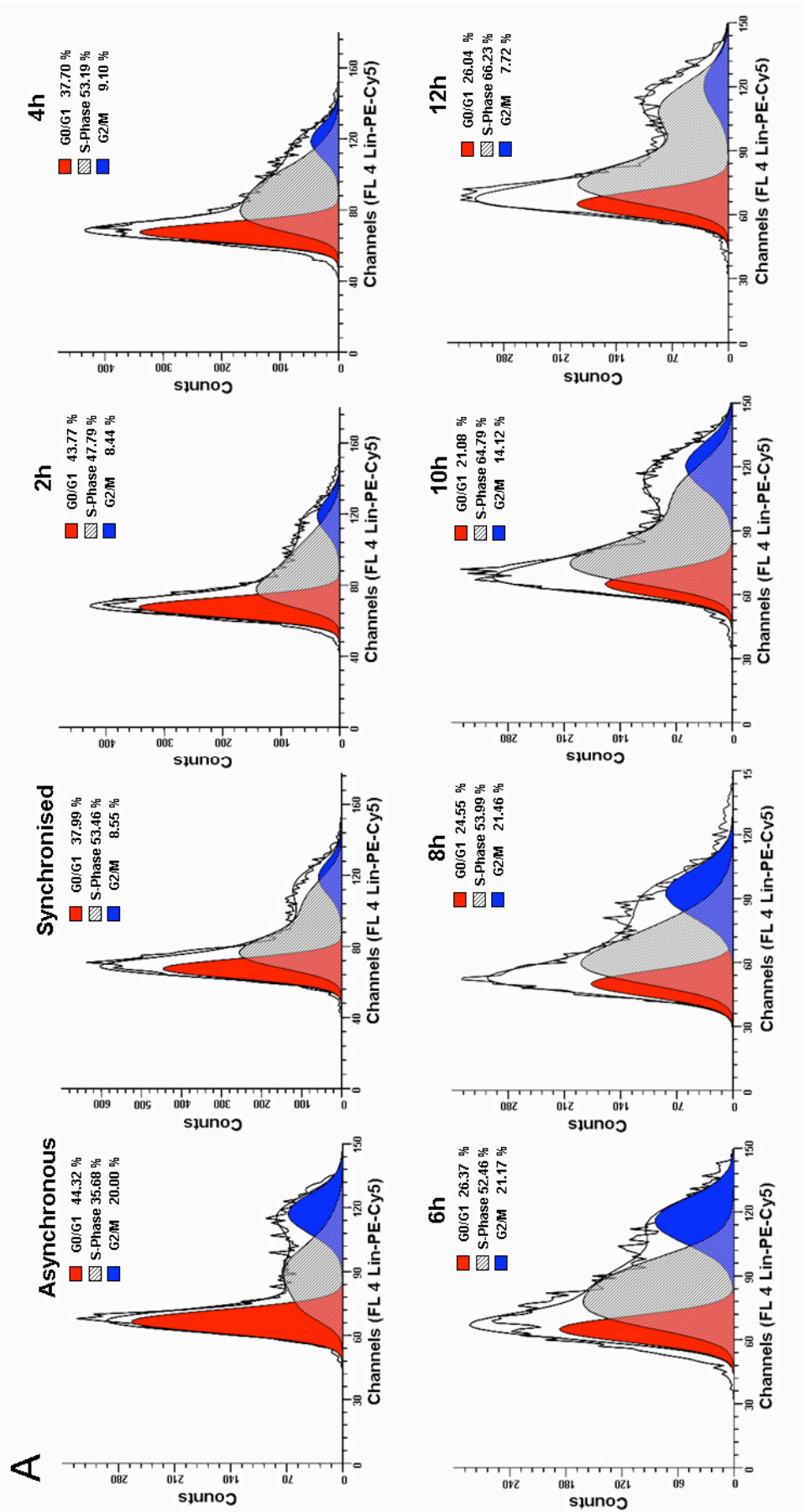
This study has previously shown that DG - cells have a reduced proliferation rate compared to the control (see Section 4.2.8), however, this phenomenon does not appear to be a result of a low mitotic index nor accompanied by an increase in multinucleate cells (see Sections 4.2.9-10). To investigate further the reasons why dystroglycan deficiency is affecting cell growth, DG + and DG - cells were analysed by flow cytometry to examine their progression through the cell cycle. Cells were synchronised at the G1/S transition by arrest with the cell cycle inhibitors mimosine and thymidine. Mimosine induces cell cycle arrest in late G1 phase by inhibiting DNA replication. The addition of excess thymidine also inhibits DNA replication and blocks cell cycle progression at the onset of S-phase. Following release from the block, cells were harvested every hour over a 12 hour period. DNA was stained using propidium iodide, and the cells were analysed by flow cytometry. The aim of this experiment was to investigate whether DG - cells accumulated at a particular stage of the cell cycle or if overall progression was slower, in order to give some insight into how dystroglycan could be affecting cell growth.

Figure 4.12 illustrates the cell cycle profiles of DG + (A) and DG - (B) cells over a 12 hour period. From these profiles, it appears that the synchronisation of DG - cells was marginally more successful than that of DG + fibroblasts, considering that following release from the block, 53% DG - were in G0/G1 compared with only 38% of the DG + cells. Clearly, both cell types failed to synchronise fully, since less than 60% of cells were arrested in G0/G1. As a consequence, the results are difficult to interpret. However, the distribution patterns of each cell type differ considerably and it may be possible to deduce some information about how dystroglycan deficiency influences cell cycle progression. Namely, it appears that four hours after release from the block, there is an accumulation of DG - cells in S-phase that persists until approximately eight hours (Figure 4.12 B and

Table I) before shifting rapidly into G2/M at 10 hours post-release (Figure 4.12 B). In contrast, DG + cells progress much more steadily with a gradual input through S-phase and a constant pool of cells in G2/M (Figure 4.12 A and Table I). Dystroglycan expression has previously been shown to peak during S-phase (Hosokawa et al., 2002) and in DG knockdown mouse mammary epithelial cells there was an accumulation of cells in S-phase (Sgambato et al., 2006), suggesting it has a role in its progression, and the results shown here suggest that dystroglycan deficiency perturbs this process. Further investigation is required to produce more conclusive results.

	DG +			DG -		
	% G0/G1	% S-phase	% G2/M	% G0/G1	% S-phase	% G2/M
Asynch	44.32	35.68	20.00	42.72	33.45	23.83
Synch	37.99	53.46	8.55	53.34	41.96	4.70
2 h	43.77	47.79	8.44	47.19	52.81	0.00
4 h	37.70	53.19	9.10	32.60	67.40	0.00
6 h	26.37	52.46	21.17	31.68	68.32	0.00
8 h	24.55	53.99	21.46	28.11	71.89	0.00
10 h	21.08	64.79	14.12	34.71	47.94	17.34
12 h	26.04	66.23	7.72	36.69	46.67	16.64

Table I: Percentage DG + and DG - cells in each phase of the cell cycle in asynchronous populations (Asynch), after synchronisation treatment (Synch) and at each time point are shown.



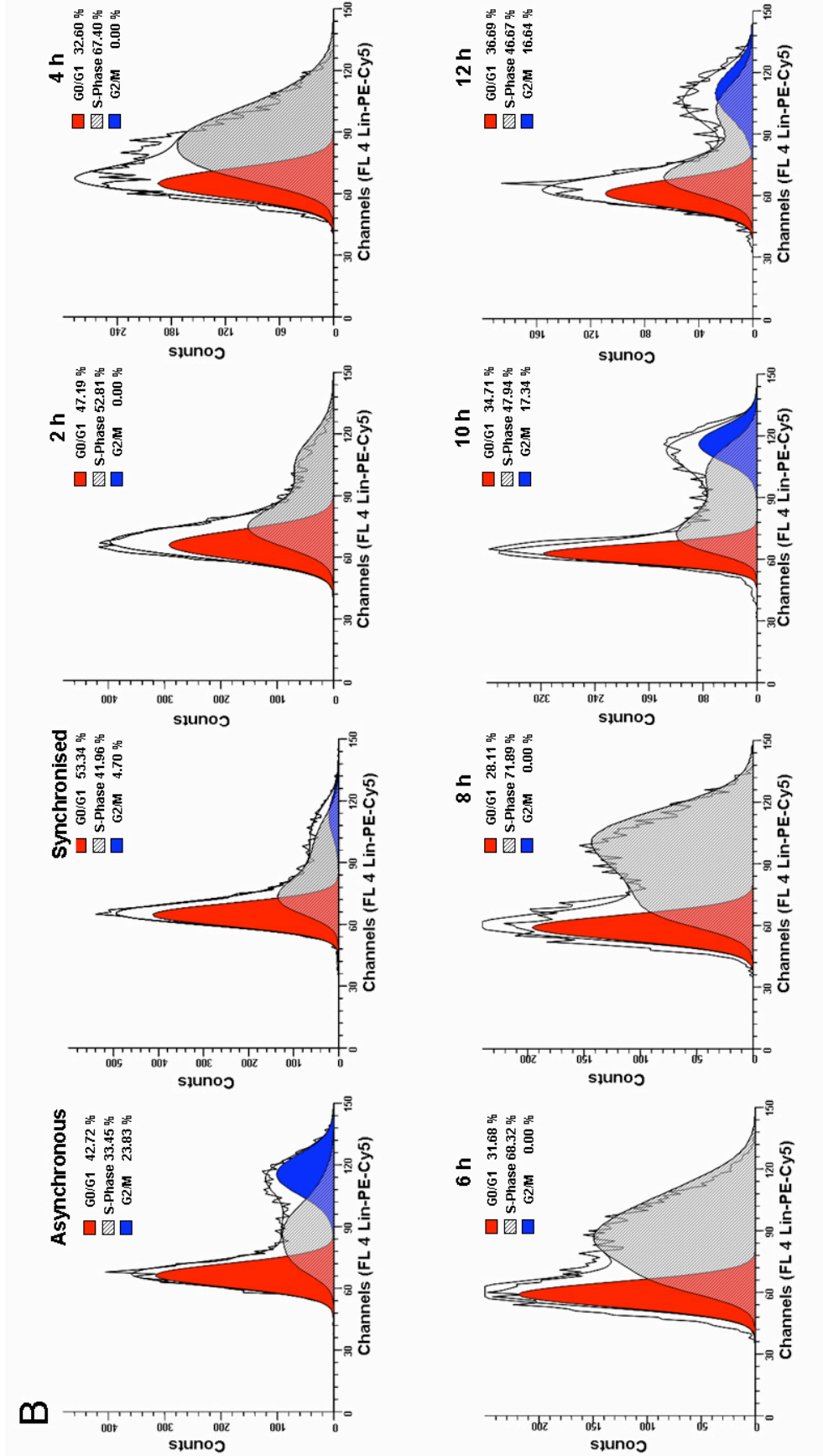


Figure 4.12: Cell cycle profiles of DG + (A) and DG - (B) cells following release from G1/S arrest. Cells were synchronised by double thymidine/mimosine block, collected, and their DNA stained with propidium iodide prior analysis by flow cytometry.

4.2.12 Reduced growth rate of DG - cells is a consequence of increased apoptosis

Previous characterisation of dystroglycan deficient myoblasts showed that there was an increased incidence of apoptotic cells in the population (Montanaro et al., 1999), which has also been reported in morpholino-mediated dystroglycan knockdown in zebrafish (Parsons et al., 2002) and *Xenopus* retina (Lunardi et al., 2006). To investigate further the apparent growth defect observed in DG - cells (see Section 4.2.7), the percentage of apoptotic cells in the population was determined using an Annexin V assay. This assay exploits the finding that, early in apoptosis, the cell experiences a loss of plasma membrane asymmetry manifested by the externalisation of phosphatidyl serine (PS) to the outer surface of the cell (membrane flipping). Annexin V binds to PS with high affinity, meaning that fluorescently labelled Annexin V can be used to differentiate between apoptotic and necrotic cells when counterstained with propidium iodide (Koopman et al., 1994). Using this technique, dead cells contain both fluorescent markers, whereas apoptotic cells only stain for Annexin V.

The results in Figure 4.13 indicate an increase in the prevalence of apoptotic cells in the DG - population (~32%) compared to that of the DG + population (~12%). This level of apoptotic cell death could account for the decreased growth rate exhibited by DG - cells (see Section 4.2.7) and suggests that dystroglycan is important for cell viability. This may explain why cells with a high level of dystroglycan knockdown could not be maintained as a stable cell line.

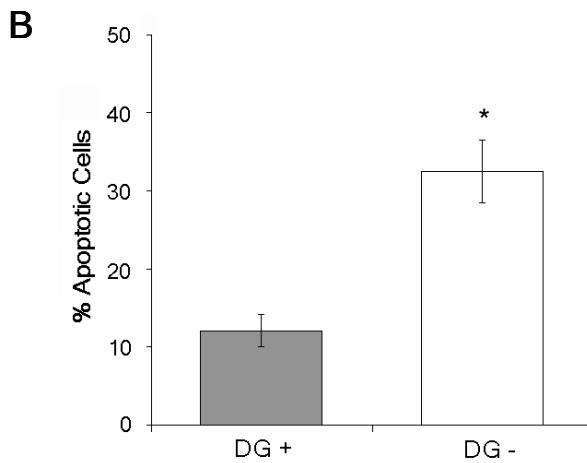
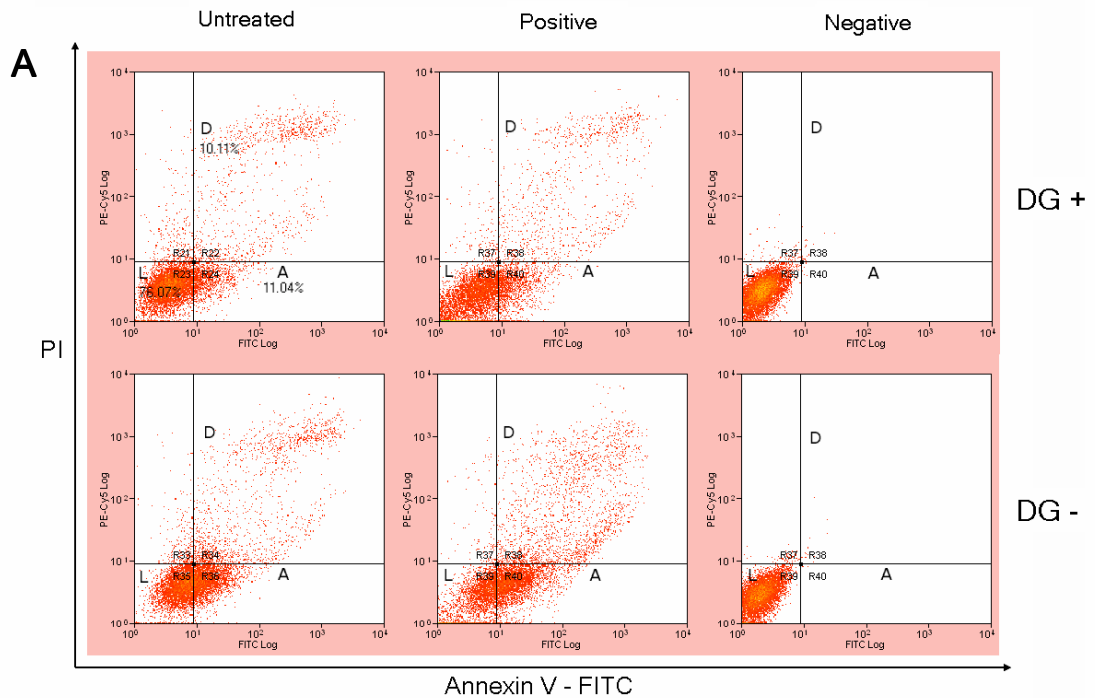


Figure 4.13: Dystroglycan deficiency causes increased apoptosis. A: DG + and DG - cells (Untreated) were stained with Annexin V-FITC and PI before being analysed by flow cytometry. Graphs show plots of PI vs. Annexin V-FITC. Positive control cells (Positive) were treated with staurosporine to induce apoptosis and negative control cells (Negative) had the fluorescent markers excluded from the protocol. L = live cells; D = dead cells; A = apoptotic cells. Flow cytometry plots are representative examples of 3 individual experiments. Percentage apoptotic cells following Staurosporine treatment: ~33% DG + and ~41% DG -. B: Quantification of Annexin V data. ~32% untreated DG - cells were found to be apoptotic compared with ~12% untreated DG + cells. Results are presented as a mean of three separate experiments (\pm SE, n = 3, * p < 0.05)

4.2.13 ERK-MAP kinase expression is reduced in DG - fibroblasts

A previous study has identified an interaction between the cytoplasmic tail of β -dystroglycan and components of the ERK-MAP kinase signalling pathway (Spence et al., 2004b). To investigate whether there are any alterations to ERK-MAP kinase signalling in response to dystroglycan depletion, levels of total ERK expression in DG + and DG - cells were investigated by immunoblotting total cell lysates using anti-ERK1/2 antisera. As shown in Figure 4.14, there was found to be a significant decrease in total ERK in DG - cells compared with DG + cells, suggesting that knockdown of dystroglycan expression causes levels of ERK to be reduced. This finding may provide an explanation for the increased incidence of apoptosis in dystroglycan depleted cells (See Section 4.2.12), since activation of the ERK-MAP kinase cascade leads to the production of cell survival signals (Xia et al., 1995) and presumably a decrease in ERK levels will cause a reduction in survival signals.

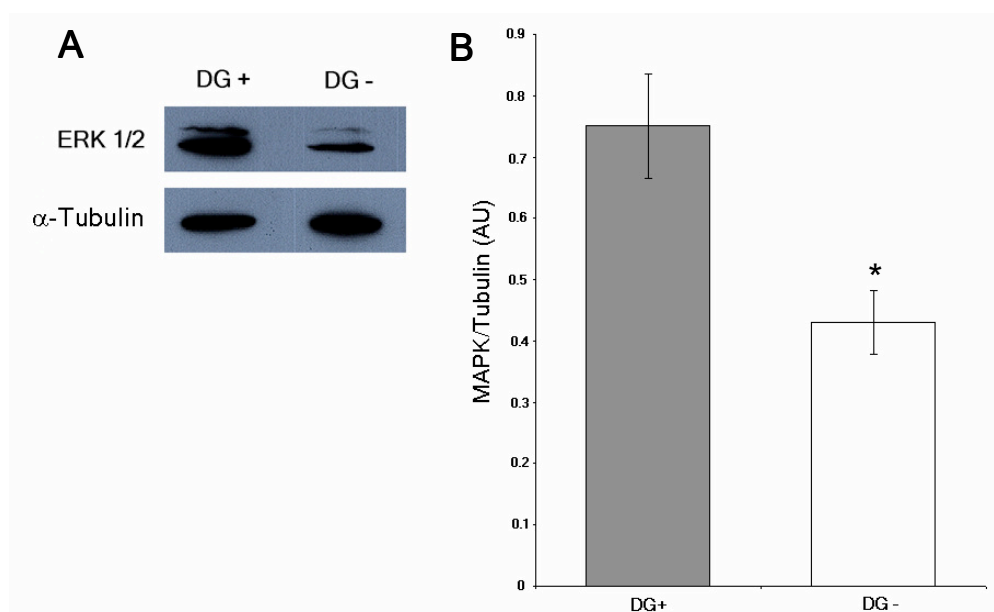


Figure 4.14: ERK-MAP kinase expression is reduced in DG - cells. Levels of ERK1/2 expression were calculated relative to an α -tubulin loading control. A: The ERK1/2 protein expression levels of DG + and DG - Swiss 3T3 fibroblast cell lysates were determined by western analysis, relative to an α -tubulin loading control. B: Bands were quantified by measuring integrated density using NIH Image software. The results show that there was a significant reduction in ERK1/2 protein expression in DG - cells compared with the control (\pm SE, n = 3, * p < 0.05).

4.2.14 Effect of DA and DN Rho GTPase constructs on DG - cells

Rho, Rac and Cdc42 are members of the Rho family of small GTPases and are important regulators of actin cytoskeleton dynamics by inducing the formation of distinctive actin-based structures within the cell and act by linking membrane receptors to assembly and disassembly of actin (reviewed in (Hall, 1998)). Previous work implicates dystroglycan signalling via the small GTPase, Cdc42 in the assembly of actin-rich filopodia (Chen et al., 2003). To assess whether dystroglycan deficiency has an effect on the action of the small GTPases, DG + and DG - cells were transiently transfected with dominant-active (DA) and dominant negative (DN) c-myc-tagged Cdc42, Rac1 and RhoA.

4.2.14.1 Dystroglycan deficiency reduces filopodia in cells transfected with DA Cdc42

Previous studies have shown that, when fibroblasts are transfected with a DA Cdc42 construct, cells are induced to produce actin-rich filopodial protrusions (Nobes and Hall, 1995). Overexpression of dystroglycan in fibroblasts was later discovered to induce the same phenotype (Chen et al., 2003), which was found to be ezrin- and Cdc42-dependent (Spence et al., 2004a) and modulated through the Rho GEF Dbl (Batchelor et al., 2007). Dystroglycan is thought to function as a scaffold in this pathway, serving to recruit essential components to the membrane, thus allowing for activation of the actin polymerisation machinery.

In the present study, the effect of dystroglycan deficiency on filopodia formation in response to constitutively active Cdc42 was investigated in order to determine if dystroglycan is crucial for this process. To achieve this, semi-confluent DG + and DG - cells were transiently transfected with DA Cdc42, followed by fixation and indirect immunofluorescence analysis, using anti-myc antisera to visualise transfected cells and rhodamine phalloidin to stain for F-actin. Transfected cells with more than 30 filopodia

per cell were scored positively for the filopodia phenotype. Quantification of the filopodia phenotype was carried out on fixed cells, therefore in the absence of movement to decipher between filopodial and fixed protrusions, a classification system was utilised whereby filopodia were defined as protrusions containing both actin and Cdc42, while at the same time devoid of focal adhesions at the tip. Representative example images of DG + and DG - cells transfected with DA Cdc42 are shown in Figure 4.15 A. According to this data, DA Cdc42-transfected DG + cells (top panel) exhibit long filopodial protrusions similar to those described by Nobes and Hall in their early DA Cdc42 microinjection experiments (Nobes and Hall, 1995). In contrast, DA Cdc42-transfected DG - cells displayed notably less filopodia than DG + cells, and those that did exist were scattered sparsely throughout the cell (Figure 4.15 A (lower panel) and B). From these results, it is apparent that dystroglycan deficiency inhibits the cells ability to produce filopodia in response to active Cdc42. Perhaps, because these cells were not completely devoid of dystroglycan, filopodia production was not inhibited completely, and the remaining expressed protein may be clustered in those areas where filopodia have formed.

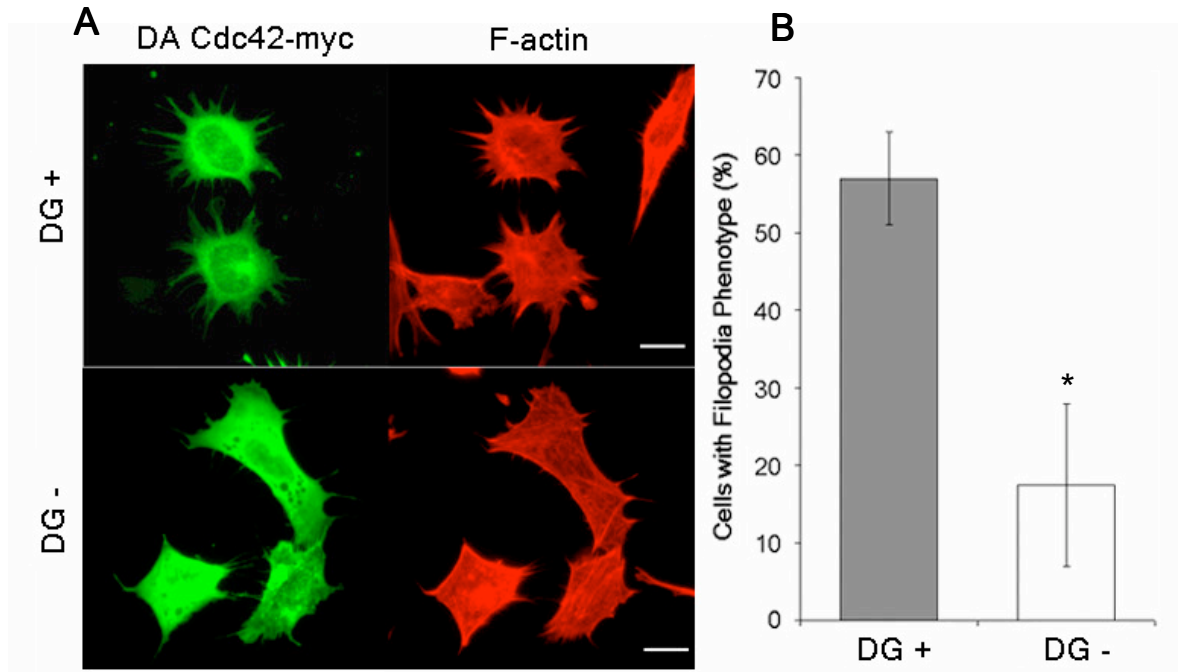


Figure 4.15: Dystroglycan depletion reduces filopodia formation. A: DG - and DG + cells transiently transfected with DA Cdc42-myc were stained for F-actin with rhodamine phalloidin and anti-myc antisera to identify transfected cells. DG - cells had very few filopodia following transfection (bottom panel) compared to DG + (top panel). Scale bar = 20 μ m. B: Transfected cells with > 30 filopodia were scored positively for the filopodia phenotype. DG - cells were inhibited in their ability to form filopodia in response to active Cdc42, compared to DG + cells (\pm SE, n = 3, *p < 0.05). 100 cells were counted per replicate.

4.2.14.2 Dystroglycan deficiency prevents formation of lamellipodia in DA Rac1 transfected cells

The finding that dystroglycan deficiency inhibits filopodia formation in response to active Cdc42 (see Section 4.2.14.1) led to further investigation into how dystroglycan deficiency affects other Rho GTPases and their activity. It has been previously shown that constitutively active Rac1 induces the formation of lamellipodia in fibroblasts (Ridley et al., 1992). Consequently, in order to investigate if dystroglycan is involved in Rac1 signalling, semi-confluent DG + and DG - cells were transiently transfected with DA Rac1, fixed and subsequently stained with both anti-myc antisera and rhodamine phalloidin to allow for analysis by indirect immunofluorescence.

For the purpose of quantification, the extent of lamellipodia formation was categorised into three morphologies, since visual analysis of both cell lines revealed that not all cells had a complete lamellipodia surrounding the cell. Cells with a complete lamellipodia were categorised as “full”, those with > 50% lamellipodia around periphery of the cell were termed “intermediate” and those with aberrant lamellipodia formation were denoted “irregular.” Examples of each of these lamellipodia morphologies are shown in Figure 4.16 A. From these results, it appears that DG - cells have a reduced ability to form a complete lamellipodia and an increase in irregular lamellipodia morphology compared to DG + cells (Figure 4.16 B). Examination of the proportion of cells with the intermediate phenotype reveals that the two cell types are virtually indistinguishable.

Interestingly, the sporadic formation of lamellipodia in DG - cells in response to DA Rac1 can be compared to earlier findings that filopodia formation was perturbed in these cells following transfection with DA Cdc42 (see Section 4.2.14.1). To reiterate, the ability of DG - cells to form any filopodia or lamellipodia is possibly due to the residual dystroglycan expressed in these cells since they are not a total knockdown. These results suggest that dystroglycan deficiency inhibits lamellipodia formation by inhibiting the activation of Rac1.

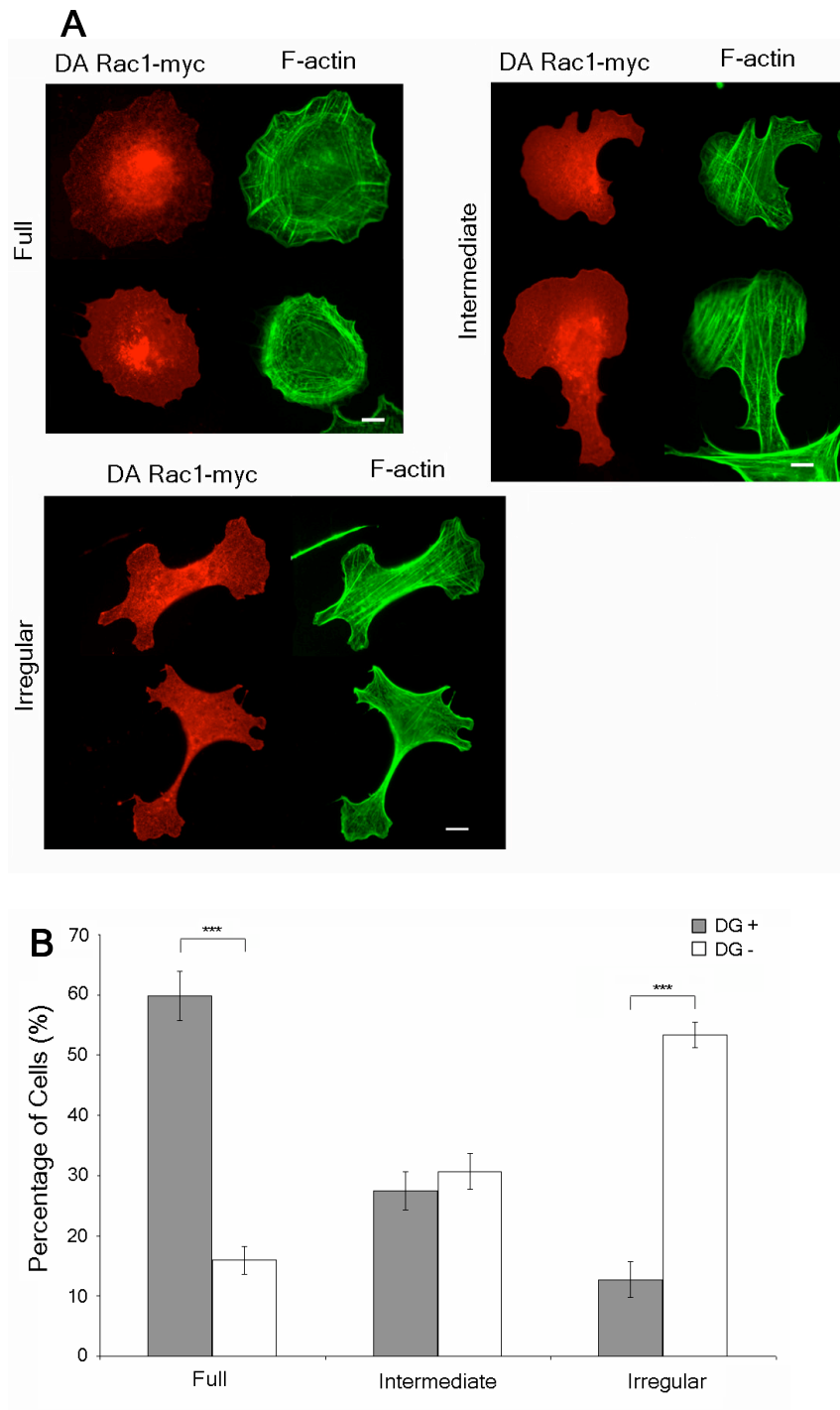


Figure 4.16: Dystroglycan depletion reduces lamellipodia formation. A: DG - and DG + cells transiently transfected with DA Rac1-myc were stained for F-actin and myc with AlexaFluor 488 phalloidin (green) and anti-myc antisera (red), respectively. Myc staining was employed in order to identify transfected cells. Cells were categorised into one of three different morphologies: Full, cells with a complete lamellipodia surrounding the periphery of the cell; Intermediate, cells with an incomplete lamellipodia that surrounds the majority of the cell (> 50%); Irregular, cells with sporadic lamellipodia encompassing < 50% of cell periphery. Example images from both DG + and DG - cell populations are shown to illustrate the different morphologies seen. Scale bar = 20 μ m. B: The relative proportion of each lamellipodial morphology in Rac1 transfected DG - and DG + cells (\pm SE, n = 4, *** p < 0.001). 100 cells were counted per replicate.

4.2.14.3 Effect of dystroglycan deficiency on RhoA activity

Based on previous findings that dystroglycan deficiency inhibits filopodia and lamellipodia formation in response to active Cdc42 and Rac1, respectively (see Section 4.2.14.1-2), the effect of dystroglycan deficiency on RhoA activity was also investigated. RhoA influences actin cytoskeletal organisation by inducing the formation of stress fibres and focal adhesions (Ridley and Hall, 1992). Semi-confluent DG - and DG + cells were transiently transfected with myc-tagged DA RhoA prior to analysis of their actin cytoskeleton by indirect immunofluorescence. Figure 4.17 shows representative cellular morphologies of DG - and DG + cells post-transfection. Overall, transfected DG - and DG + cells did not appear to have any distinguishing features and, as such, were very similar to the morphology of untransfected cells. A likely reason for this finding is that the cells were maintained in 10% serum throughout the course of this experiment; under these conditions, stress fibres are usually present. Subsequently, cells were cultured in serum-free media for 16 hours prior to transfection with DA RhoA. The results of this experiment were inconclusive because transfected cells could not be clearly identified following staining with anti-myc antisera and indirect immunofluorescence analysis due to a high level of non-specific background fluorescence and low transfection efficiency (see Appendix IX).

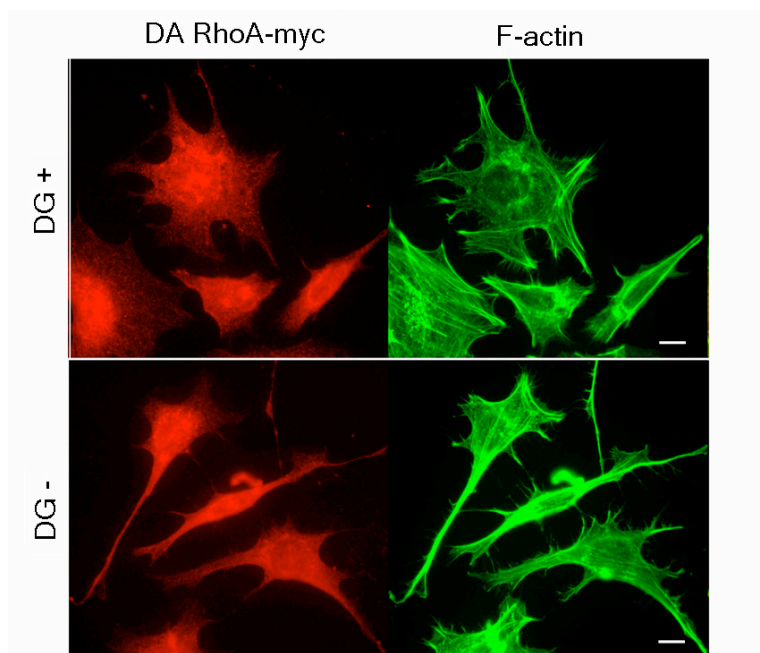


Figure 4.17: Effect of dystroglycan depletion on RhoA activity. A: DG - and DG + cells transiently transfected with DA RhoA-myc were stained with Alexa Fluor 488 phalloidin (green) and anti-myc antisera (red) to identify F-actin and transfected cells, respectively. Visual inspection of the cells did not reveal any obvious morphological differences between transfected and untransfected cells. Scale bar = 20 μ m.

4.2.14.4 Effect of dystroglycan deficiency on dominant negative Rho GTPases

Following on from the investigation of dystroglycan deficiency on the function of dominant active RhoA, Rac1 and Cdc42, a similar investigation was carried out to explore possible effects dystroglycan deficiency might have on the function of dominant negative Rho GTPases, which have been modified so they are constitutively inactive. DG + and DG - cells were transfected with DN Cdc42, DN Rac1 and DN RhoA. As is apparent from Figure 4.18, the expression levels of the transfected myc-tagged DN Cdc42, DN Rac1 and DN RhoA constructs were very low. High background staining attributable to the anti-myc antibody, ultimately made it difficult to distinguish between transfected and untransfected cells. For this reason, drawing conclusive results from this experiment is difficult. However, perhaps the similarity between transfected and untransfected cells results from the transfection of dominant negative constructs, which would not be expected to affect

actin morphology. Probably these cells require stimulation to see the effect of the DN constructs as Swiss 3T3 cells do not have a prominent actin phenotype when unstimulated.

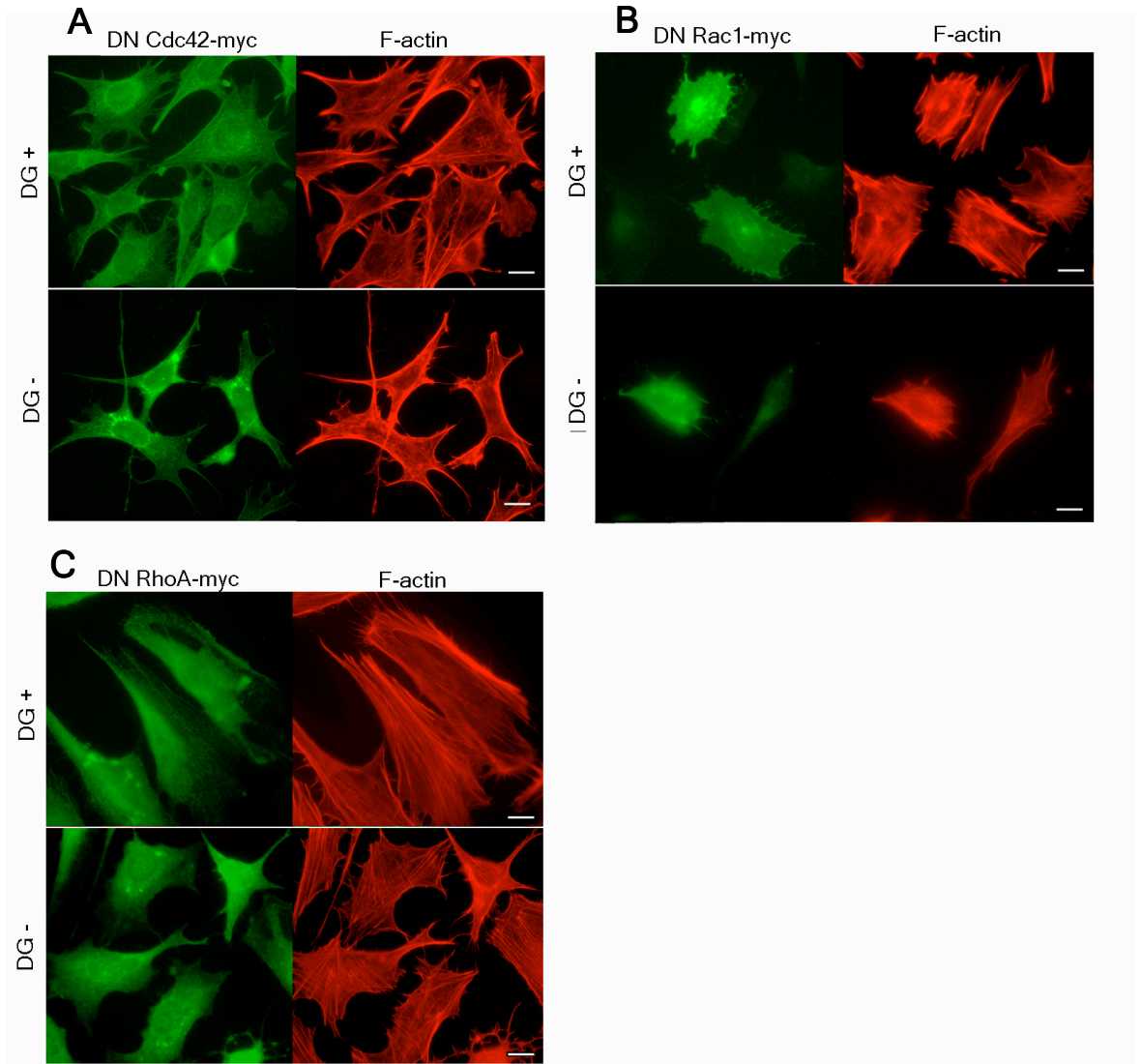


Figure 4.18: Effect of dystroglycan deficiency on dominant negative Rho GTPases. DG - and DG + cells transiently transfected with the myc-tagged DN Rho GTPase constructs; DN Cdc42 (A), DN Rac1 (B) and DN RhoA (C). Cells were stained with anti-myc antisera (green) to identify transfected cells and rhodamine phalloidin to visualise F-actin (red). Upon visual inspection, transfected and untransfected cells appear morphologically similar. Scale bar = 20 μ m.

4.2.15 Ezrin expression is upregulated but mislocalised in DG - fibroblasts

The ERM proteins, ezrin, radixin and moesin, are cytoskeletal linkers involved in modulating the actin cytoskeleton (Bretscher et al., 2002). An interaction between ezrin and the juxtamembrane region of the dystroglycan cytoplasmic tail has recently been identified and was shown to be crucial for the induction of the Cdc42-mediated filopodia phenotype previously described (see Section 4.2.14.1) (Spence et al., 2004a). In the present study, the expression level and localisation of ezrin in dystroglycan-deficient cells was investigated. To achieve this, ezrin protein expression levels in DG + and DG - cells were determined by western blot analysis relative to an α -tubulin loading control (Figure 4.19 A). Generated bands were subsequently quantified using NIH image, the results of which revealed that there was an increased expression of ezrin in DG - cells (Figure 4.19 B). To investigate this finding further, the localisation of endogenous ezrin was examined in DG + and DG - cells by indirect immunofluorescence using an anti-ezrin antibody (Figure 4.19 C). According to this study, ezrin staining is spread diffusely throughout DG - cells and there does not appear to be any strong staining at the plasma membrane. In contrast, DG + cells demonstrate punctate ezrin staining, which is localised to the tips of filopodia (inset in Figure 4.19 C). Collectively, these results suggest that dystroglycan deficiency reduces the recruitment of ezrin to the membrane, and as a consequence, cells subsequently upregulate expression of the protein, possibly as a compensatory mechanism. To further investigate this apparent upregulation of ezrin expression, it would be interesting to carry out subcellular fractionation of DG + and DG - cells. This method allows the separation of total protein content from the membrane, cytosol and cytoskeletal fractions of the cell and could be used to investigate whether there is indeed less ezrin associated with the membrane in dystroglycan depleted cells.

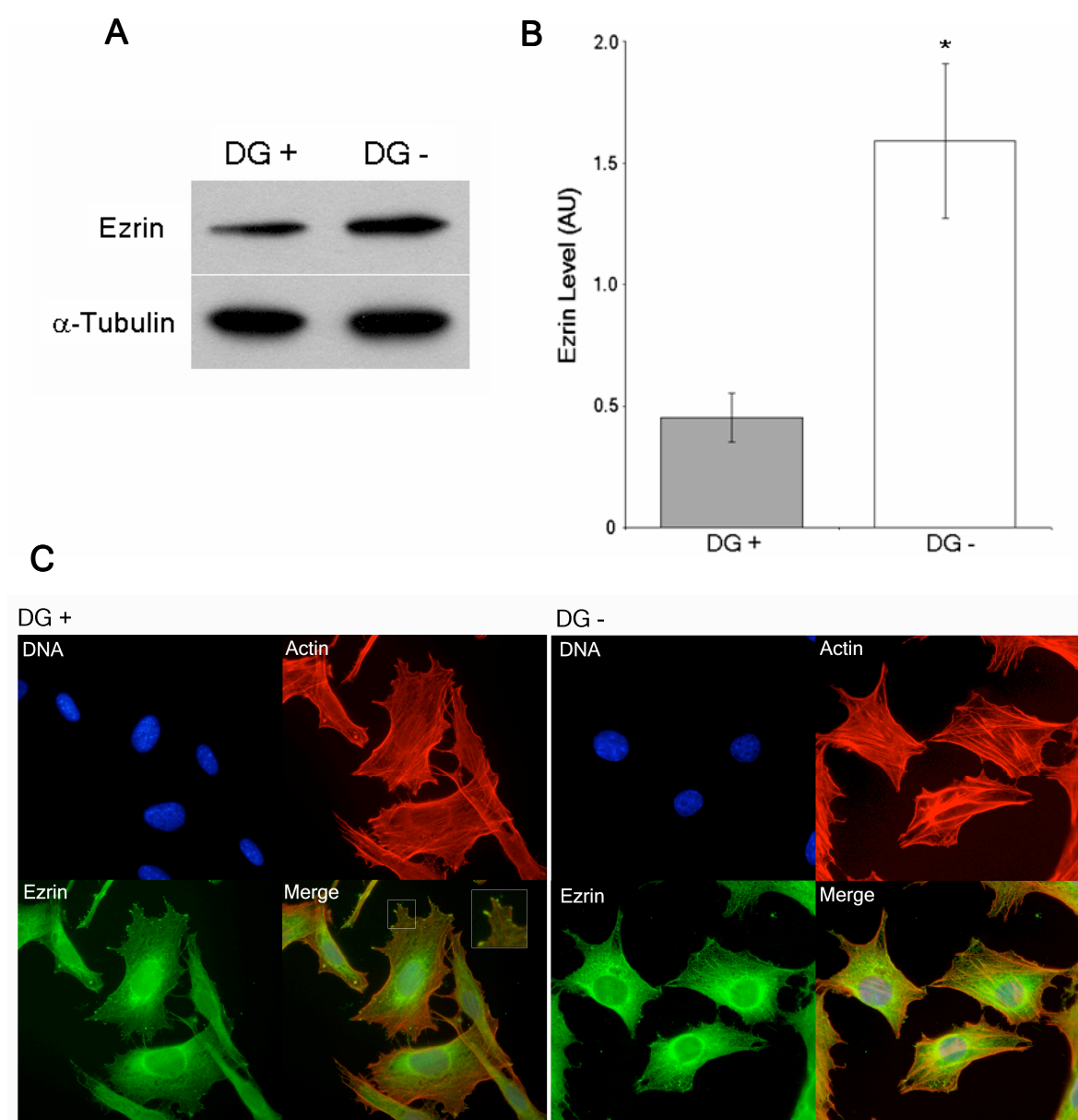


Figure 4.19: Effect of dystroglycan deficiency on ezrin expression and localisation. A: The ezrin protein expression levels of DG + and DG - cell lysates were determined by western analysis, relative to an α -tubulin loading control. B: Bands were quantified by measuring integrated density using NIH Image software. The results show that there is a significant increase in ezrin expression in DG - cells. (\pm SE, $n = 4$, * $p < 0.05$). C: Indirect immunofluorescence images of DG + and DG - cells stained for ezrin (green), actin (red) and DNA (blue). Inset shows a magnified image of punctate ezrin staining at the tips of filopodia in DG + cells. This was not seen in DG - cells.

4.3 Discussion

Dystroglycan provides a crucial link between the actin cytoskeleton and the extracellular matrix and maintaining structural stability is undoubtedly a key function of the protein. However, emerging evidence implicates dystroglycan in more complex roles within the cell including transducing cellular signals, cytoskeletal organisation and cell polarity determination. A valuable technique for elucidating the function of a protein is through loss of function studies, such as knockout animal models and RNA interference. Several studies into dystroglycan deficiency have been carried out previously, although they have placed particular emphasis on developmental processes, neuromuscular diseases and cancer. The present study investigated the function of dystroglycan in fibroblasts by the characterisation of dystroglycan deficient Swiss 3T3 cells in an attempt to determine its role in fundamental cellular processes.

Dystroglycan deficient Swiss 3T3 fibroblasts (DG -) were generated by RNAi and dystroglycan was downregulated by ~60% in the resultant stable cell line (Section 4.2.2). Initially, a knockdown of ~80% was achieved, but this level of deficiency could not be maintained in a stable line, which perhaps reflects the functional importance of dystroglycan within the cell. A control cell line expressing an shRNA construct that did not reduce dystroglycan expression (DG +) was also generated to control for any non-specific effects of the RNAi process (Section 4.2.1.2). Morphological analysis of DG - cells revealed that they were smaller and more elongated than DG + cells (Section 4.2.3). In addition to this, DG - cells were found to contain fewer focal adhesions and had a reduced ability to form large mature focal adhesions (Section 4.2.4). Actin stress-fibres visualised by staining with rhodamine-phalloidin appeared less robust in DG - cells compared to those in the control, however biochemical analysis confirmed that DG - cells

did not have a decrease in F-actin content (Section 4.2.5). Furthermore, dystroglycan deficiency resulted in cells exhibiting a slower proliferation rate but this was not accompanied by an increase in multinucleate cells or a decreased mitotic index (Section 4.2.8-10). There was, however, an increased incidence of apoptosis (Section 4.2.12) and a decrease in ERK 1/2 expression in the DG - population (Section 4.2.13). Cell motility and polarity were found to be unaffected by dystroglycan deficiency (Section 4.2.6-7), however filopodia formation was shown to be inhibited in DG - cells transfected with dominant active Cdc42 and they were also unable to form a complete lamella in response to dominant active Rac1 (Section 4.2.14.1-2). Additionally, ezrin expression was found to be upregulated, but mislocalised, in DG - cells (Section 4.2.15).

There have been several previous studies into dystroglycan deficiency in various animal models and cell culture systems. As discussed in Chapter 3, the dystroglycan knockout mouse was embryonic lethal due to its inability to form a basement membrane (Williamson et al., 1997). Dystroglycan deficiency in other organisms produced less severe, but nonetheless detrimental phenotypes, for example, RNAi-mediated knockdown of dystroglycan in drosophila resulted in a loss of cell polarity during oogenesis (Deng et al., 2003) and morpholino knockdown in zebrafish caused a muscular dystrophy-type phenotype (Parsons et al., 2002). In addition, brain selective deletion of dystroglycan in mice resulted in the development of congenital muscular dystrophy-like defects (Moore et al., 2002) and selective deletion in differentiated striated muscle resulted in a mild dystrophic phenotype, thought to be partially compensated by satellite cells expressing dystroglycan (Cohn et al., 2002). Dystroglycan deficient cells were found to be smaller and more ellipsoidal in morphology than DG + cells (see Section 4.2.3). A previous study into RNAi knockdown of dystroglycan in myotubes reported that at low density cells

appeared flatter and more spread than DG + cells (Montanaro et al., 1999). Possible reasons for these conflicting results are that different cell types respond in different ways to dystroglycan deficiency or it may reflect the level at which dystroglycan has been depleted in each case. There have also been RNAi-mediated dystroglycan knockdown studies involving mouse myoblasts (Montanaro et al., 1999) and mouse mammary epithelial cells (Sgambato et al., 2006) and results obtained from these studies will be discussed further in this section.

A plausible explanation for the altered cell morphology exhibited by DG - cells is that they could not spread out onto the substrate effectively due to depleted dystroglycan expression levels. To address this possibility, the quantity and size of focal adhesions in DG + and DG - cells was investigated. Focal adhesion structures are sites of close contact between cytoskeletal and extracellular matrix components that provide a structural link between the cell and its substrate. In addition to their structural role, focal adhesions also act as points of communication between the cell and its surroundings where signal transduction can occur in order to control cellular processes such as cell growth and motility. The results presented here showed that dystroglycan depletion in fibroblasts resulted in a slight reduction of focal adhesions per unit area and in addition to this, a lesser proportion of larger mature adhesions were produced (Section 4.2.4). These results concur with previous findings that implicate dystroglycan in cell adhesion. Dystroglycan and its binding partner utrophin have previously been shown to co-localise in adhesion structures in a variety of non-muscle cells (Belkin and Burridge, 1995a; Belkin and Burridge, 1995b; Belkin and Smalheiser, 1996; James et al., 1996; James et al., 2000; Khurana et al., 1995) and an interaction between β -dystroglycan and FAK (focal adhesion kinase), via GRB2 has previously been identified. FAK is a tyrosine kinase involved in focal adhesion assembly (Cavaldesi et al., 1999). Since there was an apparent reduction in

quantity and size of focal adhesions in DG - cells, it suggests that dystroglycan is important for their assembly or maintenance. This is a plausible concept considering that the formation of adhesion complexes is known to be regulated by tyrosine phosphorylation of cytoskeletal components (Burrige and Chrzanowska-Wodnicka, 1996) and tyrosine phosphorylation of β -dystroglycan was found to regulate its binding to utrophin in an adhesion-dependent manner (James et al., 2000). Given that dystroglycan acts as a scaffold for cell signalling proteins, such as components of the ERK-MAP kinase signalling cascade (Spence et al., 2004b), perhaps this adhesion-dependent release from its cytoskeletal binding partner, utrophin, enables it to fulfil cell signalling roles. This theory is supported by the finding that active ERK is targeted to newly forming focal adhesions during cell spreading (Fincham et al., 2000). The reduction, as opposed to complete absence, of focal adhesions in DG - cells is likely due to maintenance of integrin-mediated adhesion and the presence of residual dystroglycan expression. Even so, the reduced level of cell adhesions resulting from dystroglycan depletion supports a role for dystroglycan in the formation and organisation of focal adhesion structures. A reduction in cell adhesions may also provide some explanation as to why morphologically, dystroglycan-depleted fibroblasts appeared much smaller and less well spread than DG + cells (see Section 4.2.3).

DG - cells stained for F-actin with rhodamine-phalloidin appeared to have a reduction in actin stress fibres, since the fluorescent intensity was reduced compared to that of DG + cells when visualised by immunofluorescence. Biochemical analysis of F-actin content revealed that DG - cells contained a similar proportion to DG + cells and therefore this decrease was not due to a defect in actin polymerisation (Section 4.2.5). Another explanation could be, rather than a decrease in F-actin content, perhaps there is a decrease in actin bundling in DG - cells, which may result in less robust stress fibres.

Although, dystroglycan itself has been shown to have actin-bundling properties, this result is more likely to be a consequence of impaired cell signalling as opposed to a direct consequence of dystroglycan depletion because overexpression of the cytoplasmic domain of β -dystroglycan, which is the actin-bundling region, did not result in increased stress fibre formation *in vivo* (Chen et al., 2003).

Cell motility is an intricately coordinated cytoskeletal process that requires lamellipodia and filopodia formation at the leading edge and focal adhesion assembly and disassembly at the leading and retracting edges respectively (Small and Resch, 2005). Following on from the results that implicate dystroglycan in the formation of focal adhesions (Section 4.2.4) and in filopodia and lamellipodia assembly (Chen et al., 2003) (Spence et al., 2004a) (Section 4.2.14.1-2), the effect of dystroglycan deficiency on cell motility was investigated by wound healing assay (Section 4.2.6). The results showed that this level of dystroglycan deficiency in fibroblasts did not result in a cell motility defect. However, since DG - cells were not completely devoid of dystroglycan, perhaps residual dystroglycan expression was adequate for correct cell motility. Alternatively, other adhesion molecules, such as integrins, may be functioning redundantly and could compensate in the absence of dystroglycan. Overexpression of the cytoplasmic domain of β -dystroglycan in vascular endothelial cells caused a cell motility defect (Hosokawa et al., 2002), which suggests that the dystroglycan-ECM interaction is required for normal cell motility. A similar result might be expected in cells depleted of dystroglycan, however, an alternative explanation is that overexpression of the cytoplasmic domain, which was not membrane associated, may sequester components required for cell motility, thus explaining the observed defect.

Dystroglycan has previously been implicated in maintaining epithelial cell polarity (Deng et al., 2003; Muschler et al., 2002). Correct cell polarity is a fundamental requirement in all cells as it is required for many aspects of cell survival including cell division, movement and differentiation. Since this is the first study to characterise the cytoskeletal changes resulting from dystroglycan deficiency in fibroblastic cells, the ability of these cells to polarise was investigated to determine if dystroglycan has a widespread function in determining cell polarity. Cdc42 is a key player in regulating cell polarity (Etienne-Manneville, 2004) and local activation at the leading edge leads to filopodia formation, structures which are able to assess the environment as the cell moves forwards. This is where dystroglycan may be involved since, as previously discussed, it is involved in recruiting components leading to Cdc42 activation and filopodia formation (Batchelor et al., 2007). A useful method for inducing fibroblasts to polarise is by way of a scratch-wound assay, in which a confluent cell layer is scratched and cells at the wound edge polarise and migrate into the wound. The microtubule organising centre (MTOC) can be used as a marker for cell polarity since it reorientates to the front of the nucleus in the direction of cell migration (Kupfer et al., 1982). DG⁻ cells did not appear to have a polarity defect since cells at the wound edge were polarised to the same extent as DG⁺ cells (Section 4.2.7). This suggests that, in Swiss 3T3 fibroblasts, dystroglycan is not required for maintaining correct cell polarity. However, this does not necessarily preclude a function for dystroglycan in cell polarity, since residual expression may be adequate in concert with other cell adhesion molecules, such as integrins, which can function redundantly.

The cell cycle profile of dystroglycan knockdown cells was markedly altered from that of the control in that there appeared to be a prolonged accumulation of DG⁻ cells in

S-phase resulting in a slower progression through the cell cycle compared to DG + cells (Section 4.2.11). A similar result has been reported previously in a study that looked at depletion of dystroglycan in HC11 murine mammary epithelial cells. The same study also showed that dystroglycan expression levels are cell cycle regulated in untreated HC11 cells and in synchronised cultures, dystroglycan expression gradually increases following release from the block and peaks at around 12 hours, which corresponded with S-phase entry (Sgambato et al., 2006). Another group have also reported this cell cycle regulated expression in bovine aortic endothelial cells in which dystroglycan expressions levels increase as the cells entered S-phase (Hosokawa et al., 2002). This suggests a role for dystroglycan in cell cycle progression and strengthens the possibility that dystroglycan may play a role in cytokinesis, which will be discussed in Chapter 5.

Findings obtained during the course of this study have shown that dystroglycan-deficient fibroblasts had a reduced proliferation rate compared to DG + cells, but did not show an increase in multinucleate cells or reduced mitotic index. There was however, found to be a 3-fold increase in apoptotic cells in the DG - population, shown by Annexin V assay (Section 4.2.12), which is likely to account for the observed proliferation defect. Consistent with these results, studies into RNAi-induced dystroglycan knockdown in myoblasts and murine mammary epithelial cells found an increase in apoptosis in response to dystroglycan deficiency (Montanaro et al., 1999; Sgambato et al., 2006). It has also been reported that there was an increase in apoptotic cells in morpholino-mediated dystroglycan knockdown in *Xenopus Laevis* retina (Lunardi et al., 2006) and zebrafish embryo (Parsons et al., 2002). The observed increase in apoptosis in DG - cells may be due to the disruption of the ERK-MAP (ERK, extracellular signal-regulated kinase; MAP, mitogen-activated protein) kinase cascade, which transduces cell survival signals (Xia et

al., 1995). The cytoplasmic tail of β -dystroglycan has previously been shown to interact with the MAP kinase signalling components MEK2 and ERK. β -Dystroglycan is thought to act as a membrane scaffold that can influence activation of the ERK-MAP kinase signalling pathway by sequestering components in different cellular compartments (Spence et al., 2004b). In the present study, total ERK expression levels were found to be significantly reduced in DG - fibroblasts (Section 4.2.13). These results suggest that depletion of dystroglycan expression in fibroblasts has a significant impact on total levels of ERK within the cell, possibly resulting in a reduction in cell survival signals and leading to an increase in apoptotic cell death. In this experiment, total levels of ERK were determined, consisting of both its active and inactive forms. Therefore, to further substantiate this result, it would be useful to examine the levels of active ERK in response to dystroglycan depletion. This could be achieved by using antisera specific for the phosphorylated form of ERK.

Alternatively, since dystroglycan is also an ECM receptor, perhaps its involvement in apoptosis is analogous to that of the integrins, since disruption of integrin-mediated adhesion to the ECM has previously been reported to induce apoptosis (Frisch and Ruoslahti, 1997). This was addressed in a study investigating dystroglycan-induced apoptosis in myoblasts by disruption of its interaction with laminin, which determined that it was mediated through caspase activation. An interaction between the cytoplasmic tail of β -dystroglycan and GRB2 and FAK was proposed to link dystroglycan to the phosphoinositide 3-kinase (PI3K)/Protein kinase B (AKT) pathway that initiates cell survival signals and if disrupted, ultimately triggers activation of the caspase-mediated apoptotic pathway (Langenbach and Rando, 2002). The results presented here, concur with this theory since presumably dystroglycan depletion results in decreased ECM

binding, thus potentially disrupting the PI3K/AKT pathway and inducing apoptosis. These results support a role for dystroglycan as an important modulator of signal transduction pathways and further research is required in order to understand the precise mechanisms linking dystroglycan to cell survival.

DG - cells were transfected with DA and DN Rho-GTPase constructs to gain insight into how dystroglycan may be influencing cytoskeletal reorganisation. The Rho GTPase proteins, RhoA, Rac1 and Cdc42 are crucial regulators of actin cytoskeletal dynamics. Active RhoA induces the formation of stress fibres, active Rac1 induces lamellipodia formation and active Cdc42 induces filopodia protrusions (Nobes and Hall, 1995). Previous evidence has shown that dystroglycan is implicated in Cdc42-mediated filopodia formation and this was found to be dependent upon β -dystroglycan binding to the cytoskeletal linker protein, ezrin (Spence et al., 2004a). Ezrin is known to bind to the GDP/GTP exchange factor (GEF), Dbl, which acts upon Cdc42 and Rho (Vanni et al., 2004). A recent study has shown that dystroglycan recruits an ezrin-Dbl complex to the cell periphery, where it interacts with active Cdc42. Mislocalised truncated mutants of dystroglycan inhibited filopodia formation and this could be restored upon membrane targeting, suggesting that dystroglycan is essential for the correct localisation of ezrin and the Cdc42 activation machinery prior to filopodia formation (Batchelor et al., 2007). In the present study, DG + cells transfected with a constitutively active Cdc42 construct produced an abundance of filopodia whereas DG - cells, transfected with the same construct, remained spread out and filopodia were only present in discrete patches that were sporadically located across the cell membrane (Section 4.2.14.1). The finding that depletion of dystroglycan was sufficient to inhibit filopodia formation strengthens the existing argument that dystroglycan is fundamentally important for mediating Cdc42-

dependent filopodia formation by recruiting essential components to the membrane. Interestingly, a similar result was exhibited by DG - cells transfected with active Rac1, since in DG + cells a complete lamellipodia formed around the periphery of the cell, whereas transfected DG - cells displayed an unusual morphology in which lamellipodial protrusions were produced in small sections of the membrane and appeared to be extending in opposite directions (Section 4.2.14.2). This adds new complexity to the current understanding of the influence dystroglycan has on cytoskeletal dynamics, since Dbl is specific for Cdc42 and RhoA, this must be a consequence of the disruption of a different Rho GTPase signalling pathway. One possible candidate is the PAK (P21-activated kinase) pathway, which regulates processes such as cell motility and polarity (Bagrodia and Cerione, 1999) and is a downstream effector of Cdc42 and Rac1 (Manser et al., 1994). These results suggest that perhaps residual dystroglycan is indirectly recruiting active Cdc42 and Rac1 and promoting cytoskeletal changes in localised patches of the cell membrane. Active Cdc42 and Rac1 transfected cells displayed a more obvious phenotype than cells transfected with active RhoA, which in the presence of serum looked unaffected by the transfection (Section 4.2.14.3). The addition of serum to growth medium has previously been shown to induce RhoA activation and stress fibre formation due to the presence of growth factors contained within the serum (Ridley and Hall, 1992). Therefore in a second attempt to investigate the effect of dystroglycan deficiency on RhoA activation, cells were serum starved prior to transfection with DA RhoA. This experiment did not, however, produce conclusive results due to a low transfection efficiency and high level of non-specific background fluorescence. Further investigation is therefore required to produce more conclusive results on the effect of dystroglycan deficiency on RhoA activity, perhaps by using a different transfection technique. Transfection of dominant negative Rho GTPase constructs did not induce a phenotype in either cell type, since DG +

and DG - cells morphology appeared unaltered. This result was not surprising considering that unstimulated Swiss 3T3 cells do not display a prominent actin phenotype (Section 4.2.14.4).

Dystroglycan interacts with the ERM cytoskeletal linker protein, ezrin via a juxtamembrane binding site contained on the cytoplasmic tail of β -dystroglycan (Spence et al., 2004a). The localisation of ezrin in DG - cells was investigated to determine if dystroglycan is critical for its membrane recruitment. The results showed that that ezrin did not localise to the membrane in DG - cells, instead most of the staining was cytoplasmic with a large proportion in the perinuclear area, whereas, in DG + cells, ezrin localised to punctate spots at the tips of filopodia (Section 4.2.15). This suggests that dystroglycan is important for the recruitment of ezrin to the membrane in fibroblast cells. Interestingly, the ezrin expression levels were found to be elevated in response to dystroglycan knockdown, which implies that mis-localisation leads to upregulation of the protein as a compensation mechanism. This result was very interesting with respect to the relationship between dystroglycan and ezrin because published evidence has found that ezrin expression is upregulated in cancer cells, particularly those with high metastatic potential (Akisawa et al., 1999; Khanna et al., 2004; Yu et al., 2004), whereas dystroglycan expression has been shown to be reduced, or completely absent, in a number of cancer cell lines and primary tumours (Henry et al., 2001; Jing et al., 2004; Losasso et al., 2000; Muschler et al., 2002; Sgambato et al., 2003). The significance of this is not yet fully understood, though what is clear is that reduced dystroglycan expression on the cell surface will undoubtedly influence the contacts between the ECM and cytoskeleton and disrupt intracellular signalling cascades, perhaps mediated through ezrin, which may eventually lead to the promotion of tumour metastasis.

This study is the first to characterise the effects of dystroglycan deficiency on the cytoskeleton in fibroblast cells and has strengthened existing evidence that dystroglycan plays important roles within the cell in addition to its function as a structural molecule. The findings obtained during the course of this research were consistent with previous studies into dystroglycan deficiency in other cell types and support a role for dystroglycan in cell adhesion, filopodia formation, cell cycle progression and viability. Additionally, this study has provided evidence to suggest that dystroglycan may also be involved in the function of Rac1 in lamellipodia formation. Further research into dystroglycan is required in order to fully elucidate its multifaceted function within the cell, which may help us understand how these processes are deregulated in diseases such as muscular dystrophy and cancer.

Chapter 5

Investigating dystroglycan localisation during cytokinesis

Chapter 5

Investigating dystroglycan localisation during cytokinesis

5.1 Introduction

Cytokinesis, the process by which a cell separates itself into two daughter cells, is the final stage of eukaryotic cell division. Proper control of cytokinesis is vitally important to maintain the integrity of the cell, and for such separation to be successful, there must exist fine coordination between microtubules and the actin cytoskeleton. Much of the knowledge surrounding cytokinesis has been obtained from studying the process in model organisms such as *Saccharomyces cerevisiae*, *Schizosaccharomyces pombe*, *Xenopus laevis* and *Drosophila melanogaster*. Because all work in the present study was carried out in cultured mammalian cells, however, mammalian cell cytokinesis will be reviewed briefly.

Cytokinesis is the final stage of mitosis; a process by which replicated DNA is separated and divided into two identical daughter cells. Mitosis consists of six distinct stages: prophase, prometaphase, metaphase, anaphase, telophase and finally cytokinesis. During prophase, DNA condenses into chromosomes and microtubules start to form the mitotic spindle. At prometaphase, the nuclear membrane is dissolved and microtubules attach to paired chromosomes through protein structures called kinetochores. During metaphase the spindle microtubules align the paired chromosomes along the centre of the cell, termed the metaphase plate, which are then separated by the spindle and move to opposite poles of the cell at anaphase. By telophase, separated chromatids have arrived at opposite at the spindle poles and new membranes form around daughter nuclei. Cytokinesis, the ultimate separation and segregation of two daughter cells, commences at late telophase.

The process of cell separation is achieved by the concerted efforts of actin and myosin II, both of which are recruited to the cell midzone at late anaphase (Sanger et al., 1989) to form an actomyosin contractile ring (Schroeder, 1970). The contractile ring is closely associated with the plasma membrane and is assembled perpendicular to bundled microtubules, which lie along the long axis of the cell, thus ensuring correct orientation of the plane of cell division. The Rho GTPase, RhoA, is the pivotal regulatory element controlling this process, and does so by influencing a number of crucial components either directly or through its numerous effectors (Reviewed in (Piekny et al., 2005)). A restricted pool of RhoA is activated at the cell midzone by the RhoGEF, ECT2 (Tatsumoto et al., 1999), which is associated with components of the central spindle, thus contributing to cleavage furrow site specification (Yuce et al., 2005). The precise timing of the interactions between RhoA and ECT2 is thought to be regulated by the destruction of cyclins (Mishima et al., 2004).

Active RhoA binds to the formin homology protein, mDia1, alleviating its autoinhibition (Alberts, 2001; Kato et al., 2001), which, in conjunction with profilin, nucleates the polymerisation of unbranched actin filaments to assemble the actomyosin contractile ring (Romero et al., 2004). In addition, RhoA activates its effector Rho kinase/ROCK, which in turn phosphorylates myosin II on its regulatory light chain. This phosphorylation allows myosin II to assemble into filaments (Amano et al., 1996) and Rho kinase/ROCK also inhibits the phosphatase that dephosphorylates myosin II (Kimura et al., 1996). The motor activity of myosin II translocates bundled actin filaments, which drives the contractile ring to tighten, ultimately resulting in the ingression of the plasma membrane to form the cleavage furrow (Schroeder, 1970). Furrowing of the membrane serves to push the mitotic spindle into a dense matrix consisting of spindle microtubules and associated proteins. This structure, referred to as the midbody, is thought to maintain

the divide between the daughter cells prior to complete separation (Glotzer, 2001). Following complete membrane ingression, the cells remain connected by a thin, microtubule-rich cytoplasmic bridge, which is important for stabilisation during the final stages of cytokinesis. Completion of cytokinesis requires midbody abscission and membrane remodelling to form two daughter cells (Figure 5.1).

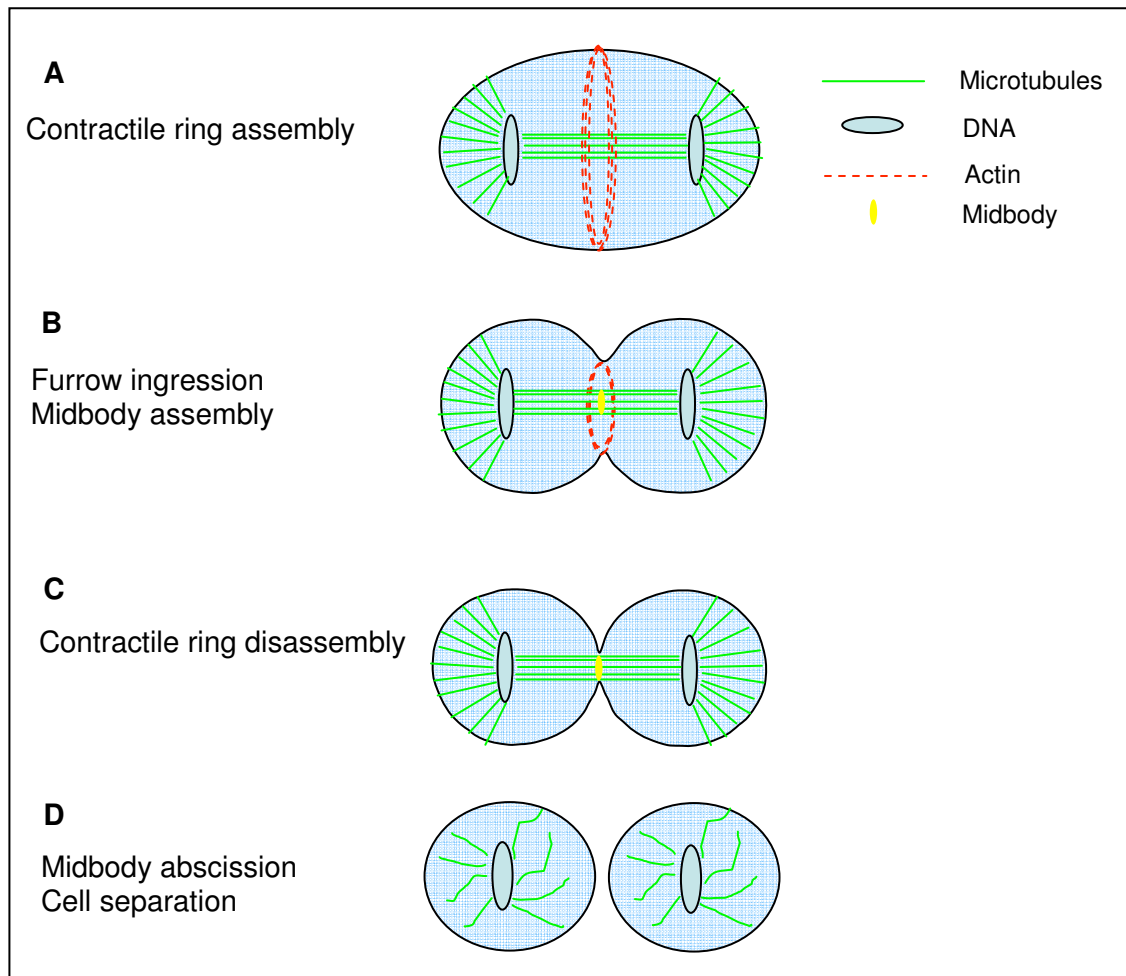


Figure 5.1: Changes in the cytoskeleton during cytokinesis. A: Actin, myosin II and modulating proteins including polymerising machinery are recruited to the cleavage site, specified by mitotic spindle factors, and assemble the contractile ring. B: Myosin II motor activity forces contractile ring to ingress forming membrane furrow. C: After complete ingression, the contractile ring disassembles and midbody proteins associated with the mitotic spindle maintain segregation between daughter cells. D: Membrane fusion events complete cell separation.

Full understanding of the timing and regulatory mechanisms governing cytokinesis is still at the early stages and there are a number of key questions yet to be answered. In particular; what structural components are required to stabilise the contractile ring and what links it to the plasma membrane? A role for membrane glycoproteins, at the cleavage furrow has previously been identified and the interaction with ezrin/radixin/moesin (ERM) proteins is thought to be important (Po et al., 1999; Tsukita et al., 1994; Yonemura et al., 1993). The ERM family are cytoskeletal linker proteins that connect the cytoskeleton to the plasma membrane in a multitude of cellular structures such as membrane ruffles, adherens junctions and microvilli, and have also been shown to be involved in cytokinesis (Sato et al., 1991). However, since the majority of research on the function of ERM protein and membrane glycoproteins at the cleavage furrow has been carried out on cells of the immune system, a universal structural component or mechanism has yet to be discovered.

In the present study, a possible role for the widely-expressed adhesion molecule, dystroglycan in cytokinesis was investigated by examining endogenous staining of dystroglycan and the localisation of several different fluorescently-tagged dystroglycan constructs in dividing cells. This study proposes that dystroglycan forms part of a complex that tethers the actomyosin contractile ring to the plasma membrane and stabilises this interaction during cleavage furrow ingression. The current body of work also leads us to question whether dystroglycan is acting as a scaffold to recruit upstream components of the contractile ring regulatory machinery.

5.2 Results

5.2.1 Dystroglycan localises to the cleavage furrow and midbody of dividing Ref52 fibroblasts

In order to study the localisation of β -dystroglycan during cytokinesis, untreated Ref52 fibroblasts were visualised by immunofluorescence staining with an anti- β -dystroglycan antibody. Figure 5.2 (A) shows that, during interphase, β -dystroglycan staining is found throughout the membrane and co-localises with actin in membrane protrusions. In contrast, cells undergoing cytokinesis exhibit a strong concentration of β -dystroglycan at the cleavage furrow (Figure 5.2 (B)) and in cells at later stages of division, once the cleavage furrow had further contracted, there was concentrated staining at the cell midbody (Figure 5.2 (C)). These cells were also stained for filamentous-actin using rhodamine phalloidin and a strong band, likely corresponding to the contractile ring, co-localised with β -dystroglycan staining at the cleavage furrow and midbody. This striking localisation suggests that dystroglycan is involved in cytokinesis and led to further investigation.

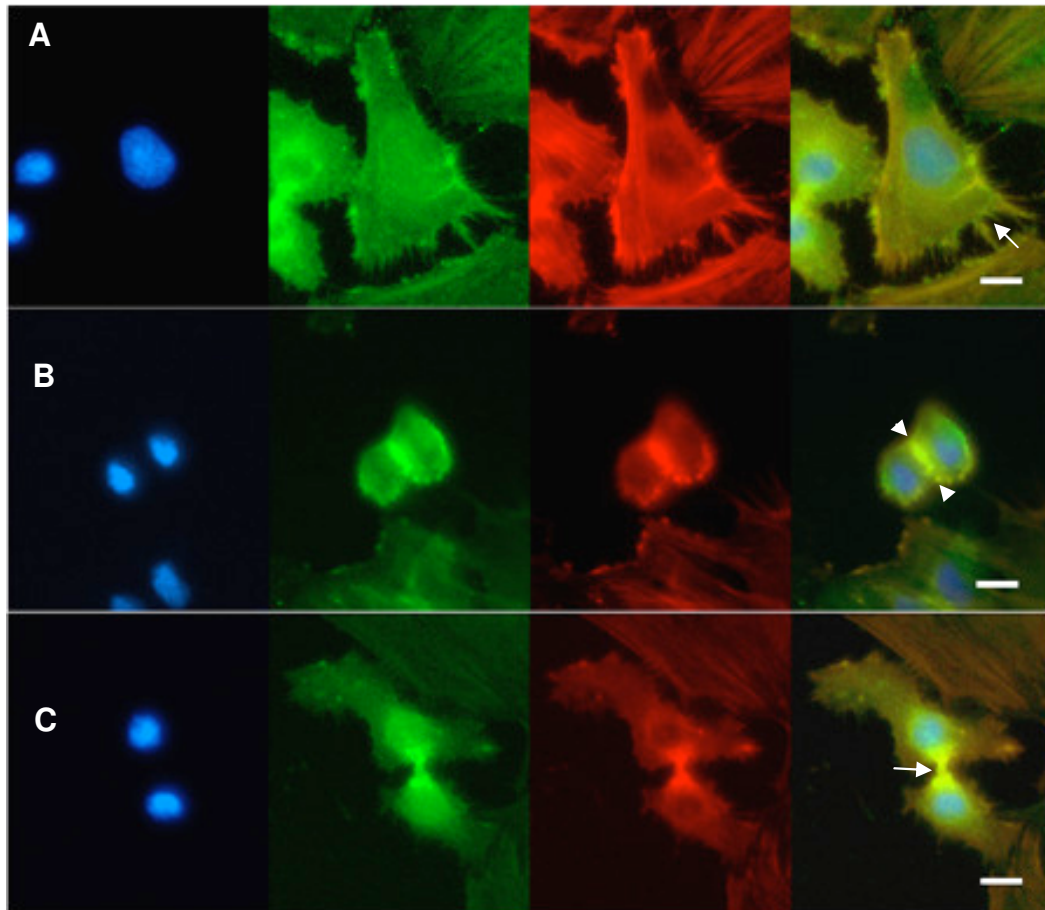


Figure 5.2: Endogenous dystroglycan localises to the cleavage furrow of Ref52 cells. Immunofluorescence images of fixed Ref52 fibroblasts stained for dystroglycan (green), actin (red phalloidin) and DNA (blue). A: Ref52 cell during interphase. Dystroglycan is expressed throughout the cell membrane and co-localises with actin in membrane protrusions (arrow, top panel). B: Dividing Ref52 cell in early telophase. Dystroglycan co-localises with actin at the cleavage furrow (double arrowheads). C: Dividing Ref52 cell in late telophase. Dystroglycan co-localises with actin at the cell midbody once the cleavage furrow has contracted completely (arrow, bottom panel). Scale bar = 10 μm .

5.2.2 *Dystroglycan-GFP localises to the cleavage furrow of stably-expressing Swiss 3T3 fibroblasts*

To further examine the localisation of dystroglycan in cytokinesis, Swiss 3T3 cells stably expressing full-length dystroglycan fused to a GFP tag ($\alpha\beta\text{DG-GFP}$) were screened for dividing cells by fluorescent microscopy. Cells undergoing cytokinesis were monitored by live-cell imaging. As a control, Swiss 3T3 cells stably expressing GFP alone were analysed. The lower panel of Figure 5.3 shows sequential images of a dividing Swiss 3T3

cell stably expressing $\alpha\beta$ DG-GFP, taken 1 minute apart. As the cell progresses through cytokinesis, the fluorescence concentrates at the cleavage furrow and later in the midbody. In contrast, fluorescence is distributed throughout the cytoplasm and appears to be excluded from the cleavage furrow as the cell divides in the GFP control. This suggests that dystroglycan is being recruited to the cleavage furrow during cell division.

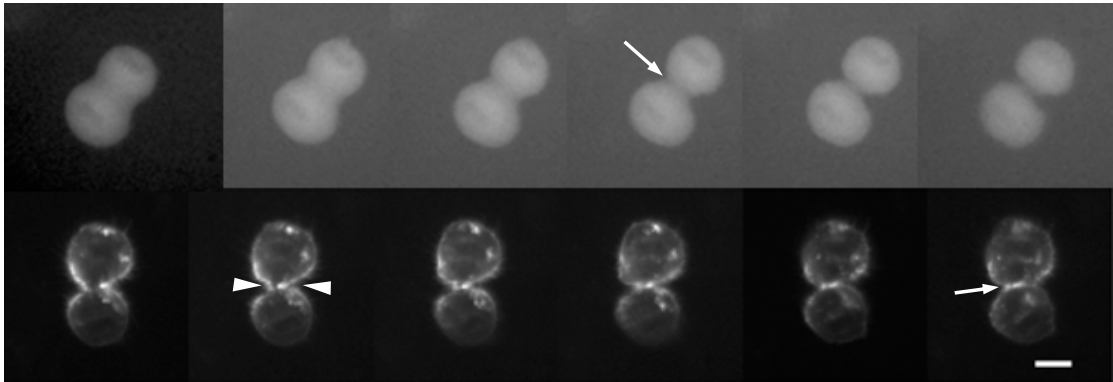


Figure 5.3: Dystroglycan-GFP localises to the cleavage furrow of dividing Swiss 3T3 cells. Live cell imaging of dividing Swiss 3T3 fibroblasts stably transfected with GFP (top panel) or $\alpha\beta$ DG-GFP (bottom panel). $\alpha\beta$ DG-GFP is localised to the cleavage furrow (double arrowheads, bottom panel) and the midbody (arrow, bottom panel), whereas GFP alone is excluded from this region (arrow, top panel). Images were captured at 1 minute intervals. $n = 3$ movies. Scale bar = 10 μ m.

5.2.3 Dystroglycan co-localises with ezrin in dividing Ref52 cells

Earlier results suggest that dystroglycan is recruited to the cleavage furrow during cytokinesis and it has previously been shown in the literature that ERM proteins also localise to the cleavage furrow and are thought to be involved in linking the actin cytoskeleton to the plasma membrane during cell division (Sato et al., 1992; Sato et al., 1991). Since β -dystroglycan can interact with ezrin (Spence et al., 2004a), co-localisation of these two proteins during cytokinesis was investigated. To achieve this, Ref52 cells were seeded onto glass coverslips overnight, then fixed and stained for endogenous β -dystroglycan and ezrin. Coverslips were screened for dividing cells using a fluorescent microscope. According to Figure 5.4, β -dystroglycan and ezrin co-localise at the cleavage

furrow in the early stages (A) and at the midbody at later stages of cytokinesis (B - C).

There was no bleedthrough between the fluorescence channels and this was controlled for by using a fluorescence microscope containing narrow band pass filters.

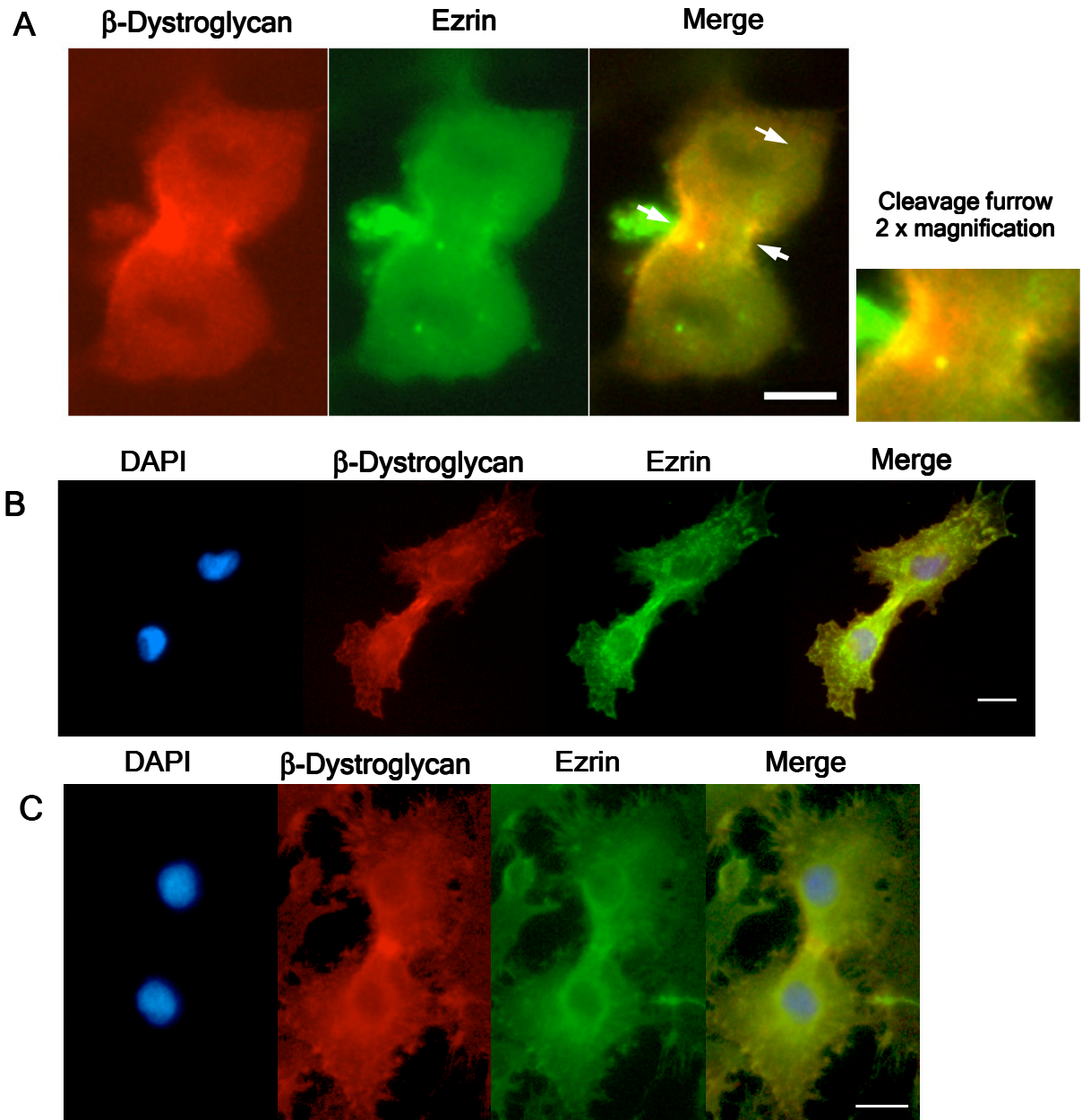


Figure 5.4: Dystroglycan co-localises with ezrin at the cleavage furrow. Ref52 cells undergoing cytokinesis were stained for β -dystroglycan (red) and ezrin (green). Nuclei were visualised by staining with DAPI (blue). β -Dystroglycan and ezrin were found to co-localise at the cleavage furrow (A) and midbody (B and C) (n = 10). Scale bar = 10 μ m.

5.2.4 Investigating the localisation of dystroglycan-GFP constructs during cytokinesis

The striking observation that dystroglycan is concentrated at the cleavage furrow and midbody during cytokinesis has been described thus far, however, the functional role of dystroglycan in cytokinesis is yet to be understood. To address this, the cellular localisation of different GFP-tagged dystroglycan constructs (see Figure 5.5 and Appendices I and II) was investigated during cytokinesis. An advantage of using GFP fusion proteins is that their localisation can be tracked using live cell imaging. This is hugely beneficial for studying a dynamic process such as cytokinesis as it allows visualisation of the protein throughout the progression of cell division, as opposed to immuno-staining of fixed cells when only a single stage in the process can be captured. Within any population of transfected cells the level of GFP expression varied markedly from one cell to another. Cells expressing the GFP-fusion proteins at high levels (i.e. cells emitting very bright fluorescence) for prolonged periods (> 24hours) were inviable due to the toxicity of the GFP-fusion. These cells failed to divide and on close examination under the microscope, exhibited noticeable membrane blebbing, which is a hallmark of apoptosis (Kerr et al., 1972). Therefore, high transfection efficiency was vital for the success of this study since it was necessary to find cells that were both expressing the fusion protein and undergoing cell division. Consequently, HeLa cells were preferentially used in this set of experiments because they could achieve a higher rate of transient transfection than Ref52 or Swiss 3T3 cells. Moreover, HeLa cells have been used in many studies on cell cycle and cytokinesis due to their rapid rate of cell division, ease of growth and symmetrical shape and were therefore considered to be a good choice of cell type for these experiments.

For the purpose of this study, several attempts were made to synchronise cells in order to maximise the opportunity for visualising cytokinesis. Initially, cells post-transfection were first treated with the microtubule depolymerising drug, nocodazole, in

order to block the cells at the G2/M phase of the cell cycle. In theory, following release from the block, all of the transfected cells should be preparing to undergo cytokinesis. However, this method was unsuccessful because, even after numerous modifications to the protocol such as varying the concentration of nocodazole and replating rounded up cells by mitotic shake-off, treated cells did not divide. In a second attempt to synchronise the cells, a double thymidine block was carried out, prior to nocodazole arrest (from (Kimura et al., 2000), see Methods Section 2.2.16.1). In this case, although there appeared to be numerous rounded-up cells following treatment, they did not divide and there was a high degree of cell death, which may have been a consequence of the procedure, which exposed the cells to several toxic reagents within a short space of time. Ultimately, the method used was simply to transfect the cells, leave them to recover overnight and subsequently screen the dish under the fluorescent microscope for dividing cells. Too much exposure to fluorescent light eventually resulted in cell death, but if transfected dividing cells were identified quickly, the localisation of the GFP-tagged dystroglycan could be studied.

The dystroglycan-GFP constructs ($\alpha\beta$ DG-GFP, DG Δ E-GFP, DG Δ C β and Myr C β -GFP) used in this study have been previously characterised and shown to exhibit expected membrane targeted expression in several different mammalian cell lines (Batchelor et al., 2007; Chen et al., 2003; Spence et al., 2004a).

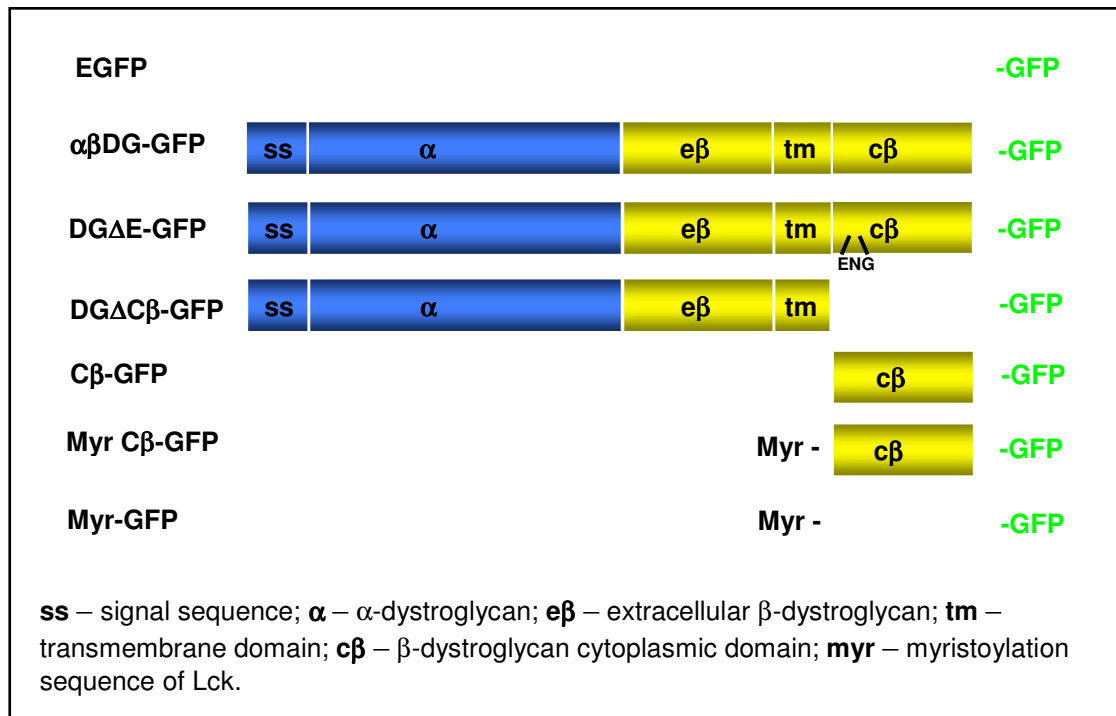


Figure 5.5: Schematic representation of the dystroglycan-GFP fusion constructs used in this study. EGFP – empty vector; $\alpha\beta$ DG-GFP – Full-length dystroglycan fused to a C-terminal GFP tag; DG Δ E-GFP – Full-length dystroglycan containing a mutated ezrin-binding site fused to GFP; DG Δ C β -GFP – Truncation mutant of dystroglycan with the cytoplasmic tail deleted fused to GFP; C β -GFP – Cytoplasmic tail of β -dystroglycan fused to GFP; Myr C β -GFP – Cytoplasmic tail of β -dystroglycan containing an N-terminal myristoylation sequence fused to GFP; Myr-GFP – Myristoylation sequence of Lck fused to GFP.

5.2.4.1 Dystroglycan-GFP localisation in dividing HeLa cells

Earlier results have shown that the full-length dystroglycan-GFP construct ($\alpha\beta$ DG-GFP) localises to the cleavage furrow and midbody in stably expressing Swiss 3T3 cells (Section 5.2.2), however, HeLa cells were found to be more reliable for transient transfection. Since all previous investigation has been undertaken using fibroblast cell lines, it was important to first investigate the localisation of $\alpha\beta$ DG-GFP in HeLa cells to confirm that this construct also localises to the cleavage furrow in epithelial cells. HeLa cells were transiently transfected with $\alpha\beta$ DG-GFP and co-stained for α -tubulin and DNA. Transfected cells were then screened using fluorescence microscopy for cells undergoing cell division. As shown in Figure 5.6, dystroglycan-GFP was localised strongly to the

midbody of HeLa cells that were in the late stages of cytokinesis. Co-staining of these cells for α -tubulin reveals that the strong localisation of dystroglycan-GFP corresponds to the point at which there is a gap between the microtubule bundles forming the central spindle, where the midbody protein complex is located.

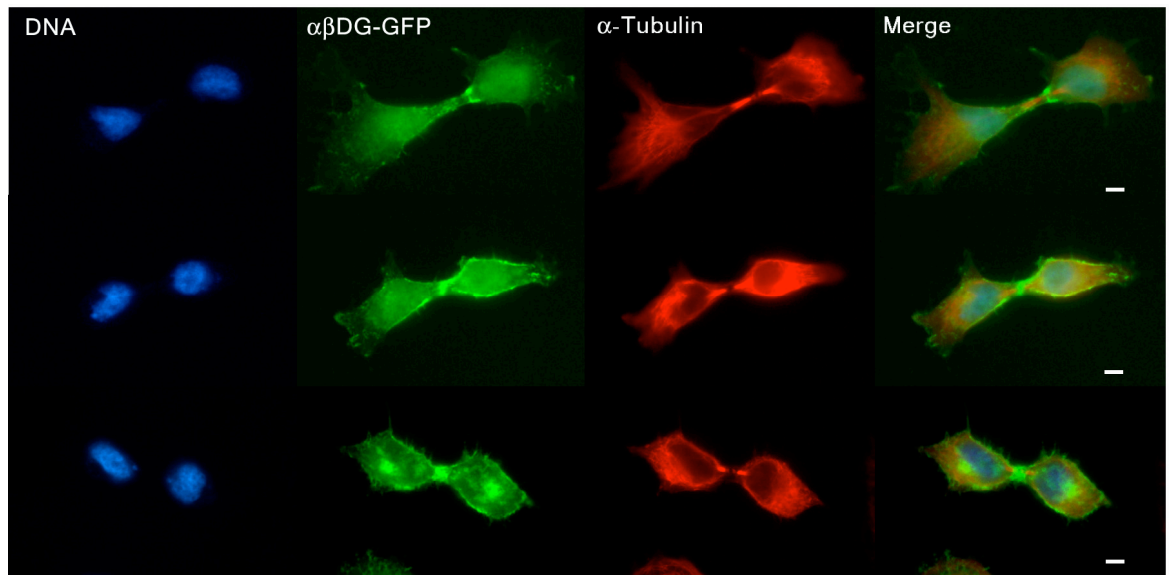


Figure 5.6: Dystroglycan-GFP is concentrated at the midbody in dividing HeLa cells. HeLa cells transfected with $\alpha\beta$ DG-GFP (green) were co-stained for α -tubulin (red) and DNA (blue). Dystroglycan-GFP is concentrated strongly at the midbody, flanked by α -tubulin (n = 5). Scale bar = 5 μ m.

Next, the progress of dividing cells was studied by live cell imaging. Figure 5.7 shows dystroglycan-GFP strongly localising to the cleavage furrow during the early stages of division, after which the localisation is less restricted until late cytokinesis where it concentrates at the midbody. This experiment confirms that dystroglycan localisation to the cleavage furrow is consistent in different cell types and it also showed that this new approach of imaging live transfected HeLa cells was successful and could be utilised to investigate the localisation of other dystroglycan-GFP constructs.

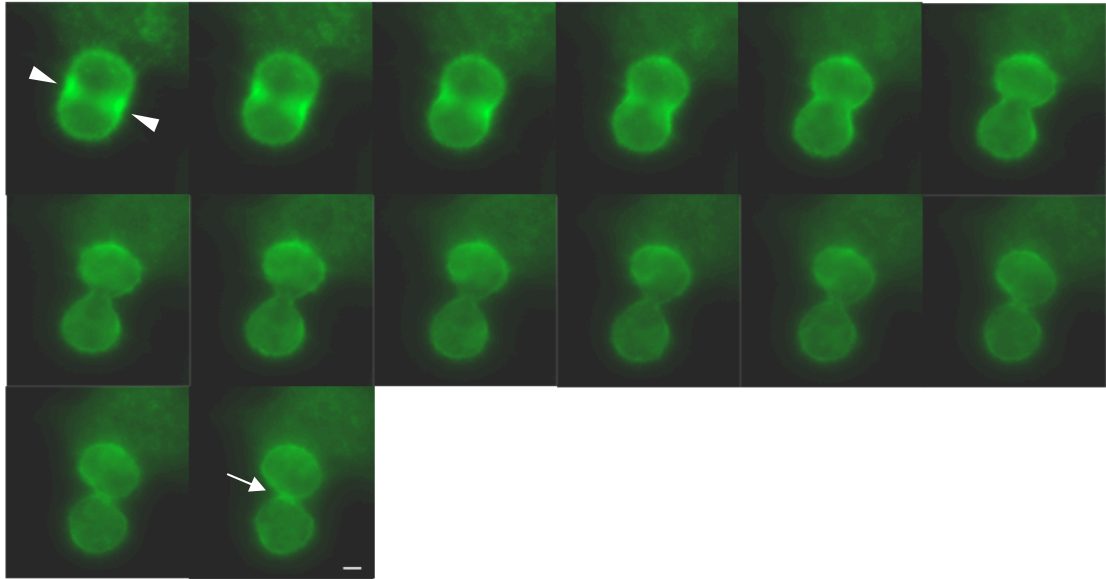


Figure 5.7: Dystroglycan-GFP localises to the cleavage furrow and midbody of dividing HeLa cells. Live cell imaging of a dividing HeLa cell transiently transfected with $\alpha\beta$ DG-GFP. Dystroglycan strongly localises to the cleavage furrow (double arrowheads) and later the midbody (arrow). Images were taken at 1 minute intervals ($n = 4$ movies). Scale bar = 5 μ m.

5.2.4.2 Myristolated-GFP does not localise to the cleavage furrow or midbody in dividing HeLa cells

To ensure that the increased fluorescence at the cleavage furrow and midbody previously described, and attributed to dystroglycan concentration, was not due to concentration of the membrane at these points but shows genuine recruitment of dystroglycan, HeLa cells were transfected with a control GFP construct containing the N-terminal myristoylation sequence of Lck (MGCVCSS) which targets the protein to the plasma membrane. This control differs from the previous GFP control (Section 5.2.2) because GFP is targeted to the plasma membrane. Figure 5.8 (A) shows that in HeLa (i) and REF52 (ii) cells transfected with Myr-GFP, the construct is membrane localised and therefore correctly targeted. Thus, if the cleavage furrow localisation was due to membrane density then this should also be evident in cells transfected with Myr-GFP. According to Figure 5.8 (B), which shows a dividing cell transfected with Myr-GFP, this construct was excluded from

the cleavage furrow (Figure 5.8 B) and therefore the concentration of fluorescence observed in earlier experiments was not due to membrane density, but is attributed to genuine recruitment of dystroglycan.

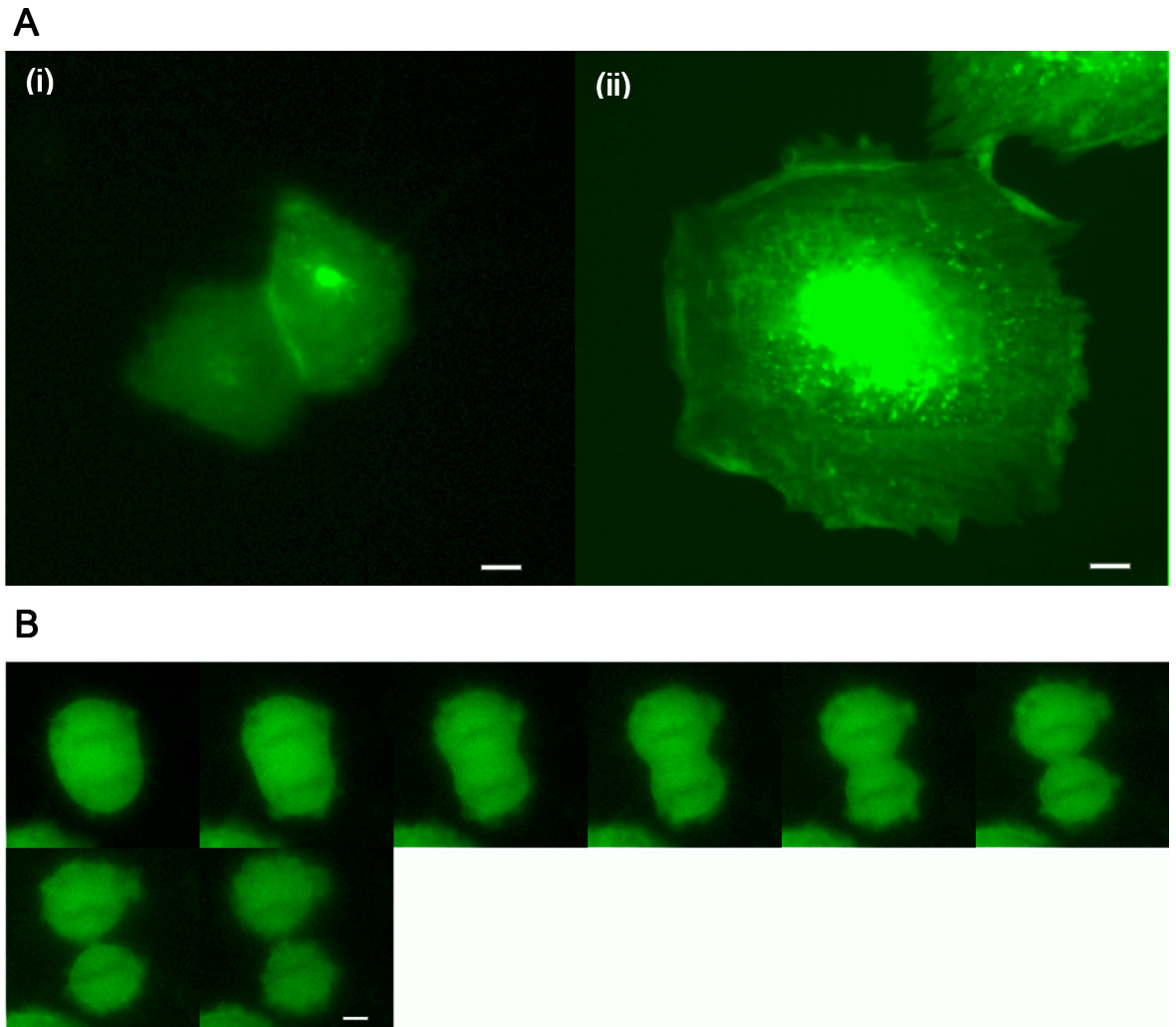


Figure 5.8: Myristoyl-tagged GFP does not localise to the cleavage furrow of dividing HeLa cells. A: Myristoyl-tagged GFP is correctly targeted to the membrane in transfected HeLa cells (i) and Ref52 cells (ii). Myr-GFP can be seen at cell-cell junctions (i) and at the membrane surface (ii). B: Live cell imaging of a dividing HeLa cell transiently transfected with myristoylated-GFP, which targets to the membrane. Myr-GFP not only fails to localise to the cleavage furrow or midbody, but it actually appears to be excluded from these areas (arrow) (n = 4 movies). Scale bar = 5 μ m.

5.2.4.3 Dystroglycan requires its C-terminal cytoplasmic tail for cleavage furrow localisation

The cytoplasmic tail of β -dystroglycan contains protein binding sites for many interacting proteins, including ezrin (discussed in Chapter 1). To determine whether this region is required for the localisation of dystroglycan during cytokinesis a dystroglycan-GFP construct with the cytoplasmic tail deleted (DG Δ C-GFP) was transfected into HeLa cells. If dystroglycan is recruited to the cleavage furrow at the start of cytokinesis by one of its cytoskeletal binding partners, perhaps ezrin, then it would require its cytoplasmic tail for its localisation. By transfecting a truncated form of dystroglycan, it may be possible to determine if dystroglycan recruitment is dependent upon its cytoskeletal contacts. Figure 5.9 shows that DG Δ C-GFP did not accumulate specifically at the cleavage furrow or midbody of the dividing cell (compare with Figure 5.7), which suggests that dystroglycan requires cytoplasmic interactions for its localisation. Cells transfected with DG Δ C-GFP exhibited strong staining of the plasma membrane, which was more apparent than cells transfected with the other DG-GFP constructs. A possible reason for this may be that, in the absence of the cytoplasmic domain, β -dystroglycan cannot be phosphorylated and/or turned over and is retained at the plasma membrane.

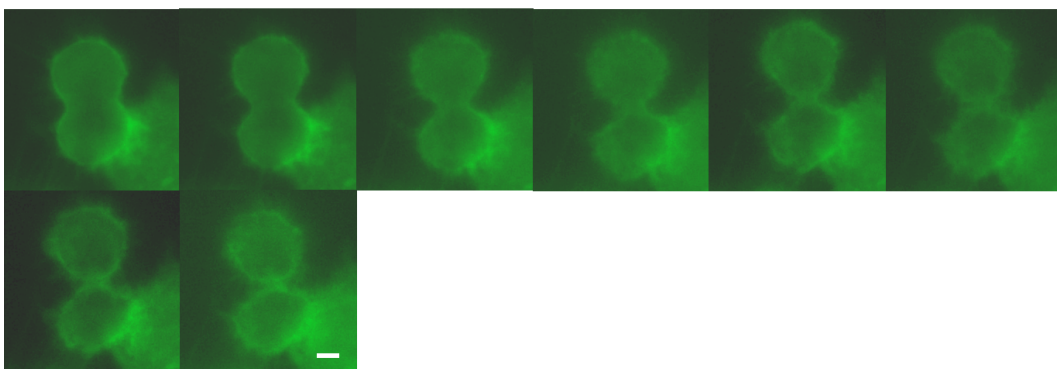


Figure 5.9: Dystroglycan requires its cytoplasmic domain for cleavage furrow localisation. Live cell imaging of a dividing HeLa cell transiently transfected with DG Δ C-GFP. This mutated protein does not accumulate at the cleavage furrow or midbody in these cells, suggesting that the cytoplasmic region of β -dystroglycan is essential for its localisation. Images were taken at 1 minute intervals ($n = 8$ movies). Scale bar = 5 μ m.

5.2.4.4 Expression of the cytoplasmic tail of β -dystroglycan

Further investigations into the recruitment of dystroglycan to the cleavage furrow during cytokinesis were attempted by transfecting cells with a construct expressing only the cytoplasmic tail of β -dystroglycan, lacking the transmembrane domain, fused to GFP (C β -GFP). As shown in Figure 5.10 (A), in non-dividing HeLa cells transfected with C β -GFP, the expressed protein does not localise to the membrane, but remains cytoplasmic and a high proportion of the expressed protein accumulates in the nucleus. In this present study, no dividing HeLa cells expressing C β -GFP were observed, despite achieving $\geq 50\%$ transfection efficiency. A possible reason for this may be that by expressing the cytoplasmic domain of β -dystroglycan alone, it may be sequestering crucial factors away from the cleavage furrow and thus preventing cytokinesis. There was, however, no evidence of failure in cytokinesis, such as the presence of multinucleate cells.

To further address this, cells were transfected with a C β -GFP construct containing an N-terminal myristoylation sequence, to target the protein to the membrane. As shown in Figure 5.10 (B), C β -Myr is correctly targeted to the plasma membrane in transfected HeLa cells as it is clearly visible in surface filopodia. If the cytoplasmic tail alone sequesters cleavage furrow components away from the membrane, then this construct should allow for their membrane association, assuming that the β -dystroglycan cytoplasmic tail is sufficient for cleavage furrow localisation. Unfortunately, the transfection efficiency of MyrC β -GFP in HeLa cells was very low and no dividing cells expressing the protein could be found.

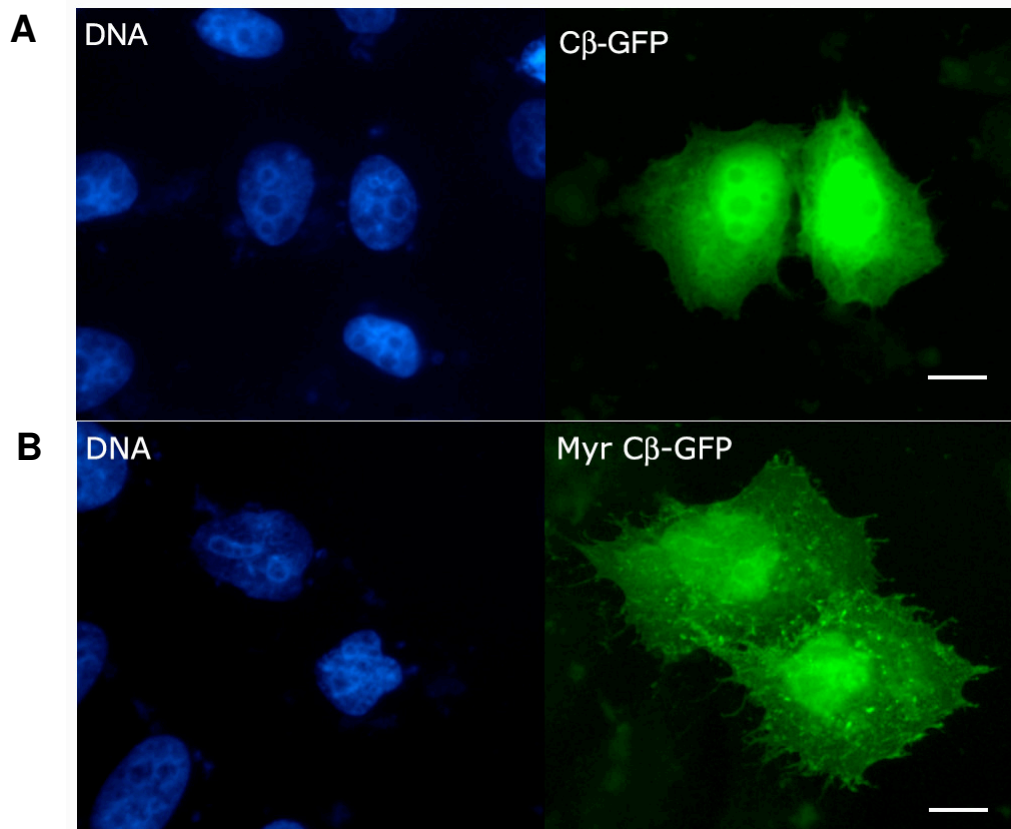


Figure 5.10: Myristoyl-tagged C β -GFP is correctly targeted to the plasma membrane.

A: HeLa cells transiently transfected with the cytoplasmic tail of β -dystroglycan fused to GFP (green) and stained for DNA (blue). This construct is cytoplasmic and accumulates in the nucleus. B: HeLa cells transiently transfected with the cytoplasmic tail of β -dystroglycan containing a myristoyl tag fused to GFP. This construct is membrane targeted and is visible in membrane surface protrusions. Scale bar = 10 μ m.

5.2.4.5 Dystroglycan does not require ezrin binding for cleavage furrow localisation

Previous data had suggested that dystroglycan accumulation at the cleavage furrow is modulated through the β -dystroglycan cytoplasmic tail, but we do not yet know what signals its recruitment. A likely candidate is ezrin, since the ERM proteins are known to localise to the cleavage furrow (Sato et al., 1991). One site responsible for ezrin binding is located on the cytoplasmic tail of β -dystroglycan and is dependent upon a group of basic residues at the juxtamembrane region (Spence et al., 2004a). To investigate whether ezrin-binding is required for cleavage furrow localisation, HeLa cells were transfected with a dystroglycan-GFP construct in which these basic residues were mutated to prevent ezrin

from binding (DG Δ E GFP). As shown in Figure 5.11, this mutant construct accumulates at the cleavage furrow in dividing cells, suggesting that ezrin binding is not essential for its localisation during cytokinesis. This construct did not appear to concentrate at the midbody, which may indicate that ezrin-binding is required for maintaining dystroglycan localisation during the latter stages of cytokinesis. This suggests that perhaps ezrin binding, although perhaps not essential for cleavage furrow recruitment of dystroglycan, may still play a role in this process.

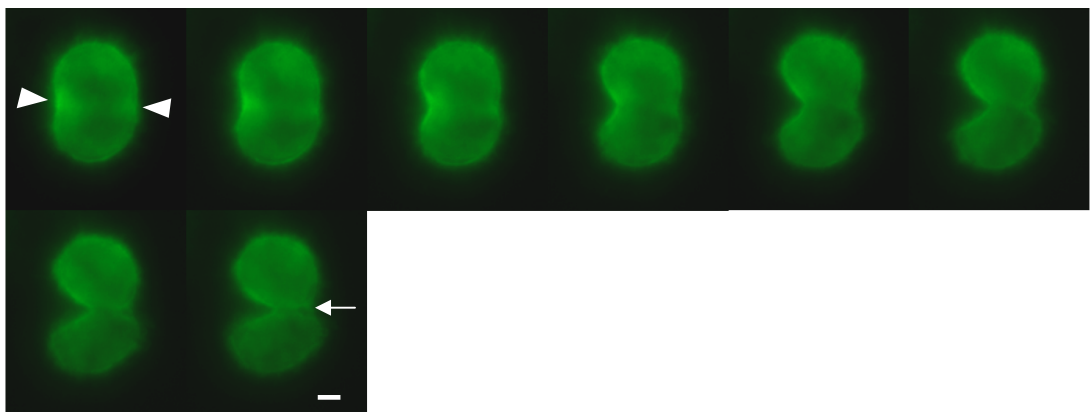


Figure 5.11: Dystroglycan does not require ezrin binding for cleavage furrow localisation. Live cell imaging of a dividing HeLa cell transiently transfected with DG Δ E GFP. This mutated protein localises to the cleavage furrow of dividing cells (double arrowheads), though did not appear to accumulate at the midbody (arrow) (n = 4 movies). Scale bar = 5 μ m.

5.3 Discussion

Cytokinesis is a highly dynamic process that requires seamless coordination between the actin and microtubule networks. However, many aspects of its mechanism are poorly understood. For example, the proteins required by the actomyosin contractile ring at the cleavage furrow to fortify its structure and modulate its interactions with the mitotic spindle and the plasma membrane have not been extensively studied.

In this chapter, the localisation of the widely expressed cell adhesion molecule, dystroglycan, during cell division was investigated. This study provides evidence to show that dystroglycan accumulates at the cleavage furrow and midbody in fibroblasts and HeLa cells and that it co-localises with actin and ezrin during cytokinesis. Also, by transiently transfecting cells with different mutated and truncated GFP constructs of dystroglycan, it was determined that localisation at the cleavage furrow requires the cytoplasmic domain of β -dystroglycan, but not the ability to bind to the ERM family member, ezrin. However, it is speculated that ezrin binding may be required to maintain dystroglycan at the midbody during late cytokinesis.

The accumulation of dystroglycan at the cleavage furrow, shown in this study by endogenous staining of dystroglycan (Figure 5.2) and expression of GFP-dystroglycan constructs in dividing fibroblasts (Figure 5.3) and HeLa cells (Figure 5.6-5.7), is highly plausible considering that several other membrane glycoproteins have previously been shown to accumulate there. One such example is CD44, a widely-expressed heavily glycosylated transmembrane protein which was found to localise to the cleavage furrow in dividing BHK cells and mouse L fibroblasts (Tsukita et al., 1994). Also, the membrane glycoprotein CD43, which is expressed on thymocytes and T-cells, accumulates at the cleavage furrow of dividing basophilic leukaemia cells (Yonemura et al., 1993) and the rat homologue of CD43 has been localised to the cleavage furrow of dividing rat thymocytes

(de Petris, 1984). Dystroglycan shares several characteristics with both of these proteins in that they all contain a single transmembrane region, are heavily glycosylated and bind to ERM proteins through a positively charged cluster of residues at the juxta-membrane region (Legg and Isacke, 1998; Spence et al., 2004a; Yonemura et al., 1998). This suggests that dystroglycan may share a common function with CD43 and CD44 at the cleavage furrow.

Membrane glycoproteins are attractive candidates for the putative membrane anchor thought to link the contractile ring to the plasma membrane during cytokinesis, due to their location at the membrane and ability of the cytoplasmic tail to act as a scaffold for intracellular binding partners. Other adhesion molecules found at the cleavage furrow are L-selectin (Po et al., 1999), leukocyte adhesion molecule-1 (Pilarski et al., 1991) and membrane immunoglobulins (de Petris, 1984). Expression of these proteins is restricted to cells of the immune system, which may signify some functional redundancy between different cell types.

The localisation of dystroglycan to the cleavage furrow in dividing HeLa cells was investigated by transient transfection of various dystroglycan-GFP constructs (Figure 5.5). Subsequent localisation of these constructs by live-cell imaging gave some insight into the possible function of dystroglycan during cytokinesis.

To initially investigate the possibility that that the GFP-tag could be targeting dystroglycan to the cleavage furrow, the localisation of GFP was observed in dividing stable GFP-expressing Swiss 3T3 fibroblasts. This was found not to be the case, since in dividing cells, GFP appeared to be excluded from the cleavage furrow (Figure 5.3). This was also found to be the case in cells expressing GFP containing a myristoyl group, which targets the protein to the membrane (Figure 5.8). This result indicates that the strong signal observed at the cleavage furrow in dystroglycan-GFP expressing cells is not due to

membrane density. Moreover, specific immuno-staining showed that endogenous β -dystroglycan localises to the cleavage furrow (Figure 5.2) and this cannot be attributed to GFP targeting.

Expression of a truncated mutant of dystroglycan, lacking the cytoplasmic domain did not localise to the cleavage furrow of dividing HeLa cells, suggesting that this region is essential for its accumulation (Figure 5.9). The β -dystroglycan cytoplasmic domain contains many protein-protein interaction domains including the ezrin-binding site. Previous studies investigating the localisation of CD43 showed that the region required for cleavage furrow localisation was the first half of the cytoplasmic domain adjacent to the transmembrane region. The authors speculated that this domain may be expressed in other membrane proteins which would explain why cells lacking CD43 could divide (Yonemura et al., 1993). This same argument could be used to explain why cells expressing truncated dystroglycan did not fail in cytokinesis.

Previous studies have shown that CD43 and CD44 co-localise with ERM family members, ezrin, radixin and moesin at the cleavage furrow (Tsukita et al., 1994; Yonemura et al., 1993). The ERM proteins are cytoskeletal cross-linkers that are members of the Band 4.1 superfamily of proteins. ERM proteins link the actin cytoskeleton to the plasma membrane through interaction with transmembrane receptors and are involved in mediating cytoskeletal reorganisation. Radixin was the first of the ERM proteins to be observed at the cleavage furrow in mammalian cells (Sato et al., 1991) but since the ERM family proteins are highly homologous (Funayama et al., 1991; Gould et al., 1989; Lankes and Furthmayr, 1991; Turunen et al., 1989), it is now accepted that ezrin and moesin also localise to the cleavage furrow (Sato et al., 1992). This has been confirmed in the present study by distinctive staining of ezrin at the cleavage furrow and midbody which co-localised with dystroglycan (Figure 5.4). Since the ERM proteins are able to bind directly

to actin filaments (Turunen et al., 1994), they are likely to function in tethering the cytoskeleton to transmembrane receptors, such as dystroglycan at the plasma membrane during furrow ingression.

ERM proteins and CD43 have been localised specifically to small actin-rich protrusions called microvilli within the cleavage furrow and it has been determined that in thymocytes and basophilic leukaemia cells there was an increase in microvilli at the cleavage furrow compared to the rest of the cell (Yonemura et al., 1993). However, this observation was not consistent with earlier studies undertaken in mastocytoma and PtK2 cells (Knutton et al., 1975; Sanger et al., 1984). The function of microvilli at the cleavage furrow has not been extensively studied, although after the initial discovery it was thought that their role was to increase the membrane surface area and thus physically unfold enough membrane to create two cells from a single cell (Knutton et al., 1975). With current understanding of the terminal stages of cytokinesis during which new membrane insertion is critical, this early hypothesis may actually be fairly accurate (Reviewed in (Finger and White, 2002)).

The formation of actin-rich membrane protrusions is mediated through activation of the Rho-family GTPase, Cdc42. Dystroglycan has recently been found to be involved in mediating changes in the actin cytoskeleton that induce the formation of filopodia and microvilli (Chen et al., 2003) in an ezrin- and Cdc42-dependent manner (Spence et al., 2004a). These structures are highly dynamic and are important for many processes including cell movement and axon guidance (Nobes and Hall, 1995). Most recently, it has been shown that dystroglycan recruits a complex containing ezrin and the Rho GDP/GTP exchange factor (GEF), Dbl, which activates both Rho and Cdc42 GTPases (Batchelor et al., 2007). Taken together, this evidence adds new complexity to the possible function of dystroglycan in the cleavage furrow because it may act as a scaffolding molecule to recruit

a complex containing ezrin and Dbl to the membrane, in order to induce the formation of membrane protrusions and thus contribute towards termination of cytokinesis.

The cytoplasmic domain of β -dystroglycan contains binding sites for multiple interacting proteins and is essential for correct functionality of the protein. In this study, HeLa cells were transfected with the cytoplasmic domain alone, lacking the transmembrane domain, fused to GFP (C β -GFP) in order to investigate its effect on cytokinesis. Fibroblasts transfected with C β -GFP were previously shown to have a significantly reduced number of filopodia, compared to cells expressing the full-length protein (Chen et al., 2003). This was thought to be due to the C β -GFP construct, which remains cytoplasmic, sequestering important factors such as ezrin away from the membrane (Spence et al., 2004a). This may also explain the lack of dividing cells in the C β -GFP-expressing population in the present study (see section 5.2.4.4). Functional redundancy by other membrane glycoproteins may be overridden if the cytoplasmic domain is sequestering effector proteins required for cytokinesis. There is evidence in the literature that a similar effect occurs during the expression of truncated ERM proteins. For example, when the C-terminal domain of radixin is expressed in NIH 3T3 cells, it does not localise to the cleavage furrow, but produces a multinucleate phenotype and it is thought that this domain may sequester components required for F-actin formation and indirectly affect cytokinesis (Henry et al., 1995). Also, the overexpression of the C-terminal domain of drosophila moesin in *S.pombe* produces multinucleate cells (Edwards et al., 1994). There was no noticeable increase in multinucleate cells after transfection with C β -GFP in the present study, although this possibility has not yet been fully investigated. Perhaps, since the transfected cells were analysed very quickly following transfection, they had not yet been expressing the protein for long enough to show an obvious multinucleate

phenotype. Alternatively, C β -GFP may be sequestering factors required for an earlier stage in cell division and as a result the process is halted prior to nuclear division.

Hela cells were transfected with a construct encoding the C-terminal cytoplasmic tail tagged with a myristoyl group (MyrC β -GFP) to investigate if membrane relocation could rescue the apparent cytokinesis defect in C β -GFP-expressing cells (Figure 5.10). Also, by observing the localisation of MyrC β -GFP during cytokinesis, it may indicate whether any outside signalling is required for dystroglycan recruitment to the cleavage furrow. Unfortunately, the localisation of this MyrC β -GFP could not be determined due to a very low transfection ratio. However, studies investigating CD43 localisation during cytokinesis have shown that outside-in signalling was not required and the C-terminal domain was both necessary and sufficient for its localisation to the cleavage furrow (Yonemura et al., 1993).

Dystroglycan containing a mutated ezrin binding site (DG Δ E) was found to localise to the cleavage furrow (Figure 5.11), which suggests that ezrin binding is not required for cleavage furrow localisation. However, this does not necessarily mean that there is no interaction between these proteins at the cleavage furrow; just that ezrin does not recruit dystroglycan. This is consistent with previous data which showed that dystroglycan recruits ezrin to filopodia (Spence et al., 2004a). Localisation studies using truncated mutants of CD43 carried out in leukocytes, showed that the first half of the cytoplasmic region (i.e. closest to the membrane and containing the ERM binding region) was sufficient for cleavage furrow localisation (Yonemura et al., 1993). It is important to consider that the CD43 study was carried out prior to the identification of the ERM-binding site and the entire first half of the cytoplasmic domain was expressed. Since the mutant construct used in the present study contained a specific mutation in the ERM-binding site, this promotes the notion that another factor must be involved in order to

signal the recruitment of dystroglycan to the cleavage furrow, perhaps mediated through ligand binding to α -dystroglycan on the outer surface of the membrane. Furthermore, expression of DG Δ E did not result in failure of the cells to complete cytokinesis. This can be explained by the possibility that other transmembrane glycoproteins, such as CD44, may be functioning redundantly. Surprisingly, unlike full-length dystroglycan, DG Δ E did not appear to localise to the midbody (Figure 5.11), which suggests that ezrin is required to maintain dystroglycan at the cleavage furrow. Perhaps ezrin-binding masks a proteolytic cleavage site and at some point between furrow ingression and midbody formation, dystroglycan is vulnerable to proteolytic enzymes, such as matrix metalloproteinases (MMPs). A cleavage site recognised by MMPs has previously been identified on the extracellular portion of β -dystroglycan (Yamada et al., 2001), which suggests that it is sensitive to degradation in some circumstances.

The analysis of synchronised DG - cells by flow cytometry suggested that there was an accumulation of cells in S-phase resulting in a slower progression through the cell cycle than the control population (See Section 4.2.11). Also, by Annexin V assay, it was shown that there was an increase in apoptotic cells in the DG - population (Section 4.2.12)). An increase in apoptotic cells has also been reported in other dystroglycan knockdown studies involving myotubes (Montanaro et al., 1999) and mouse mammary epithelial cells (Sgambato et al., 2006). If dystroglycan is a fundamental component of the complex required for structural stability of the contractile ring-plasma membrane interface and the recruitment of components required for microvilli formation at the cleavage furrow, then perhaps other membrane glycoproteins cannot function efficiently in the absence of dystroglycan. This could possibly explain the increased incidence of apoptosis observed in DG - cells. Furthermore, β -Dystroglycan expression levels have been reported to dramatically change in synchronised cultures of murine mammary epithelial cells and

bovine aortic endothelial cells as they progress through the cell cycle (Hosokawa et al., 2002; Sgambato et al., 2006). This also supports a possible role for dystroglycan in cytokinesis.

In conclusion, the data presented in this chapter provides evidence that dystroglycan accumulates at the cleavage furrow of dividing cells. Cleavage furrow localisation was shown to be dependant upon the cytoplasmic tail of β -dystroglycan but not the ability to bind the ERM family member, ezrin. The interaction with ezrin may however be important for retention of dystroglycan at the midbody during the final stages of cytokinesis. These findings suggest that dystroglycan plays a role in cytokinesis, possibly as a component of a membrane complex that tethers the actin cytoskeleton to the plasma membrane and/or a scaffolding molecule for upstream components of cleavage furrow signalling pathways. A proposed model for the function of dystroglycan at the cleavage furrow is illustrated in Figure 5.12. This study has opened up new avenues of investigation into the function of dystroglycan and more research will be required to fully elucidate its role during cytokinesis.

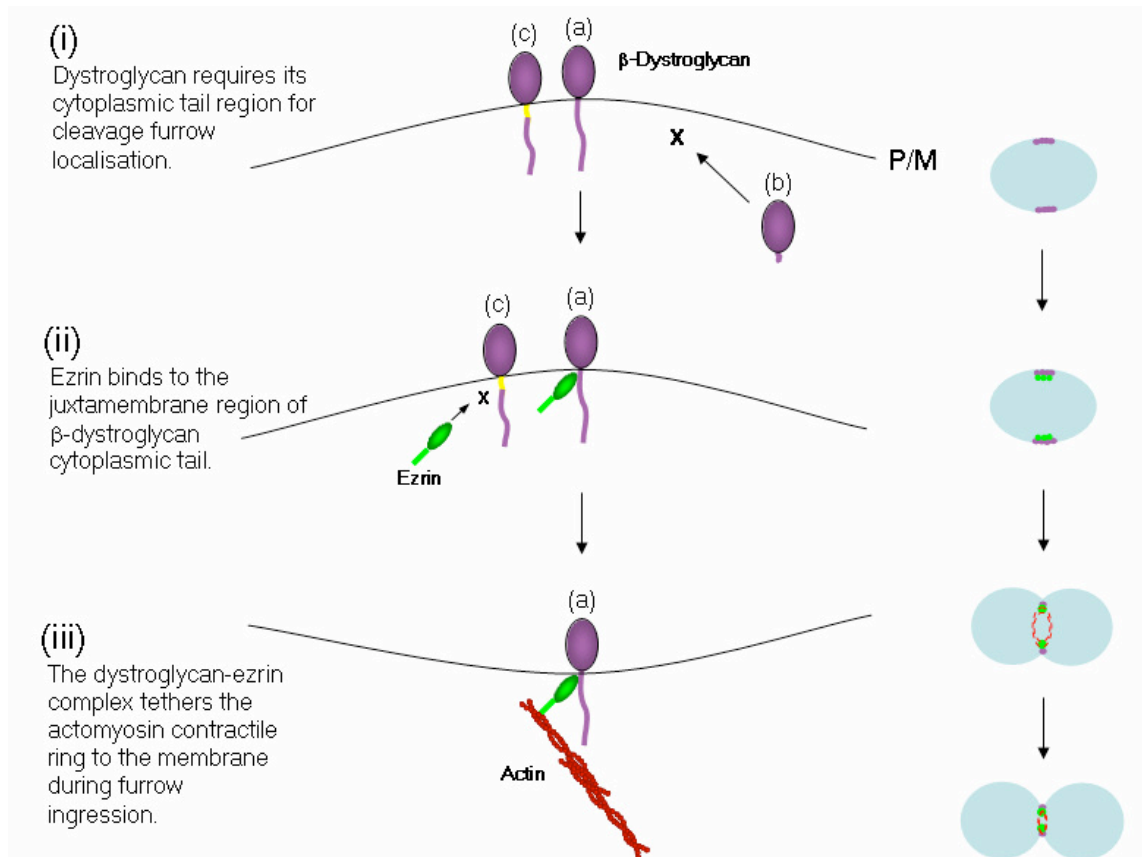


Figure 5.12: Model of dystroglycan function at the cleavage furrow. (i): β -Dystroglycan localises to the site of furrow ingression ((a) and (c)) and requires its cytoplasmic tail region for this localisation (b). (ii): β -Dystroglycan does not require ezrin binding for cleavage furrow localisation (c), but perhaps recruits ezrin and requires this interaction for its function at the cleavage furrow (a). (iii): The β -dystroglycan-ezrin complex tethers the actomyosin contractile ring to the cell membrane during cleavage furrow ingression. P/M = plasma membrane.

Chapter 6:

Final Discussion

Chapter 6

Final Discussion

Dystroglycan is a widely expressed cell adhesion molecule comprising two subunits, α -dystroglycan (peripheral membrane protein) and β -dystroglycan (transmembrane protein) that links the actin cytoskeleton to the extracellular matrix (Ervasti and Campbell, 1993; Ibraghimov-Beskrovnaya et al., 1992). Dystroglycan provides an important structural link tethering the cell to the surrounding matrix and is pivotal in maintaining tissue integrity. Dystroglycan is now known to also have important functions out with its structural role, as a receptor for extracellular binding partners and a regulator of intracellular signal transduction. Much research has focussed on the role of dystroglycan in development and disease, whereas relatively little is known about how dystroglycan functions at the cellular level. β -Dystroglycan has been shown to interact with a whole host of cytosolic and cytoskeletal binding partners, many of which are involved in signal transduction, suggesting that dystroglycan may be involved in regulating fundamental cellular processes such as proliferation, motility and cytoskeletal rearrangements. However, the mechanisms by which dystroglycan regulates these intracellular interactions and the downstream effects are just starting to be elucidated. The aim of this study was to build on current understanding of dystroglycan function at the cellular level by generating dystroglycan deficient fibroblasts and characterising their phenotype, with particular emphasis on how the cytoskeleton is affected.

Complete targeted disruption of the dystroglycan gene in mice resulted in embryonic lethality (Williamson et al., 1997) and as a consequence other methods to study dystroglycan deficiency were developed. One group used dystroglycan null ES cells to generate dystroglycan chimaeric mice, which had skeletal muscles effectively devoid of

dystroglycan expression (Cote et al., 1999). In this study, two different approaches were made to create dystroglycan deficient fibroblasts. In the first method, the dystroglycan null ES cells used to generate dystroglycan chimaeric mice (Cote et al., 1999) were differentiated into an immortal fibroblast cell line (Section 3.2.1). Further analysis of these cells was, however, abandoned following the discovery that they were, in fact, expressing dystroglycan (Section 3.2.3). Possible explanations for this were thoroughly investigated, such as the possibility that dystroglycan expression could be re-initiated following gene disruption (Section 3.2.4). However, it was confirmed using genomic PCR that the cells did not contain the gene targeted cassette (Section 3.2.6). Further investigation into how these cells did come to express dystroglycan was not considered to be worthwhile and consequently another method to generate dystroglycan deficient fibroblasts was employed.

Dystroglycan knockdown fibroblasts were produced by RNAi, in which the dystroglycan expression level was reduced by > 60 % (Sections 4.2.1 - 4.2.2). This level of knockdown was a possible limitation since residual dystroglycan expression may be adequate for many cellular processes in which dystroglycan is involved. Nonetheless, the resultant cells were significantly altered when compared to control cells, which suggests that this level of knockdown was sufficient to study dystroglycan deficiency. Other groups have reported a reduction in dystroglycan expression of ~80 - 90% different cell lines during transient expression of shRNA constructs (Jones et al.; Montanaro et al., 1999; Sgambato et al., 2006). Interestingly, in this study dystroglycan expression was found to be decreased by ~80% shortly after retroviral infection of the shRNA construct, but this level of knockdown could not be maintained in a stable cell line. Together, these results suggest that perhaps there is a limiting threshold level of dystroglycan expression required for cell survival.

The cytoplasmic tail region of β -dystroglycan associates with the actin cytoskeleton via binding partners such as utrophin (James et al., 1996) and has also been found to associate with F-actin directly (Chen et al., 2003). Dystroglycan localises to areas of close association between the actin-rich structures and the plasma membrane, for example focal adhesions (Belkin and Smalheiser, 1996; James et al., 1996) and membrane protrusions (Spence et al., 2004a) and, in view of this, it is reasonable to suppose that depletion of dystroglycan may have some detrimental effects on the actin cytoskeleton. Dystroglycan deficient fibroblasts were found to be less than 50% smaller in area than control cells and this was thought to be a consequence of the cell inability to spread effectively onto the substrate (Section 4.2.3). This hypothesis was supported by the results obtained from analysing the quantity and size of vinculin-containing focal adhesions, which showed that dystroglycan deficient fibroblasts contained less focal adhesions per cell area than control cells and there was also found to be a slight decrease in the number of mature focal adhesions (Section 4.2.4). Interestingly, similar characteristics have been reported in cells deficient in focal adhesion proteins, such as fibroblasts isolated from vinculin null mice, which were found to be less spread than control cells (Xu et al., 1998). Dystroglycan has been localised to the area surrounding classical vinculin-rich focal adhesions (James et al., 1996) and it is therefore interesting that, in this study, there were less focal adhesions in dystroglycan-deficient cells, suggesting perhaps that dystroglycan is required for their formation and/or maintaining their stability. Focal adhesion assembly and disassembly is regulated by tyrosine phosphorylation (Burrige and Chrzanowska-Wodnicka, 1996) and the phosphorylation of a tyrosine residue on the cytoplasmic tail of β -dystroglycan has been shown to be adhesion-dependent (James et al., 2000). Together, these results strongly suggest that dystroglycan is involved in the regulation of focal

adhesion assembly; however, further investigation is required to provide better understanding of the mechanisms by which this occurs.

To assess whether dystroglycan deficiency had any effect on the organisation of the F-actin network, dystroglycan deficient fibroblasts stained for F-actin were analysed by fluorescence microscopy. The fluorescent intensity of the F-actin appeared reduced in comparison to control cells, however there was no apparent reduction in F-actin content as determined by biochemical assay (Section 4.2.5). Further confirmation of this quantification could be carried out by staining cells with enough rhodamine-phalloidin to saturate the binding of F-actin before measuring the fluorescent intensity, which may be a more accurate measure of F-actin concentration (Cooper, 1987). An alternative possibility for the reduction in fluorescent intensity is perhaps that dystroglycan deficient cells have a reduction in bundled actin filaments, since the fluorescent intensity of phalloidin-stained F-actin increases when actin filaments are very close together. Dystroglycan has been shown to have F-actin bundling activity *in vitro* and to be involved in formation of filopodia, which are composed of bundled actin filaments (Chen et al., 2003) and the results obtained in this study suggest that dystroglycan may be involved in bundling actin filaments, perhaps by anchoring actin stress fibres to the membrane at focal adhesion complexes. Further investigation is required to confirm these findings; in particular it would be interesting to see if re-expression of dystroglycan in dystroglycan deficient cells was sufficient to increase the fluorescent intensity of phalloidin staining to normal levels.

Dystroglycan has recently been implicated in the formation of filopodial membrane protrusions by recruiting upstream components of the Cdc42 pathway to the plasma membrane resulting in localised activation of Cdc42, which was found to be dependent on dystroglycan binding to the cytoskeletal linker protein, ezrin (Batchelor et al., 2007; Chen et al., 2003; Spence et al., 2004a). The results presented here strengthen this evidence

because the ability of dystroglycan deficient fibroblasts to induce filopodia in response to dominant active Cdc42 was found to be inhibited (Section 4.2.14.1). Further confirmation of this result could be achieved by repeating this analysis following re-expression of dystroglycan in dystroglycan deficient cells. In addition, this investigation has generated new questions about how dystroglycan could be involved upstream of Rho GTPase signalling pathways since lamellipodia formation was inhibited in dystroglycan deficient cells in response to dominant active Rac1, suggesting that dystroglycan may also be regulating upstream components of the Rac1 pathway (Section 4.2.14.2). A previous study carried out in rat skeletal muscle subjected to atrophy, in which DGC components are depleted, found that Rac1 activity in these cells was reduced (Chockalingam et al., 2002). A recent study, also in muscle cells, found that binding of laminin-1 to α -dystroglycan initiated the tyrosine phosphorylation of syntrophin allowing it to bind to Grb2, which activates Sos1, which in turn activates the Rac1 pathway (Zhou et al., 2006). Results obtained in this current study provided the first evidence to suggest that dystroglycan mediates Rac1 signalling in non-muscle cells and further investigation is required to determine the intermediate components linking dystroglycan to Rac1 signalling in fibroblasts. This study also aimed to determine whether dystroglycan deficiency affected RhoA activity, however conclusive evidence could not be obtained due to low expression of the dominant active RhoA construct (Section 4.2.14.3). Optimisation of the transfection conditions, for example by varying the DNA concentration and the length of exposure to the transfection media, may improve the transfection efficiency. Low expression of the dominant negative Rho GTPase constructs also resulted in inconclusive results, but in hindsight the expression of any of these constructs was unlikely to affect cell morphology in unstimulated cells (Section 4.2.14.4). Dominant negative Rho GTPases were found to inhibit the cytoskeletal rearrangements induced by the addition of growth factors (Nobes

and Hall, 1995; Ridley and Hall, 1992), but since dystroglycan mediates interactions upstream in the signalling pathway, stimulation of dystroglycan deficient cells prior to transfection with dominant negative Rho GTPases is unlikely to give any information about its function.

Dystroglycan binds to the cytoskeletal linker protein, ezrin and this interaction is known to be important for the ability of dystroglycan to mediate Cdc42-dependent filopodia formation (Spence et al., 2004a). The expression level and localisation of ezrin was investigated in dystroglycan deficient cells to gain further insight into the correlation between them. Interestingly, ezrin appeared to be upregulated in dystroglycan deficient cells but there appeared to be an increased cytoplasmic localisation and decreased localisation at the plasma membrane (Section 4.2.15). This suggests that perhaps the absence of dystroglycan reduces the recruitment of ezrin to the membrane and ezrin expression is upregulated as a compensatory mechanism. However, this result is unexpected because ezrin interacts with membrane proteins other than dystroglycan (Yonemura et al., 1998), so would presumably still be able to localise to the membrane. More detailed analysis of ezrin localisation and expression in dystroglycan deficient cells is required to further investigate the relationship between dystroglycan and ezrin..

Dystroglycan has been shown to be important for epithelial polarisation in the *Drosophila* oocyte and in mammary epithelial cells (Deng et al., 2003; Muschler et al., 2002; Schneider et al., 2006). This coupled with recent evidence to suggest that dystroglycan functions upstream of the Cdc42 pathway, which is a key player in establishing cell polarity (Etienne-Manneville, 2004), suggests that dystroglycan may have a general role in cell polarity determination. This was investigated in dystroglycan-deficient fibroblasts by assessing their ability to polarise and move towards a wound. Results obtained from this study found that dystroglycan-deficient fibroblasts were not

defective in their ability to polarise or move towards a wound suggesting that dystroglycan is not essential for maintaining fibroblast cell polarity, otherwise residual dystroglycan expression or functional redundancy with other adhesion molecules may be the reason that there was no obvious polarity defect in dystroglycan deficient cells (Sections 4.2.6 - 4.2.7).

Other studies investigating dystroglycan deficiency in mouse mammary epithelial cells (Sgambato et al., 2006), muscle myotubes (Montanaro et al., 1999) and *Xenopus* retina (Lunardi et al., 2006) have reported an increased incidence of apoptosis compared to their normal counterparts and it has also been proposed that dystroglycan is involved in maintaining cell survival signals in muscle cells (Langenbach and Rando, 2002). In the present study, dystroglycan deficient fibroblasts were found to have a decrease in total ERK1/2 expression levels (Section 4.2.13). Since the ERK-MAP kinase signalling pathway produces cell survival signals, this data is in agreement with the results obtained by Langenbach *et al*, however further investigation is required to determine the expression levels of active ERK in DG - cells. The data presented here provides the first evidence that dystroglycan deficiency causes increased apoptosis in fibroblasts, which suggests that dystroglycan may have an important function in maintaining cell survival signals in a variety of cell types (Section 4.2.12-13).

This study has shown that dystroglycan accumulates at the cleavage furrow in dividing Ref52 fibroblasts (Section 5.2.1). Moreover, dystroglycan was found to co-localise with its binding partner ezrin at the cleavage furrow (Section 5.2.3), a protein that has previously been shown to localise there (Sato et al., 1992). Further investigation using HeLa cells transfected with different dystroglycan-GFP constructs revealed that dystroglycan requires its cytoplasmic tail region for localisation, but it was not dependent upon its ability to bind to ezrin (Section 5.2.4). The requirement of the extracellular region of dystroglycan for cleavage furrow localisation could not be assessed due to low

transfection efficiency of the construct in HeLa cells, but this would be a valuable piece of data to gather in the future. Studies involving CD43, another transmembrane glycoprotein that localises to the cleavage furrow found that the extracellular portion of the protein was not required for its localisation (Yonemura et al., 1993), which may also be the case for dystroglycan. A possible role for dystroglycan in cytokinesis may be as a membrane tether to link the actin contractile ring to the membrane during furrow ingression. This finding draws new light on the observation that dystroglycan expression levels fluctuate as cells passed through the cell cycle (Hosokawa et al., 2002; Sgambato et al., 2006), since it offers a possible reason as to why dystroglycan expression may be cell cycle regulated. In this study, dystroglycan deficient fibroblasts did not exhibit an obvious defect in cytokinesis since there was no increase in multinucleate cells or reduction in mitotic index (Sections 4.2.9 - 4.2.10). A possible reason for this may be that other membrane proteins were functioning redundantly or that residual dystroglycan was adequate for correct cytokinesis to occur. Dystroglycan deficient cells did, however, show an altered cell cycle profile in which cells appeared to accumulate in S-phase for several hours, whereas control cells did not (Section 4.2.11). Due to incomplete synchronisation of the cell cultures, this experiment needs to be repeated to give more conclusive results. Interestingly, S-phase accumulation had also been reported in another study in which dystroglycan expression was depleted (Sgambato et al., 2006). Any relationship between these observations and the function of dystroglycan at the cleavage furrow warrants further investigation as it will provide valuable insight into the role of dystroglycan in cell cycle progression. The evidence presented here strongly suggests that dystroglycan is involved in cytokinesis and future research will be required to elucidate the mechanisms by which this occurs. In order to continue with this investigation, the experimental conditions need to be optimised to improve the rate of cell survival following transfection, for example it would be beneficial

to carry out live cell imaging inside a microscope incubation chamber. One way in which this could be achieved would be to re-clone the dystroglycan constructs into vectors expressing fluorescent tags that are less toxic to the cells than GFP. In this study, cells were removed from the incubator to carry out their analysis which meant that there was limited time to capture dividing cells since cell survival outside the incubator was short-lived.

This study explored the effects of dystroglycan deficiency in fibroblasts and the data presented here contributes to our understanding of the function of this protein at the cellular level. To follow on from this research, it would be interesting to see if re-introduction of dystroglycan into dystroglycan deficient fibroblasts could rescue any of the phenotypes caused by dystroglycan depletion. Since the shRNA expressed by dystroglycan deficient fibroblasts is directed towards mouse DAG1, re-expression would need to be carried out using the dystroglycan gene from a different species. A rescue of dystroglycan expression in DG - cells was attempted by transfecting cells with $\alpha\beta$ DG-GFP, however expression very low, possibly because this is a mouse gene and was also downregulated by the constitutively expressed shRNA. A further rescue attempt was made using full-length chick dystroglycan expressed in pCMV-Tag1, which was thought to be sufficiently altered from the mouse gene so that it was not affected by shRNA knockdown. This construct unfortunately had very low transfection efficiency in DG - cells and therefore could not be used to rescue dystroglycan expression. A drawback to using RNAi mediated dystroglycan depletion was that a complete knockdown was not achieved and there is the possibility that residual dystroglycan expression may mask any phenotype that would otherwise be seen in a complete knockout system. Although in this study a higher level of dystroglycan knockdown could not be maintained in a stable cell line, it would

perhaps be beneficial to study fibroblasts that were transiently transfected with siRNA constructs to see if a greater level of knockdown could be attained.

Following on from the evidence to suggest that ezrin expression was upregulated in dystroglycan deficient cells, it may also be interesting to investigate the expression levels and localisation of other dystroglycan-associated proteins, such as utrophin. This information may help to explain some of the phenotypes observed in dystroglycan deficient cells and could lead to further elucidation of the signalling pathways in which dystroglycan is involved.

Further investigation into the role of dystroglycan at the cleavage furrow would benefit from high resolution imaging and optimisation of the transfection procedure. Re-cloning of the GFP construct encoding the cytoplasmic domain containing a membrane targeting sequence would be advantageous because its localisation to the cleavage furrow would tell us whether outside signalling is required for this localisation. The identification of dystroglycan binding partners at the cleavage furrow perhaps by isolation of midbody fractions may help to explain its function during cell division.

In conclusion, this study has enhanced our knowledge of dystroglycan function at the cellular level and identified possible new roles for dystroglycan. Future research into the numerous signal transduction pathways that dystroglycan has been linked to will provide further understanding of the very important role that dystroglycan plays within the cell and this may lead to new insights into how these processes are deregulated in muscular dystrophy and during cancer progression.

Appendices

B

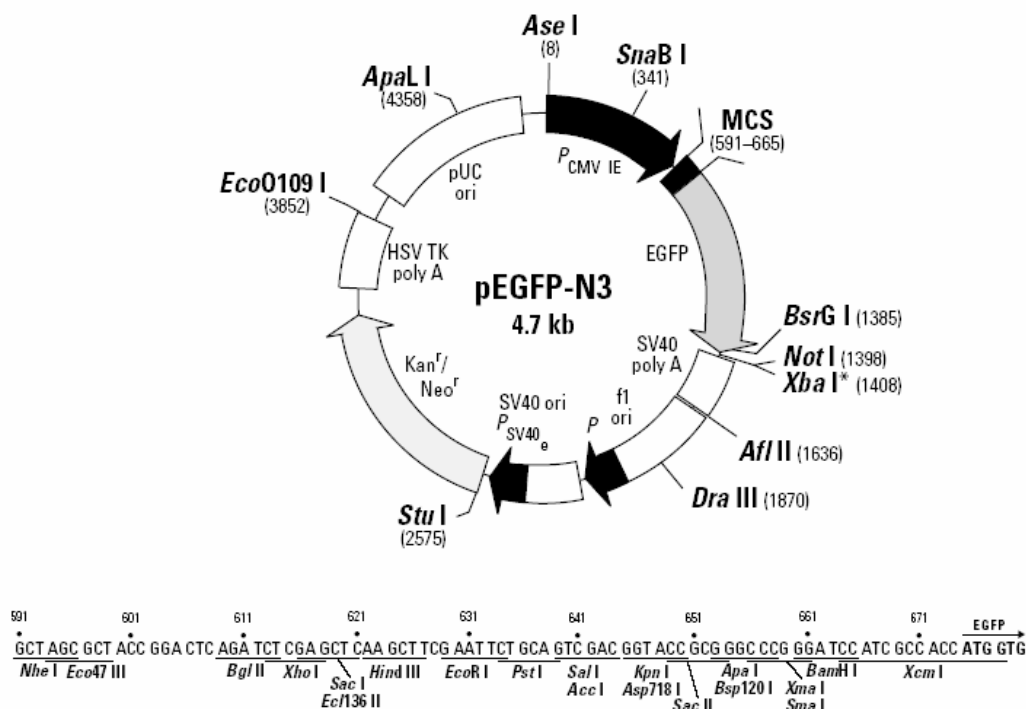


Figure B: The C β -GFP construct was generated by amplification of the cytoplasmic domain of β -dystroglycan by PCR from $\alpha\beta$ DG-GFP using the following primers; 5'TTGCTCGAGATGTATCGCAAGAAGAGGAAGGGC and 5'GATCCCGGGCCAGGGGGAACATACGGAGGGGGTGA and cloned into the TOPO vector, pCR4 (Invitrogen). The cytoplasmic domain insert was then sub-cloned into the Xho I and Sma I sites of pEGFP-N3.

Appendix II: DNA Constructs

Name	Description	Source/Reference
N17Cdc42	Dominant negative Cdc42 sequence cloned between BamHI and NheI sites in CMVneo-myc-1. AMP ^R	A. Hall (Nobes and Hall, 1995)
V12Cdc42	Constitutively activated Cdc42 sequence cloned between BamHI and NheI sites in CMVneo-myc1. AMP ^R	A. Hall (Nobes and Hall, 1995)
N17 Rac1	Dominant negative Rac1 sequence cloned between BamHI and NheI sites in CMVneo-myc-1. AMP ^R	A. Hall (Ridley et al., 1992)
V12 Rac1	Constitutively activated Rac1 sequence cloned between BamHI and NheI sites in CMVneo-myc1. AMP ^R	A. Hall (Nobes and Hall, 1995)
N19RhoA	Dominant negative RhoA sequence cloned between BamHI and NheI sites in CMVneo-myc-1. AMP ^R	A. Hall (Nobes and Hall, 1995)
V14RhoA	Constitutively activated RhoA sequence cloned between BamHI and NheI sites in CMVneo-myc1. AMP ^R	A. Hall (Nobes and Hall, 1995)
$\alpha\beta$ DG-GFP	Full-length dystroglycan cloned into SalI and SmaI sites of pEGFP-N3 vector.	Y-J Chen (Chen et al., 2003)
$\alpha\beta$ DG Δ C β -GFP	Dystroglycan cytoplasmic deletion mutant cloned into SalI and SmaI sites of pEGFP-N3 vector.	Y-J Chen (Chen et al., 2003)
$\alpha\beta$ DG Δ E-GFP	Full-length dystroglycan with ezrin binding site mutated (RKKRK to RENGK) cloned into SalI and SmaI sites of pEGFP-N3 vector.	Y-J Chen (Chen et al., 2003)
C β -GFP	Cytoplasmic tail of β -dystroglycan cloned into XhoI and SmaI sites of pEGFP-N3 vector.	This work
Myr C β -GFP	N-terminal myristoylation sequence of Lck (MGCVCSS) subcloned into the 5' end of the C β -GFP construct in pEGFP-N3 vector.	C.L.Batchelor (Batchelor et al., 2007)
Myr -GFP	N-terminal myristoylation sequence of Lck (MGCVCSS) cloned into NheI and XhoI sites of pEGFP-N1 vector.	C.L.Batchelor (Batchelor et al., 2007)

Appendix III: Cell Lines and Primary Cells

Cells	Description	Source
A431	Human epithelial carcinoma cell line	E. Avizienyte (Beatson Institute)
C2C4	Mouse myoblast cell line	S. Hughes (Kings College London)
C2C7	Mouse myoblast cell line	S. Hughes (Kings College London)
CHO-k1	Chinese hamster ovary cell line	G. Gould (University of Glasgow)
Cos-7	African green monkey kidney cell line	M. Frame (Beatson Institute)
HeLa	Human epithelial cell line	B. Earnshaw (Edinburgh University)
Ref52	Rat embryo fibroblast cell line	D. Helfman (Cold Spring Harbour Laboratories)
Swiss 3t3	Mouse fibroblast cell line	M. Frame (Beatson Institute)
2aa	Swiss 3t3 fibroblasts stably expressing dystroglycan-GFP	H.J. Spence (Chen et al., 2003)
3aa	Swiss 3t3 fibroblasts stably expressing GFP.	H.J. Spence (Chen et al., 2003)
3H1	DAG1 ^{-/-} ES cells	S. Carbonetto (McGill University) (Cote et al., 1999)
R1	DAG1 ^{+/+} ES cells	S. Carbonetto
SNL	STO feeder cells	S. Carbonetto
3C12	DAG ^{-/-} derived fibroblasts	S. Carbonetto
DAG1 ^{-/-} Clones A,B,C,D	DAG ^{-/-} derived fibroblasts	This work
PT67	PT67 Cell Line is an NIH/3T3-based packaging line expressing the 10A1 viral envelope	B. Ozanne (Beatson Institute)
DG -	Swiss 3t3 cells stably expressing a antisense DAG1 RNAi construct that knocks down dystroglycan expression.	This work
DG +	Swiss 3t3 cells stably expressing the sense strand of DAG1 RNAi construct.	This work

Appendix IV: Primary Antisera

Protein	Species	Western Blotting	Immuno-cytochemistry	Description/Source
β -Dystroglycan Polyclonal 1709	Rabbit	1:1000	1:100	S.Winder Tyr 895-P 1710 (Ilsley et al., 2001)
β -Dystroglycan Polyclonal 1710	Rabbit	1:1000	1:100	S.Winder Tyr 895-P 1709 (Ilsley et al., 2001)
β -Dystroglycan Monoclonal 43DAG/8D5	Mouse	1:50	1:10	Novacastra Laboratories
β -Dystroglycan Monoclonal MANDAG2	Mouse	1:500	-	G.E. Morris (Helliwell et al., 1994)
Ezrin	Rabbit	1:1000	1:50	D.Crouch (Woodward and Crouch, 2001)
β -Actin (1-19)	Goat	1:200	-	Santa Cruz SC1616
α -Tubulin Clone B-5-1-2	Mouse	1:1000	1:1000	Sigma T5168
Desmin	Mouse	1:200	-	Sigma 1033
Keratin	Guinea pig	1:200	-	Sigma K4252
P44/42 MAP Kinase	Rabbit	1:1000	-	Cell Signaling #9102
Vimentin	Goat	1:400	-	Sigma V4630
Vinculin	Mouse	-	1:100	Sigma V9131
Myc 9E10	Mouse	-	1:50	Santa Cruz SC40
Anti-BrdU	Mouse	-	1:16	Roche 1170 376

Appendix V: Secondary Antisera

Raised against	Conjugate	Western Blotting	Immuno-cytochemistry	Description/Source
Actin	FITC	-	1:100	Sigma P5282
Goat/Sheep IgG	AP	1:70,000	-	Sigma A8062
	HRP	1:10,000	-	Sigma A9452
Guinea Pig IgG	AP	1:30,000	-	Sigma A5062
Mouse IgG	AP	1:5000	-	Sigma A3562
	HRP	1:5000	-	Sigma A4416
	FITC	-	1:100	Vector
	TRITC	-	1:100	Vector TI-2000
Rabbit IgG	AP	1:5000	-	Sigma A2556
	HRP	1:10,000	-	Sigma A0545
	FITC	-	1:100	Vector
	TRITC	-	1:100	Vector

AP = Alkaline Phosphatase
 FITC = Fluorescein
 HRP = Horseradish peroxidase
 TRITC = Texas Red
 - = N/A

Appendix VI: Stock Solutions, Buffers and Media Compositions

Actin Fractionation Buffer	50mM 1mM 0.5% (v/v) 20mM	NaCl EDTA Triton X-100 HEPES pH 7.9
Adjusting Solution (10x)	80 mM 50% (w/v) 30% (v/v) 40% (v/v)	Tris-HCl (pH 6.8) SDS Glycerol β -Mercaptoethanol Bromophenol Blue to colour
Alkaline Phosphatase Buffer	100mM 5mM 100mM	NaCl MgCl ₂ Tris-HCl (pH 9.5)
Annexin V binding buffer	10 mM 140 mM 2.5 mM	HEPES NaCl CaCl ₂
BCIP Stock	57.7 mM	BCIP prepared in DMF
Blocking Buffer	5% (v/v) 1% (w/v)	FCS BSA prepared in PBS
Coomassie Blue Stain	0.1% (w/v) 40% (v/v) 10% (v/v)	Coomassie Blue R250 Methanol Acetic Acid
Destaining Solution	5% (v/v) 10% (v/v)	Methanol Acetic Acid
ECL Solution I	100mM 25mM 396 μ M	Tris-HCl (pH 8.5) Luminol <i>p</i> -Coumaric Acid
ECL Solution II	100mM 0.02% (v/v)	Tris-HCl (pH 8.5) H ₂ O ₂
ES Cell Differentiation Medium	20% (v/v) 1% (v/v)	FCS Penicillin/Streptomycin

ES Cell Medium	20% (v/v) 1% (v/v) 10 ⁻¹¹ M 1000 U/ml	FCS Penicillin/Streptomycin β-Mercaptoethanol ESGRO in DMEM
Freezing Medium	20% (v/v) 10% (v/v)	FCS DMSO in DMEM
Maleic Acid Buffer	0.1M 0.15M	Maleic Acid NaCl adjusted to pH 7.5
Modified Sample Buffer	50mM 1% (w/v) 10% (v/v) 1μM 1mM 100μM 10mM	Tris-HCl (pH 6.8) SDS Glycerol Pepstatin PMSF TPCK Benzamidine
MOPS Buffer (10x)	0.2M 0.05M 0.01M	MOPS Sodium Acetate EDTA adjusted to pH 7.0 with NaOH
NBT Stock	30.6mM 70% (v/v)	NBT Dimethylformamide
Northern Blot Detection Buffer	0.1M 0.1M	Tris-HCl NaCl adjusted to pH 9.5
Northern Blot Washing Buffer	0.1M 0.15M 0.3% (v/v)	Maleic Acid NaCl Tween-20 adjusted to pH 7.5
Orange G Loading Buffer	30% (w/v) 100mM	Ficoll EDTA (pH 8.0) Orange G to colour

Permeabilising Buffer	20mM 0.05% (v/v)	Glycine Triton X-100 prepared in PBS
Phosphate Buffered Saline	137mM 2.68mM 10mM 1.76mM	NaCl KCl Na ₂ HPO ₄ KH ₂ PO ₄ adjusted to pH 7.4 with HCl
Resolving Gel Buffer	1.5M 0.4% (w/v)	Tris-HCl (pH 8.8) SDS
RIPA Buffer	50mM 150mM 1mM 1mM 1% (v/v) 0.5% (v/v) 0.1% (w/v) 1mM (w/v) 1mM 1mM 10µM 10µM 1µM 10µM 10µM	Tris-HCl (pH7.5) NaCl EGTA EDTA Triton X-100 Sodium Deoxycholate SDS Sodium Azide PMSF Sodium Orthovanadate TPCK Leupeptin Pepstatin A Benzamidine Aprotinin
RNA Elution Buffer	0.1mM 10mM	EDTA Tris-HCl (pH 7.5)
RNA Loading Buffer	50% (v/v) 16.6% (v/v) 10% (v/v) 10% (v/v) 2% (v/v)	Formamide (100%) Paraformaldehyde (37%) 10x MOPS Glycerol (100%) Bromophenol Blue (2.5%) prepared in DEPC-treated H ₂ O
SCC Transfer Buffer (20x)	3M 0.3M	NaCl Sodium Citrate adjusted to pH 7.0
SDS-PAGE Running Buffer (10x)	250mM 1% (w/v) 1.92M	Tris SDS Glycine (pH 8.3)

SDS-PAGE Sample Buffer (2x)	62.5mM 2% (w/v) 30% (v/v) 0.01% (w/v) 710mM	Tris-HCl (pH 6.8) SDS Glycerol Bromophenol Blue β -Mercaptoethanol
SNL (STO) Medium	10% (v/v) 1% (v/v)	FCS Penicillin/Streptomycin in DMEM
Stacking Gel Buffer	0.5M 0.4% (w/v)	Tris-HCl (pH 6.8) SDS
Stripping Buffer	0.2M 1% (w/v)	Glycine SDS adjusted to pH 2.5 with HCl
TAE (50x)	2M 1M 50mM	Tris Acetic Acid EDTA
TBST	50mM 150mM 0.05% (v/v)	Tris-HCl (pH 7.5) NaCl Tween-20
Transfer Buffer	1.25mM 1.25mM 50 μ M 10% (v/v) pH 7.2	Bicine Bis-Tris EDTA Methanol
Working Medium	10% (v/v)	FCS in DMEM or RPMI

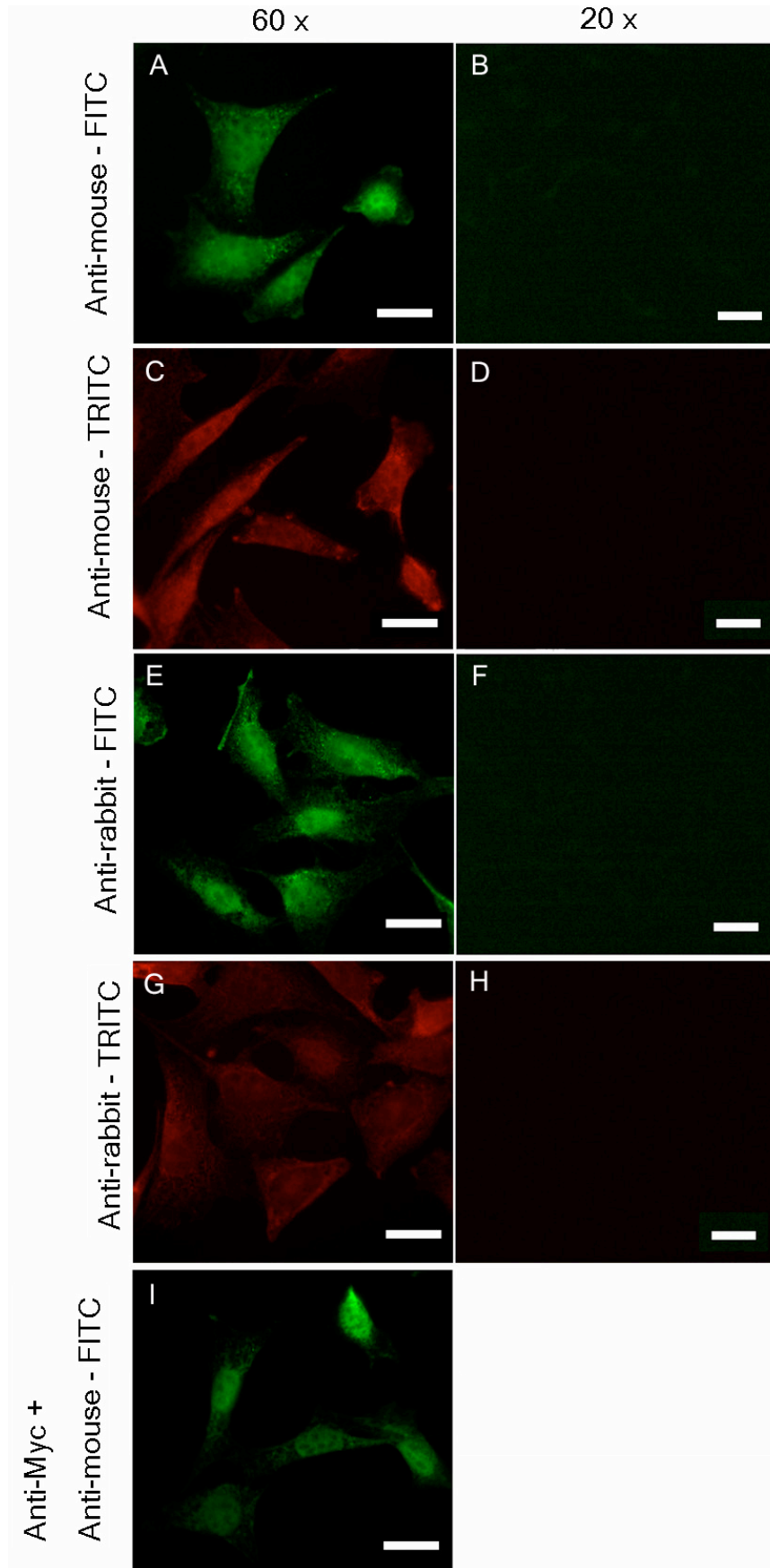
Appendix VII: RT-PCR primers

RT-PCR Primer pair	Forward primer Sequence	Reverse Primer Sequence
(a)	5' TGA CAC TGA TAA AGG TGT GCA	5' AGG GTA GTC GAC TTA AGG GGG AAC ATA CGG AGG GGG TGA
(b)	5' ATC CAT GTT CAC AAG CGC C	5' AGG GTA GTC GAC TTA AGG GGG AAC ATA CGG AGG GGG TGA
(c)	5' TGG AAT GGA CCA ACA ACA CT	5' AGG GTA GTC GAC TTA AGG GGG AAC ATA CGG AGG GGG TGA
(d)	5' TTG GTC GAC ATG TCT GTG GAC AAC TGG CTA	5' AGT GTA GCC AAG ACG GTA AGG
GAPDH	5' GAG TCA ACG GAT TTG GTC GT	5' TTG ATT TTG GAG GGA TCT CG

Appendix VIII: Genomic PCR primers

Primer	Sequence
DG001	5' CAG CCT GCG TGA GAT GAA CTA C
DG002	5' ATT CGC CAA TGA CAA GAC GCT G
DG003	5' ATG CCC AGT CAA AGT CCG TAT G
DG004	5' GCG TGC AGC ACT CAC TGA GAT G
DG006	5' GTA CTC GCC GAT AGT GGA AAC C

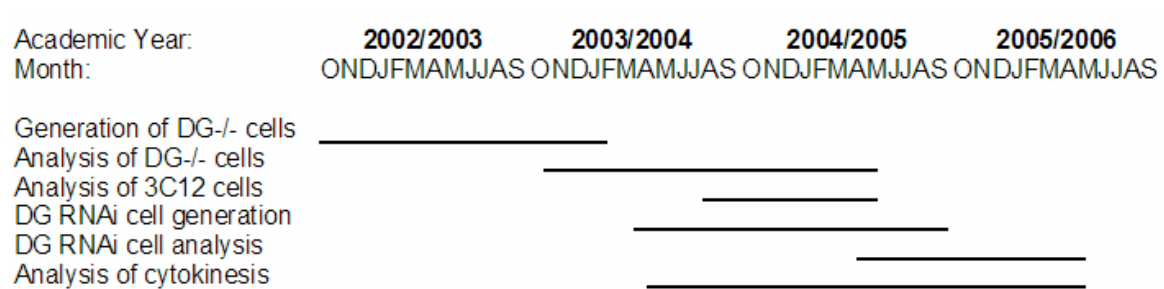
Appendix IX: Secondary Antisera Cross-reactivity



A - H: Swiss 3T3 cells were immuno-stained with secondary antisera to detect background cross-reactivity in the absence of primary antisera. In all cases, cells were counterstained with DAPI to detect for emission bleed-through and this accounts for much of the nuclear staining.

I: Untransfected Swiss 3T3 cells were immuno-stained with anti-myc antisera followed by anti-mouse secondary antisera to detect non-specific background staining. Images A, C, E, G and I: Scale bar = 20 μ m. Images B, D, F and H: Scale bar = 50 μ m

Appendix X: Experimental Timeline



References

- Akisawa, N., Nishimori, I., Iwamura, T., Onishi, S. and Hollingsworth, M. A. (1999). High levels of ezrin expressed by human pancreatic adenocarcinoma cell lines with high metastatic potential. *Biochem Biophys Res Commun* 258, 395-400.
- Alberts, A. S. (2001). Identification of a carboxyl-terminal diaphanous-related formin homology protein autoregulatory domain. *J Biol Chem* 276, 2824-30.
- Amano, M., Ito, M., Kimura, K., Fukata, Y., Chihara, K., Nakano, T., Matsuura, Y. and Kaibuchi, K. (1996). Phosphorylation and activation of myosin by Rho-associated kinase (Rho-kinase). *J Biol Chem* 271, 20246-9.
- Apel, E. D., Roberds, S. L., Campbell, K. P. and Merlie, J. P. (1995). Rapsyn may function as a link between the acetylcholine receptor and the agrin-binding dystrophin-associated glycoprotein complex. *Neuron* 15, 115-26.
- Bagrodia, S. and Cerione, R. A. (1999). Pak to the future. *Trends Cell Biol* 9, 350-5.
- Barresi, R., Michele, D. E., Kanagawa, M., Harper, H. A., Dovico, S. A., Satz, J. S., Moore, S. A., Zhang, W., Schachter, H., Dumanski, J. P. et al. (2004). LARGE can functionally bypass alpha-dystroglycan glycosylation defects in distinct congenital muscular dystrophies. *Nat Med* 10, 696-703.
- Bartoli, M., Ramarao, M. K. and Cohen, J. B. (2001). Interactions of the rapsyn RING-H2 domain with dystroglycan. *J Biol Chem* 276, 24911-7.
- Batchelor, C. L., Higginson, J. R., Chen, Y. J., Vanni, C., Eva, A. and Winder, S. J. (2007). Recruitment of Dbl by ezrin and dystroglycan drives membrane proximal Cdc42 activation and filopodia formation. *Cell Cycle* 6, 353-63.
- Batchelor, C. L. and Winder, S. J. (2006). Sparks, signals and shock absorbers: how dystrophin loss causes muscular dystrophy. *Trends Cell Biol* 16, 198-205.
- Belkin, A. M. and Burridge, K. (1995a). Association of aciculin with dystrophin and utrophin. *J Biol Chem* 270, 6328-37.
- Belkin, A. M. and Burridge, K. (1995b). Localization of utrophin and aciculin at sites of cell-matrix and cell-cell adhesion in cultured cells. *Exp Cell Res* 221, 132-40.
- Belkin, A. M. and Smalheiser, N. R. (1996). Localization of cranin (dystroglycan) at sites of cell-matrix and cell-cell contact: recruitment to focal adhesions is dependent upon extracellular ligands. *Cell Adhes Commun* 4, 281-96.
- Beltran-Valero de Bernabe, D., Currier, S., Steinbrecher, A., Celli, J., van Beusekom, E., van der Zwaag, B., Kayserili, H., Merlini, L., Chitayat, D., Dobyns, W. B. et al. (2002). Mutations in the O-mannosyltransferase gene POMT1 give rise to the severe neuronal migration disorder Walker-Warburg syndrome. *Am J Hum Genet* 71, 1033-43.

- Blake, D. J., Nawrotzki, R., Peters, M. F., Froehner, S. C. and Davies, K. E. (1996). Isoform diversity of dystrobrevin, the murine 87-kDa postsynaptic protein. *J Biol Chem* 271, 7802-10.
- Bowe, M. A., Deyst, K. A., Leszyk, J. D. and Fallon, J. R. (1994). Identification and purification of an agrin receptor from Torpedo postsynaptic membranes: a heteromeric complex related to the dystroglycans. *Neuron* 12, 1173-80.
- Bowe, M. A., Mendis, D. B. and Fallon, J. R. (2000). The small leucine-rich repeat proteoglycan biglycan binds to alpha-dystroglycan and is upregulated in dystrophic muscle. *J Cell Biol* 148, 801-10.
- Bozzi, M., Bianchi, M., Sciandra, F., Paci, M., Giardina, B., Brancaccio, A. and Cicero, D. O. (2003). Structural characterization by NMR of the natively unfolded extracellular domain of beta-dystroglycan: toward the identification of the binding epitope for alpha-dystroglycan. *Biochemistry* 42, 13717-24.
- Brancaccio, A., Schulthess, T., Gesemann, M. and Engel, J. (1995). Electron microscopic evidence for a mucin-like region in chick muscle alpha-dystroglycan. *FEBS Lett* 368, 139-42.
- Brancaccio, A., Schulthess, T., Gesemann, M. and Engel, J. (1997). The N-terminal region of alpha-dystroglycan is an autonomous globular domain. *Eur J Biochem* 246, 166-72.
- Bretscher, A., Edwards, K. and Fehon, R. G. (2002). ERM proteins and merlin: integrators at the cell cortex. *Nat Rev Mol Cell Biol* 3, 586-99.
- Brockington, M., Blake, D. J., Prandini, P., Brown, S. C., Torelli, S., Benson, M. A., Ponting, C. P., Estournet, B., Romero, N. B., Mercuri, E. et al. (2001). Mutations in the fukutin-related protein gene (FKRP) cause a form of congenital muscular dystrophy with secondary laminin alpha2 deficiency and abnormal glycosylation of alpha-dystroglycan. *Am J Hum Genet* 69, 1198-209.
- Brown, S. C., Fassati, A., Popplewell, L., Page, A. M., Henry, M. D., Campbell, K. P. and Dickson, G. (1999). Dystrophic phenotype induced in vitro by antibody blockade of muscle alpha-dystroglycan-laminin interaction. *J Cell Sci* 112 (Pt 2), 209-16.
- Burridge, K. and Chrzanowska-Wodnicka, M. (1996). Focal adhesions, contractility, and signaling. *Annu Rev Cell Dev Biol* 12, 463-518.
- Cao, W., Henry, M. D., Borrow, P., Yamada, H., Elder, J. H., Ravkov, E. V., Nichol, S. T., Compans, R. W., Campbell, K. P. and Oldstone, M. B. (1998). Identification of alpha-dystroglycan as a receptor for lymphocytic choriomeningitis virus and Lassa fever virus. *Science* 282, 2079-81.
- Cartaud, A., Coutant, S., Petrucci, T. C. and Cartaud, J. (1998). Evidence for in situ and in vitro association between beta-dystroglycan and the subsynaptic 43K rapsyn protein. Consequence for acetylcholine receptor clustering at the synapse. *J Biol Chem* 273, 11321-6.

- Cavaldesi, M., Macchia, G., Barca, S., Defilippi, P., Tarone, G. and Petrucci, T. C. (1999). Association of the dystroglycan complex isolated from bovine brain synaptosomes with proteins involved in signal transduction. *J Neurochem* 72, 1648-55.
- Chen, H. I., Einbond, A., Kwak, S. J., Linn, H., Koepf, E., Peterson, S., Kelly, J. W. and Sudol, M. (1997). Characterization of the WW domain of human yes-associated protein and its polyproline-containing ligands. *J Biol Chem* 272, 17070-7.
- Chen, Y. J., Spence, H. J., Cameron, J. M., Jess, T., Ilsley, J. L. and Winder, S. J. (2003). Direct interaction of beta-dystroglycan with F-actin. *Biochem J* 375, 329-37.
- Chiba, A., Matsumura, K., Yamada, H., Inazu, T., Shimizu, T., Kusunoki, S., Kanazawa, I., Kobata, A. and Endo, T. (1997). Structures of sialylated O-linked oligosaccharides of bovine peripheral nerve alpha-dystroglycan. The role of a novel O-mannosyl-type oligosaccharide in the binding of alpha-dystroglycan with laminin. *J Biol Chem* 272, 2156-62.
- Chockalingam, P. S., Cholera, R., Oak, S. A., Zheng, Y., Jarrett, H. W. and Thomason, D. B. (2002). Dystrophin-glycoprotein complex and Ras and Rho GTPase signaling are altered in muscle atrophy. *Am J Physiol Cell Physiol* 283, C500-11.
- Chung, W. and Campanelli, J. T. (1999). WW and EF hand domains of dystrophin-family proteins mediate dystroglycan binding. *Mol Cell Biol Res Commun* 2, 162-71.
- Cohn, R. D., Henry, M. D., Michele, D. E., Barresi, R., Saito, F., Moore, S. A., Flanagan, J. D., Skwarchuk, M. W., Robbins, M. E., Mendell, J. R. et al. (2002). Disruption of DAG1 in differentiated skeletal muscle reveals a role for dystroglycan in muscle regeneration. *Cell* 110, 639-48.
- Cooper, J. A. (1987). Effects of cytochalasin and phalloidin on actin. *J Cell Biol* 105, 1473-8.
- Cote, P. D., Moukhles, H., Lindenbaum, M. and Carbonetto, S. (1999). Chimaeric mice deficient in dystroglycans develop muscular dystrophy and have disrupted myoneural synapses. *Nat Genet* 23, 338-42.
- Cullen, M. J., Walsh, J. and Nicholson, L. V. (1994). Immunogold localization of the 43-kDa dystroglycan at the plasma membrane in control and dystrophic human muscle. *Acta Neuropathol (Berl)* 87, 349-54.
- de Petris, S. (1984). Spontaneous redistribution of cell-surface glycoproteins in lymphoid cells during cytokinesis. *Embo J* 3, 1849-55.
- Deng, W. M., Schneider, M., Frock, R., Castillejo-Lopez, C., Gaman, E. A., Baumgartner, S. and Ruohola-Baker, H. (2003). Dystroglycan is required for polarizing the epithelial cells and the oocyte in *Drosophila*. *Development* 130, 173-84.
- Deyst, K. A., Bowe, M. A., Leszyk, J. D. and Fallon, J. R. (1995). The alpha-dystroglycan-beta-dystroglycan complex. Membrane organization and relationship to an agrin receptor. *J Biol Chem* 270, 25956-9.

- Di Stasio, E., Sciandra, F., Maras, B., Di Tommaso, F., Petrucci, T. C., Giardina, B. and Brancaccio, A. (1999). Structural and functional analysis of the N-terminal extracellular region of beta-dystroglycan. *Biochem Biophys Res Commun* 266, 274-8.
- Drab, M., Haller, H., Bychkov, R., Erdmann, B., Lindschau, C., Haase, H., Morano, I., Luft, F. C. and Wobus, A. M. (1997). From totipotent embryonic stem cells to spontaneously contracting smooth muscle cells: a retinoic acid and db-cAMP in vitro differentiation model. *Faseb J* 11, 905-15.
- Driss, A., Charrier, L., Yan, Y., Nduati, V., Sitaraman, S. and Merlin, D. (2006). Dystroglycan receptor is involved in integrin activation in intestinal epithelia. *Am J Physiol Gastrointest Liver Physiol* 290, G1228-42.
- Durbeej, M. and Campbell, K. P. (1999). Biochemical characterization of the epithelial dystroglycan complex. *J Biol Chem* 274, 26609-16.
- Durbeej, M. and Campbell, K. P. (2002). Muscular dystrophies involving the dystrophin-glycoprotein complex: an overview of current mouse models. *Curr Opin Genet Dev* 12, 349-61.
- Durbeej, M., Henry, M. D. and Campbell, K. P. (1998). Dystroglycan in development and disease. *Curr Opin Cell Biol* 10, 594-601.
- Durbeej, M., Henry, M. D., Ferletta, M., Campbell, K. P. and Ekblom, P. (1998). Distribution of dystroglycan in normal adult mouse tissues. *J Histochem Cytochem* 46, 449-57.
- Durbeej, M., Larsson, E., Ibraghimov-Beskrovnaya, O., Roberds, S. L., Campbell, K. P. and Ekblom, P. (1995). Non-muscle alpha-dystroglycan is involved in epithelial development. *J Cell Biol* 130, 79-91.
- Durbeej, M., Talts, J. F., Henry, M. D., Yurchenco, P. D., Campbell, K. P. and Ekblom, P. (2001). Dystroglycan binding to laminin alpha1LG4 module influences epithelial morphogenesis of salivary gland and lung in vitro. *Differentiation* 69, 121-34.
- Edwards, K. A., Montague, R. A., Shepard, S., Edgar, B. A., Erikson, R. L. and Kiehart, D. P. (1994). Identification of *Drosophila* cytoskeletal proteins by induction of abnormal cell shape in fission yeast. *Proc Natl Acad Sci U S A* 91, 4589-93.
- Ervasti, J. M. and Campbell, K. P. (1993). A role for the dystrophin-glycoprotein complex as a transmembrane linker between laminin and actin. *J Cell Biol* 122, 809-23.
- Ervasti, J. M., Ohlendieck, K., Kahl, S. D., Gaver, M. G. and Campbell, K. P. (1990). Deficiency of a glycoprotein component of the dystrophin complex in dystrophic muscle. *Nature* 345, 315-9.
- Esapa, C. T., Bentham, G. R., Schroder, J. E., Kroger, S. and Blake, D. J. (2003). The effects of post-translational processing on dystroglycan synthesis and trafficking. *FEBS Lett* 555, 209-16.
- Etienne-Manneville, S. (2004). Cdc42--the centre of polarity. *J Cell Sci* 117, 1291-300.

- Ferletta, M., Kikkawa, Y., Yu, H., Talts, J. F., Durbeej, M., Sonnenberg, A., Timpl, R., Campbell, K. P., Ekblom, P. and Genersch, E. (2003). Opposing roles of integrin alpha6beta1 and dystroglycan in laminin-mediated extracellular signal-regulated kinase activation. *Mol Biol Cell* 14, 2088-103.
- Fincham, V. J., James, M., Frame, M. C. and Winder, S. J. (2000). Active ERK/MAP kinase is targeted to newly forming cell-matrix adhesions by integrin engagement and v-Src. *Embo J* 19, 2911-23.
- Finger, F. P. and White, J. G. (2002). Fusion and fission: membrane trafficking in animal cytokinesis. *Cell* 108, 727-30.
- Fire, A., Xu, S., Montgomery, M. K., Kostas, S. A., Driver, S. E. and Mello, C. C. (1998). Potent and specific genetic interference by double-stranded RNA in *Caenorhabditis elegans*. *Nature* 391, 806-11.
- Frisch, S. M. and Ruoslahti, E. (1997). Integrins and anoikis. *Curr Opin Cell Biol* 9, 701-6.
- Funayama, N., Nagafuchi, A., Sato, N., Tsukita, S. and Tsukita, S. (1991). Radixin is a novel member of the band 4.1 family. *J Cell Biol* 115, 1039-48.
- Galbiati, F., Volonte, D., Chu, J. B., Li, M., Fine, S. W., Fu, M., Bermudez, J., Pedemonte, M., Weidenheim, K. M., Pestell, R. G. et al. (2000). Transgenic overexpression of caveolin-3 in skeletal muscle fibers induces a Duchenne-like muscular dystrophy phenotype. *Proc Natl Acad Sci U S A* 97, 9689-94.
- Gee, S. H., Montanaro, F., Lindenbaum, M. H. and Carbonetto, S. (1994). Dystroglycan-alpha, a dystrophin-associated glycoprotein, is a functional agrin receptor. *Cell* 77, 675-86.
- Geiger, B., Tokuyasu, K. T., Dutton, A. H. and Singer, S. J. (1980). Vinculin, an intracellular protein localized at specialized sites where microfilament bundles terminate at cell membranes. *Proc Natl Acad Sci U S A* 77, 4127-31.
- Glotzer, M. (2001). Animal cell cytokinesis. *Annu Rev Cell Dev Biol* 17, 351-86.
- Gorecki, D. C., Derry, J. M. and Barnard, E. A. (1994). Dystroglycan: brain localisation and chromosome mapping in the mouse. *Hum Mol Genet* 3, 1589-97.
- Gould, K. L., Bretscher, A., Esch, F. S. and Hunter, T. (1989). cDNA cloning and sequencing of the protein-tyrosine kinase substrate, ezrin, reveals homology to band 4.1. *Embo J* 8, 4133-42.
- Grewal, P. K., Holzfeind, P. J., Bittner, R. E. and Hewitt, J. E. (2001). Mutant glycosyltransferase and altered glycosylation of alpha-dystroglycan in the myodystrophy mouse. *Nat Genet* 28, 151-4.
- Grisoni, K., Martin, E., Gieseler, K., Mariol, M. C. and Segalat, L. (2002). Genetic evidence for a dystrophin-glycoprotein complex (DGC) in *Caenorhabditis elegans*. *Gene* 294, 77-86.
- Hall, A. (1998). Rho GTPases and the actin cytoskeleton. *Science* 279, 509-14.

- Hayflick, L. and Moorhead, P. S. (1961). The serial cultivation of human diploid cell strains. *Exp Cell Res* 25, 585-621.
- Helliwell, T. R., Nguyen, T. M. and Morris, G. E. (1994). Expression of the 43 kDa dystrophin-associated glycoprotein in human neuromuscular disease. *Neuromuscul Disord* 4, 101-13.
- Henry, M. D. and Campbell, K. P. (1996). Dystroglycan: an extracellular matrix receptor linked to the cytoskeleton. *Curr Opin Cell Biol* 8, 625-31.
- Henry, M. D. and Campbell, K. P. (1998). A role for dystroglycan in basement membrane assembly. *Cell* 95, 859-70.
- Henry, M. D., Cohen, M. B. and Campbell, K. P. (2001). Reduced expression of dystroglycan in breast and prostate cancer. *Hum Pathol* 32, 791-5.
- Henry, M. D., Gonzalez Agosti, C. and Solomon, F. (1995). Molecular dissection of radixin: distinct and interdependent functions of the amino- and carboxy-terminal domains. *J Cell Biol* 129, 1007-22.
- Herzog, C., Has, C., Franzke, C. W., Echtermeyer, F. G., Schlotzer-Schrehardt, U., Kroger, S., Gustafsson, E., Fassler, R. and Bruckner-Tuderman, L. (2004). Dystroglycan in skin and cutaneous cells: beta-subunit is shed from the cell surface. *J Invest Dermatol* 122, 1372-80.
- Hnia, K., Zouiten, D., Cantel, S., Chazalette, D., Hugon, G., Fehrentz, J. A., Masmoudi, A., Diment, A., Bramham, J., Mornet, D. et al. (2007). ZZ domain of dystrophin and utrophin: topology and mapping of a beta-dystroglycan interaction site. *Biochem J* 401, 667-77.
- Hoffman, E. P., Brown, R. H., Jr. and Kunkel, L. M. (1987). Dystrophin: the protein product of the Duchenne muscular dystrophy locus. *Cell* 51, 919-28.
- Hohenester, E., Tisi, D., Talts, J. F. and Timpl, R. (1999). The crystal structure of a laminin G-like module reveals the molecular basis of alpha-dystroglycan binding to laminins, perlecan, and agrin. *Mol Cell* 4, 783-92.
- Holt, K. H., Crosbie, R. H., Venzke, D. P. and Campbell, K. P. (2000). Biosynthesis of dystroglycan: processing of a precursor propeptide. *FEBS Lett* 468, 79-83.
- Hosokawa, H., Ninomiya, H., Kitamura, Y., Fujiwara, K. and Masaki, T. (2002). Vascular endothelial cells that express dystroglycan are involved in angiogenesis. *J Cell Sci* 115, 1487-96.
- Huang, X., Poy, F., Zhang, R., Joachimiak, A., Sudol, M. and Eck, M. J. (2000). Structure of a WW domain containing fragment of dystrophin in complex with beta-dystroglycan. *Nat Struct Biol* 7, 634-8.
- Hutvagner, G. and Zamore, P. D. (2002). A microRNA in a multiple-turnover RNAi enzyme complex. *Science* 297, 2056-60.

Ibraghimov-Beskrovnaya, O., Ervasti, J. M., Leveille, C. J., Slaughter, C. A., Sernett, S. W. and Campbell, K. P. (1992). Primary structure of dystrophin-associated glycoproteins linking dystrophin to the extracellular matrix. *Nature* 355, 696-702.

Ibraghimov-Beskrovnaya, O., Milatovich, A., Ozcelik, T., Yang, B., Koepnick, K., Francke, U. and Campbell, K. P. (1993). Human dystroglycan: skeletal muscle cDNA, genomic structure, origin of tissue specific isoforms and chromosomal localization. *Hum Mol Genet* 2, 1651-7.

Ibraghimov-Beskrovnaya, O., Sheffield, V. C. and Campbell, K. P. (1993). Single base polymorphism in the DAG1 gene detected by DGGE and mismatch PCR. *Hum Mol Genet* 2, 1983.

Ilsley, J. L., Sudol, M. and Winder, S. J. (2001). The interaction of dystrophin with beta-dystroglycan is regulated by tyrosine phosphorylation. *Cell Signal* 13, 625-32.

Ilsley, J. L., Sudol, M. and Winder, S. J. (2002). The WW domain: linking cell signalling to the membrane cytoskeleton. *Cell Signal* 14, 183-9.

Jacobson, C., Cote, P. D., Rossi, S. G., Rotundo, R. L. and Carbonetto, S. (2001). The dystroglycan complex is necessary for stabilization of acetylcholine receptor clusters at neuromuscular junctions and formation of the synaptic basement membrane. *J Cell Biol* 152, 435-50.

Jacobson, C., Montanaro, F., Lindenbaum, M., Carbonetto, S. and Ferns, M. (1998). alpha-Dystroglycan functions in acetylcholine receptor aggregation but is not a coreceptor for agrin-MuSK signaling. *J Neurosci* 18, 6340-8.

James, M., Nguyen, T. M., Wise, C. J., Jones, G. E. and Morris, G. E. (1996). Utrophin-dystroglycan complex in membranes of adherent cultured cells. *Cell Motil Cytoskeleton* 33, 163-74.

James, M., Nuttall, A., Ilsley, J. L., Ottersbach, K., Tinsley, J. M., Sudol, M. and Winder, S. J. (2000). Adhesion-dependent tyrosine phosphorylation of (beta)-dystroglycan regulates its interaction with utrophin. *J Cell Sci* 113 (Pt 10), 1717-26.

Jing, J., Lien, C. F., Sharma, S., Rice, J., Brennan, P. A. and Gorecki, D. C. (2004). Aberrant expression, processing and degradation of dystroglycan in squamous cell carcinomas. *Eur J Cancer* 40, 2143-51.

Jones, J. C., Lane, K., Hopkinson, S. B., Lecuona, E., Geiger, R. C., Dean, D. A., Correa-Meyer, E., Gonzales, M., Campbell, K., Sznajder, J. I. et al. (2005). Laminin-6 assembles into multimolecular fibrillar complexes with perlecan and participates in mechanical-signal transduction via a dystroglycan-dependent, integrin-independent mechanism. *J Cell Sci* 118, 2557-66.

Jung, D., Yang, B., Meyer, J., Chamberlain, J. S. and Campbell, K. P. (1995). Identification and characterization of the dystrophin anchoring site on beta-dystroglycan. *J Biol Chem* 270, 27305-10.

- Kato, T., Watanabe, N., Morishima, Y., Fujita, A., Ishizaki, T. and Narumiya, S. (2001). Localization of a mammalian homolog of diaphanous, mDia1, to the mitotic spindle in HeLa cells. *J Cell Sci* 114, 775-84.
- Kerr, J. F., Wyllie, A. H. and Currie, A. R. (1972). Apoptosis: a basic biological phenomenon with wide-ranging implications in tissue kinetics. *Br J Cancer* 26, 239-57.
- Khanna, C., Wan, X., Bose, S., Cassaday, R., Olomu, O., Mendoza, A., Yeung, C., Gorlick, R., Hewitt, S. M. and Helman, L. J. (2004). The membrane-cytoskeleton linker ezrin is necessary for osteosarcoma metastasis. *Nat Med* 10, 182-6.
- Khurana, T. S., Kunkel, L. M., Frederickson, A. D., Carbonetto, S. and Watkins, S. C. (1995). Interaction of chromosome-6-encoded dystrophin related protein with the extracellular matrix. *J Cell Sci* 108 (Pt 1), 173-85.
- Kimura, K., Ito, M., Amano, M., Chihara, K., Fukata, Y., Nakafuku, M., Yamamori, B., Feng, J., Nakano, T., Okawa, K. et al. (1996). Regulation of myosin phosphatase by Rho and Rho-associated kinase (Rho-kinase). *Science* 273, 245-8.
- Kimura, K., Tsuji, T., Takada, Y., Miki, T. and Narumiya, S. (2000). Accumulation of GTP-bound RhoA during cytokinesis and a critical role of ECT2 in this accumulation. *J Biol Chem* 275, 17233-6.
- Knutton, S., Sumner, M. C. and Pasternak, C. A. (1975). Role of microvilli in surface changes of synchronized P815Y mastocytoma cells. *J Cell Biol* 66, 568-76.
- Kobayashi, K., Nakahori, Y., Miyake, M., Matsumura, K., Kondo-Iida, E., Nomura, Y., Segawa, M., Yoshioka, M., Saito, K., Osawa, M. et al. (1998). An ancient retrotransposal insertion causes Fukuyama-type congenital muscular dystrophy. *Nature* 394, 388-92.
- Koopman, G., Reutelingsperger, C. P., Kuijten, G. A., Keehnen, R. M., Pals, S. T. and van Oers, M. H. (1994). Annexin V for flow cytometric detection of phosphatidylserine expression on B cells undergoing apoptosis. *Blood* 84, 1415-20.
- Kunkel, G. R. and Pederson, T. (1989). Transcription of a human U6 small nuclear RNA gene in vivo withstands deletion of intragenic sequences but not of an upstream TATATA box. *Nucleic Acids Res* 17, 7371-9.
- Kunz, S., Rojek, J. M., Kanagawa, M., Spiropoulou, C. F., Barresi, R., Campbell, K. P. and Oldstone, M. B. (2005). Posttranslational modification of alpha-dystroglycan, the cellular receptor for arenaviruses, by the glycosyltransferase LARGE is critical for virus binding. *J Virol* 79, 14282-96.
- Kupfer, A., Louvard, D. and Singer, S. J. (1982). Polarization of the Golgi apparatus and the microtubule-organizing center in cultured fibroblasts at the edge of an experimental wound. *Proc Natl Acad Sci U S A* 79, 2603-7.
- Laemmli, U. K. (1970). Cleavage of structural proteins during the assembly of the head of bacteriophage T4. *Nature* 227, 680-5.

- Langenbach, K. J. and Rando, T. A. (2002). Inhibition of dystroglycan binding to laminin disrupts the PI3K/AKT pathway and survival signaling in muscle cells. *Muscle Nerve* 26, 644-53.
- Lankes, W. T. and Furthmayr, H. (1991). Moesin: a member of the protein 4.1-talin-ezrin family of proteins. *Proc Natl Acad Sci U S A* 88, 8297-301.
- Legg, J. W. and Isacke, C. M. (1998). Identification and functional analysis of the ezrin-binding site in the hyaluronan receptor, CD44. *Curr Biol* 8, 705-8.
- Li, S., Harrison, D., Carbonetto, S., Fassler, R., Smyth, N., Edgar, D. and Yurchenco, P. D. (2002). Matrix assembly, regulation, and survival functions of laminin and its receptors in embryonic stem cell differentiation. *J Cell Biol* 157, 1279-90.
- Longman, C., Brockington, M., Torelli, S., Jimenez-Mallebrera, C., Kennedy, C., Khalil, N., Feng, L., Saran, R. K., Voit, T., Merlini, L. et al. (2003). Mutations in the human LARGE gene cause MDC1D, a novel form of congenital muscular dystrophy with severe mental retardation and abnormal glycosylation of alpha-dystroglycan. *Hum Mol Genet* 12, 2853-61.
- Losasso, C., Di Tommaso, F., Sgambato, A., Ardito, R., Cittadini, A., Giardina, B., Petrucci, T. C. and Brancaccio, A. (2000). Anomalous dystroglycan in carcinoma cell lines. *FEBS Lett* 484, 194-8.
- Love, D. R., Morris, G. E., Ellis, J. M., Fairbrother, U., Marsden, R. F., Bloomfield, J. F., Edwards, Y. H., Slater, C. P., Parry, D. J. and Davies, K. E. (1991). Tissue distribution of the dystrophin-related gene product and expression in the mdx and dy mouse. *Proc Natl Acad Sci U S A* 88, 3243-7.
- Lowenstein, E. J., Daly, R. J., Batzer, A. G., Li, W., Margolis, B., Lammers, R., Ullrich, A., Skolnik, E. Y., Bar-Sagi, D. and Schlessinger, J. (1992). The SH2 and SH3 domain-containing protein GRB2 links receptor tyrosine kinases to ras signaling. *Cell* 70, 431-42.
- Lunardi, A., Cremisi, F. and Dente, L. (2006). Dystroglycan is required for proper retinal layering. *Dev Biol* 290, 411-20.
- Manser, E., Leung, T., Salihuddin, H., Zhao, Z. S. and Lim, L. (1994). A brain serine/threonine protein kinase activated by Cdc42 and Rac1. *Nature* 367, 40-6.
- Michele, D. E., Barresi, R., Kanagawa, M., Saito, F., Cohn, R. D., Satz, J. S., Dollar, J., Nishino, I., Kelley, R. I., Somer, H. et al. (2002). Post-translational disruption of dystroglycan-ligand interactions in congenital muscular dystrophies. *Nature* 418, 417-22.
- Minetti, C., Sotgia, F., Bruno, C., Scartezzini, P., Broda, P., Bado, M., Masetti, E., Mazzocco, M., Egeo, A., Donati, M. A. et al. (1998). Mutations in the caveolin-3 gene cause autosomal dominant limb-girdle muscular dystrophy. *Nat Genet* 18, 365-8.
- Mishima, M., Pavicic, V., Gruneberg, U., Nigg, E. A. and Glotzer, M. (2004). Cell cycle regulation of central spindle assembly. *Nature* 430, 908-13.

- Montanaro, F., Lindenbaum, M. and Carbonetto, S. (1999). alpha-Dystroglycan is a laminin receptor involved in extracellular matrix assembly on myotubes and muscle cell viability. *J Cell Biol* 145, 1325-40.
- Moore, S. A., Saito, F., Chen, J., Michele, D. E., Henry, M. D., Messing, A., Cohn, R. D., Ross-Barta, S. E., Westra, S., Williamson, R. A. et al. (2002). Deletion of brain dystroglycan recapitulates aspects of congenital muscular dystrophy. *Nature* 418, 422-5.
- Muschler, J., Levy, D., Boudreau, R., Henry, M., Campbell, K. and Bissell, M. J. (2002). A role for dystroglycan in epithelial polarization: loss of function in breast tumor cells. *Cancer Res* 62, 7102-9.
- Nitkin, R. M., Smith, M. A., Magill, C., Fallon, J. R., Yao, Y. M., Wallace, B. G. and McMahan, U. J. (1987). Identification of agrin, a synaptic organizing protein from Torpedo electric organ. *J Cell Biol* 105, 2471-8.
- Nobes, C. D. and Hall, A. (1995). Rho, rac, and cdc42 GTPases regulate the assembly of multimolecular focal complexes associated with actin stress fibers, lamellipodia, and filopodia. *Cell* 81, 53-62.
- Nykanen, A., Haley, B. and Zamore, P. D. (2001). ATP requirements and small interfering RNA structure in the RNA interference pathway. *Cell* 107, 309-21.
- Parsons, M. J., Campos, I., Hirst, E. M. and Stemple, D. L. (2002). Removal of dystroglycan causes severe muscular dystrophy in zebrafish embryos. *Development* 129, 3505-12.
- Peng, H. B., Ali, A. A., Daggett, D. F., Rauvala, H., Hassell, J. R. and Smalheiser, N. R. (1998). The relationship between perlecan and dystroglycan and its implication in the formation of the neuromuscular junction. *Cell Adhes Commun* 5, 475-89.
- Pereboev, A. V., Ahmed, N., thi Man, N. and Morris, G. E. (2001). Epitopes in the interacting regions of beta-dystroglycan (PPxY motif) and dystrophin (WW domain). *Biochim Biophys Acta* 1527, 54-60.
- Piekny, A., Werner, M. and Glotzer, M. (2005). Cytokinesis: welcome to the Rho zone. *Trends Cell Biol* 15, 651-8.
- Pilarski, L. M., Turley, E. A., Shaw, A. R., Gallatin, W. M., Laderoute, M. P., Gillitzer, R., Beckman, I. G. and Zola, H. (1991). FMC46, a cell protrusion-associated leukocyte adhesion molecule-1 epitope on human lymphocytes and thymocytes. *J Immunol* 147, 136-43.
- Po, J. L., Mak, A., Ginsberg, D., Huerta, P., Manoukian, R., Shustik, C. and Jensen, G. S. (1999). Mitotic separation of daughter cells in the human lymphoma B cell line Daudi involves L-selectin engagement and shedding. *Haematologica* 84, 785-93.
- Ponting, C. P., Blake, D. J., Davies, K. E., Kendrick-Jones, J. and Winder, S. J. (1996). ZZ and TAZ: new putative zinc fingers in dystrophin and other proteins. *Trends Biochem Sci* 21, 11-13.

- Rambukkana, A., Yamada, H., Zanazzi, G., Mathus, T., Salzer, J. L., Yurchenco, P. D., Campbell, K. P. and Fischetti, V. A. (1998). Role of alpha-dystroglycan as a Schwann cell receptor for *Mycobacterium leprae*. *Science* 282, 2076-9.
- Rentschler, S., Linn, H., Deininger, K., Bedford, M. T., Espanel, X. and Sudol, M. (1999). The WW domain of dystrophin requires EF-hands region to interact with beta-dystroglycan. *Biol Chem* 380, 431-42.
- Ridley, A. J. and Hall, A. (1992). The small GTP-binding protein rho regulates the assembly of focal adhesions and actin stress fibers in response to growth factors. *Cell* 70, 389-99.
- Ridley, A. J., Paterson, H. F., Johnston, C. L., Diekmann, D. and Hall, A. (1992). The small GTP-binding protein rac regulates growth factor-induced membrane ruffling. *Cell* 70, 401-10.
- Roberts, R. G., Freeman, T. C., Kendall, E., Vetrie, D. L., Dixon, A. K., Shaw-Smith, C., Bone, Q. and Bobrow, M. (1996). Characterization of DRP2, a novel human dystrophin homologue. *Nat Genet* 13, 223-6.
- Romero, S., Le Clainche, C., Didry, D., Egile, C., Pantaloni, D. and Carlier, M. F. (2004). Formin is a processive motor that requires profilin to accelerate actin assembly and associated ATP hydrolysis. *Cell* 119, 419-29.
- Russo, K., Di Stasio, E., Macchia, G., Rosa, G., Brancaccio, A. and Petrucci, T. C. (2000). Characterization of the beta-dystroglycan-growth factor receptor 2 (Grb2) interaction. *Biochem Biophys Res Commun* 274, 93-8.
- Sadoulet-Puccio, H. M. and Kunkel, L. M. (1996). Dystrophin and its isoforms. *Brain Pathol* 6, 25-35.
- Saito, F., Masaki, T., Kamakura, K., Anderson, L. V., Fujita, S., Fukuta-Ohi, H., Sunada, Y., Shimizu, T. and Matsumura, K. (1999). Characterization of the transmembrane molecular architecture of the dystroglycan complex in schwann cells. *J Biol Chem* 274, 8240-6.
- Saito, F., Moore, S. A., Barresi, R., Henry, M. D., Messing, A., Ross-Barta, S. E., Cohn, R. D., Williamson, R. A., Sluka, K. A., Sherman, D. L. et al. (2003). Unique role of dystroglycan in peripheral nerve myelination, nodal structure, and sodium channel stabilization. *Neuron* 38, 747-58.
- Sambrook, J., Fritsch, E. F. and Maniatis, T. (1989). *Molecular cloning: a laboratory manual*. Cold Spring Harbor, N.Y.: Cold Spring Harbor Laboratory.
- Sanger, J. M., Mittal, B., Dome, J. S. and Sanger, J. W. (1989). Analysis of cell division using fluorescently labeled actin and myosin in living PtK2 cells. *Cell Motil Cytoskeleton* 14, 201-19.
- Sanger, J. M., Reingold, A. M. and Sanger, J. W. (1984). Cell surface changes during mitosis and cytokinesis of epithelial cells. *Cell Tissue Res* 237, 409-17.

- Sato, N., Funayama, N., Nagafuchi, A., Yonemura, S., Tsukita, S. and Tsukita, S. (1992). A gene family consisting of ezrin, radixin and moesin. Its specific localization at actin filament/plasma membrane association sites. *J Cell Sci* 103 (Pt 1), 131-43.
- Sato, N., Yonemura, S., Obinata, T., Tsukita, S. and Tsukita, S. (1991). Radixin, a barbed end-capping actin-modulating protein, is concentrated at the cleavage furrow during cytokinesis. *J Cell Biol* 113, 321-30.
- Schneider, M., Khalil, A. A., Poulton, J., Castillejo-Lopez, C., Egger-Adam, D., Wodarz, A., Deng, W. M. and Baumgartner, S. (2006). Perlecan and Dystroglycan act at the basal side of the *Drosophila* follicular epithelium to maintain epithelial organization. *Development* 133, 3805-15.
- Schroeder, T. E. (1970). The contractile ring. I. Fine structure of dividing mammalian (HeLa) cells and the effects of cytochalasin B. *Z Zellforsch Mikrosk Anat* 109, 431-49.
- Sciandra, F., Schneider, M., Giardina, B., Baumgartner, S., Petrucci, T. C. and Brancaccio, A. (2001). Identification of the beta-dystroglycan binding epitope within the C-terminal region of alpha-dystroglycan. *Eur J Biochem* 268, 4590-7.
- Sgambato, A., Camerini, A., Faraglia, B., Pavoni, E., Montanari, M., Spada, D., Losasso, C., Brancaccio, A. and Cittadini, A. (2004). Increased expression of dystroglycan inhibits the growth and tumorigenicity of human mammary epithelial cells. *Cancer Biol Ther* 3, 967-75.
- Sgambato, A., Di Salvatore, M. A., De Paola, B., Rettino, A., Faraglia, B., Boninsegna, A., Graziani, C., Camerini, A., Proietti, G. and Cittadini, A. (2006). Analysis of dystroglycan regulation and functions in mouse mammary epithelial cells and implications for mammary tumorigenesis. *J Cell Physiol* 207, 520-9.
- Sgambato, A., Migaldi, M., Montanari, M., Camerini, A., Brancaccio, A., Rossi, G., Cangiano, R., Losasso, C., Capelli, G., Trentini, G. P. et al. (2003). Dystroglycan expression is frequently reduced in human breast and colon cancers and is associated with tumor progression. *Am J Pathol* 162, 849-60.
- Sgambato, A., Tarquini, E., Resci, F., De Paola, B., Faraglia, B., Camerini, A., Rettino, A., Migaldi, M., Cittadini, A. and Zannoni, G. F. (2006). Aberrant expression of alpha-dystroglycan in cervical and vulvar cancer. *Gynecol Oncol*.
- Singh, J., Itahana, Y., Knight-Krajewski, S., Kanagawa, M., Campbell, K. P., Bissell, M. J. and Muschler, J. (2004). Proteolytic enzymes and altered glycosylation modulate dystroglycan function in carcinoma cells. *Cancer Res* 64, 6152-9.
- Smalheiser, N. R. and Kim, E. (1995). Purification of cranin, a laminin binding membrane protein. Identity with dystroglycan and reassessment of its carbohydrate moieties. *J Biol Chem* 270, 15425-33.
- Small, J. V. and Resch, G. P. (2005). The comings and goings of actin: coupling protrusion and retraction in cell motility. *Curr Opin Cell Biol* 17, 517-23.
- Sotgia, F., Bonuccelli, G., Bedford, M., Brancaccio, A., Mayer, U., Wilson, M. T., Campos-Gonzalez, R., Brooks, J. W., Sudol, M. and Lisanti, M. P. (2003). Localization of

- phospho-beta-dystroglycan (pY892) to an intracellular vesicular compartment in cultured cells and skeletal muscle fibers in vivo. *Biochemistry* 42, 7110-23.
- Sotgia, F., Lee, H., Bedford, M. T., Petrucci, T., Sudol, M. and Lisanti, M. P. (2001). Tyrosine phosphorylation of beta-dystroglycan at its WW domain binding motif, PPxY, recruits SH2 domain containing proteins. *Biochemistry* 40, 14585-92.
- Sotgia, F., Lee, J. K., Das, K., Bedford, M., Petrucci, T. C., Macioce, P., Sargiacomo, M., Bricarelli, F. D., Minetti, C., Sudol, M. et al. (2000). Caveolin-3 directly interacts with the C-terminal tail of beta -dystroglycan. Identification of a central WW-like domain within caveolin family members. *J Biol Chem* 275, 38048-58.
- Spector, D. L., Goldman, R. D. and Leinwand, L. A. (1998). Cells: a laboratory manual. Cold Spring Harbor, NY: Cold Spring Harbor Laboratory Press.
- Spence, H. J., Chen, Y. J., Batchelor, C. L., Higginson, J. R., Suila, H., Carpen, O. and Winder, S. J. (2004a). Ezrin-dependent regulation of the actin cytoskeleton by beta-dystroglycan. *Hum Mol Genet* 13, 1657-68.
- Spence, H. J., Dhillon, A. S., James, M. and Winder, S. J. (2004b). Dystroglycan, a scaffold for the ERK-MAP kinase cascade. *EMBO Rep* 5, 484-9.
- Sudol, M. (1996). The WW module competes with the SH3 domain? *Trends Biochem Sci* 21, 161-3.
- Sugita, S., Saito, F., Tang, J., Satz, J., Campbell, K. and Sudhof, T. C. (2001). A stoichiometric complex of neuexins and dystroglycan in brain. *J Cell Biol* 154, 435-45.
- Sugiyama, J., Bowen, D. C. and Hall, Z. W. (1994). Dystroglycan binds nerve and muscle agrin. *Neuron* 13, 103-15.
- Tatsumoto, T., Xie, X., Blumenthal, R., Okamoto, I. and Miki, T. (1999). Human ECT2 is an exchange factor for Rho GTPases, phosphorylated in G2/M phases, and involved in cytokinesis. *J Cell Biol* 147, 921-8.
- Tinsley, J. M., Blake, D. J., Roche, A., Fairbrother, U., Riss, J., Byth, B. C., Knight, A. E., Kendrick-Jones, J., Suthers, G. K., Love, D. R. et al. (1992). Primary structure of dystrophin-related protein. *Nature* 360, 591-3.
- Tisi, D., Talts, J. F., Timpl, R. and Hohenester, E. (2000). Structure of the C-terminal laminin G-like domain pair of the laminin alpha2 chain harbouring binding sites for alpha-dystroglycan and heparin. *Embo J* 19, 1432-40.
- Tommasi di Vignano, A., Di Zenzo, G., Sudol, M., Cesareni, G. and Dente, L. (2000). Contribution of the different modules in the utrophin carboxy-terminal region to the formation and regulation of the DAP complex. *FEBS Lett* 471, 229-34.
- Tsukita, S., Oishi, K., Sato, N., Sagara, J., Kawai, A. and Tsukita, S. (1994). ERM family members as molecular linkers between the cell surface glycoprotein CD44 and actin-based cytoskeletons. *J Cell Biol* 126, 391-401.

- Tsukita, S. and Yonemura, S. (1999). Cortical actin organization: lessons from ERM (ezrin/radixin/moesin) proteins. *J Biol Chem* 274, 34507-10.
- Turunen, O., Wahlstrom, T. and Vaheri, A. (1994). Ezrin has a COOH-terminal actin-binding site that is conserved in the ezrin protein family. *J Cell Biol* 126, 1445-53.
- Turunen, O., Winqvist, R., Pakkanen, R., Grzeschik, K. H., Wahlstrom, T. and Vaheri, A. (1989). Cytovillin, a microvillar Mr 75,000 protein. cDNA sequence, prokaryotic expression, and chromosomal localization. *J Biol Chem* 264, 16727-32.
- Vanni, C., Parodi, A., Mancini, P., Visco, V., Ottaviano, C., Torrisi, M. R. and Eva, A. (2004). Phosphorylation-independent membrane relocalization of ezrin following association with Dbl in vivo. *Oncogene* 23, 4098-106.
- Williamson, R. A., Henry, M. D., Daniels, K. J., Hrstka, R. F., Lee, J. C., Sunada, Y., Ibraghimov-Beskrovnaya, O. and Campbell, K. P. (1997). Dystroglycan is essential for early embryonic development: disruption of Reichert's membrane in Dag1-null mice. *Hum Mol Genet* 6, 831-41.
- Winder, S. J. (1997). The membrane-cytoskeleton interface: the role of dystrophin and utrophin. *J Muscle Res Cell Motil* 18, 617-29.
- Woodward, A. M. and Crouch, D. H. (2001). Cellular distributions of the ERM proteins in MDCK epithelial cells: regulation by growth and cytoskeletal integrity. *Cell Biol Int* 25, 205-13.
- Wu, H. and Parsons, J. T. (1993). Cortactin, an 80/85-kilodalton pp60src substrate, is a filamentous actin-binding protein enriched in the cell cortex. *J Cell Biol* 120, 1417-26.
- Xia, Z., Dickens, M., Raingeaud, J., Davis, R. J. and Greenberg, M. E. (1995). Opposing effects of ERK and JNK-p38 MAP kinases on apoptosis. *Science* 270, 1326-31.
- Xu, W., Baribault, H. and Adamson, E. D. (1998). Vinculin knockout results in heart and brain defects during embryonic development. *Development* 125, 327-37.
- Yamada, H., Chiba, A., Endo, T., Kobata, A., Anderson, L. V., Hori, H., Fukuta-Ohi, H., Kanazawa, I., Campbell, K. P., Shimizu, T. et al. (1996). Characterization of dp6troglycan-laminin interaction in peripheral nerve. *J Neurochem* 66, 1518-24.
- Yamada, H., Denzer, A. J., Hori, H., Tanaka, T., Anderson, L. V., Fujita, S., Fukuta-Ohi, H., Shimizu, T., Ruegg, M. A. and Matsumura, K. (1996). Dystroglycan is a dual receptor for agrin and laminin-2 in Schwann cell membrane. *J Biol Chem* 271, 23418-23.
- Yamada, H., Saito, F., Fukuta-Ohi, H., Zhong, D., Hase, A., Arai, K., Okuyama, A., Maekawa, R., Shimizu, T. and Matsumura, K. (2001). Processing of beta-dystroglycan by matrix metalloproteinase disrupts the link between the extracellular matrix and cell membrane via the dystroglycan complex. *Hum Mol Genet* 10, 1563-9.
- Yang, B., Jung, D., Motto, D., Meyer, J., Koretzky, G. and Campbell, K. P. (1995). SH3 domain-mediated interaction of dystroglycan and Grb2. *J Biol Chem* 270, 11711-4.

- Yonemura, S., Hirao, M., Doi, Y., Takahashi, N., Kondo, T., Tsukita, S. and Tsukita, S. (1998). Ezrin/radixin/moesin (ERM) proteins bind to a positively charged amino acid cluster in the juxta-membrane cytoplasmic domain of CD44, CD43, and ICAM-2. *J Cell Biol* 140, 885-95.
- Yonemura, S., Nagafuchi, A., Sato, N. and Tsukita, S. (1993). Concentration of an integral membrane protein, CD43 (leukosialin, sialophorin), in the cleavage furrow through the interaction of its cytoplasmic domain with actin-based cytoskeletons. *J Cell Biol* 120, 437-49.
- Yoshida, A., Kobayashi, K., Manya, H., Taniguchi, K., Kano, H., Mizuno, M., Inazu, T., Mitsuhashi, H., Takahashi, S., Takeuchi, M. et al. (2001). Muscular dystrophy and neuronal migration disorder caused by mutations in a glycosyltransferase, POMGnT1. *Dev Cell* 1, 717-24.
- Yu, Y., Khan, J., Khanna, C., Helman, L., Meltzer, P. S. and Merlino, G. (2004). Expression profiling identifies the cytoskeletal organizer ezrin and the developmental homeoprotein Six-1 as key metastatic regulators. *Nat Med* 10, 175-81.
- Yuce, O., Piekny, A. and Glotzer, M. (2005). An ECT2-centralspindlin complex regulates the localization and function of RhoA. *J Cell Biol* 170, 571-82.
- Zhan, Y., Tremblay, M. R., Melian, N. and Carbonetto, S. (2005). Evidence that dystroglycan is associated with dynamin and regulates endocytosis. *J Biol Chem* 280, 18015-24.
- Zhong, D., Saito, F., Saito, Y., Nakamura, A., Shimizu, T. and Matsumura, K. (2006). Characterization of the protease activity that cleaves the extracellular domain of beta-dystroglycan. *Biochem Biophys Res Commun* 345, 867-71.
- Zhou, Y. W., Thomason, D. B., Gullberg, D. and Jarrett, H. W. (2006). Binding of laminin alpha1-chain LG4-5 domain to alpha-dystroglycan causes tyrosine phosphorylation of syntrophin to initiate Rac1 signaling. *Biochemistry* 45, 2042-52.